Discrete semiclassical methods in the theory of Rydberg atoms in external fields

P. A. Braun

Department of Theoretical Physics, Institute of Physics,
St. Petersburg University, St. Petersburg 198 904, Russia

The properties of the WKB method in the discrete representation are reviewed. The method provides the eigenvalues and the eigenvectors of the three-term recursion relations or, which is the same thing, the tridiagonal band matrices. Applications of the method to the splitting of the Rydberg atom levels in the external electric and magnetic fields are considered. Analytical treatment is given to the problem of the oscillator strength distribution in the quadratic Zeeman and the Stark-Zeeman spectra. In the case of the nonhydrogenic Rydberg atoms, the effect of the core on the pattern of the splitting is studied. Certain alternative applications of the discrete WKB method are considered in brief (the quasienergy spectra of nonlinear oscillators in resonant fields, rotational molecular spectra, calculation of infinite continued fractions).

CONTENTS

I. INTRODUCTION

Following the advent of tunable lasers, it became possible to obtain highly excited (Rydberg) atoms in individual quantum states and to study the splitting of their levels in various external fields. Because of their huge size (of the order n^2 where $n \gg 1$ is the principal quantum number of the valence electron) Rydberg atoms are highly susceptible to external perturbations. Therefore effects that would hardly be noticeable in the ground state become significant.

In particular, considerable interest has been focused on the second-order Zeeman effect. This is connected with the diamagnetic part of the operator describing the interaction of an atomic electron with an external magnetic field $H\hat{z}$,

$$V_d = \frac{H^2}{8c^2}(x^2+y^2) \ . \tag{1.1}$$

For a fixed field the diamagnetic splitting grows as n^4 when n is increased.

Consider the case of the hydrogen atom. In experiments on highly excited states (Holle *et al.*, 1985; Wintgen, Holle *et al.*, 1986; Holle *et al.*, 1988) the spin-orbital coupling can usually be neglected. Therefore the orbital part of the paramagnetic interaction $(H/2c)L_z$ is an integral of motion leading to trivial equidistant splitting according to the value of the magnetic quantum number m. The residual $n-|m|$-fold degeneracy is removed by the diamagnetic perturbation (1.1).

In fields that are not too strong, the diamagnetic splitting can be found by diagonalizing the operator V_d in a basis set of parabolic orbitals $|nn_1n_2\rangle$ with fixed n. Because of axial symmetry V_d can connect only states with the same value of the sum $n_1+n_2=n-|m|-1$. It can also change by 0 or ± 2 the value of the difference $k\equiv n_1-n_2$. Consequently the resulting set of equations for the coefficients of the zero-order eigenfunction is a three-term recursion (TTR) relation:

$$p_k C_{k-2}+(w_k-E')C_k+p_{k+2}C_{k+2}=0 \ . \tag{1.2}$$

Here E' is the energy correction value due to the diamagnetic perturbation. Its connection with the total energy of the perturbed atom is

$$E=-1/2n^2+mH/2c+E' \ .$$

The diagonal $w_k=\langle nn_1n_2|V_d|nn_1n_2\rangle$ and the off-diagonal $p_k=\langle nn_1-1n_2+1|V_d|nn_1n_2\rangle$ matrix elements of the perturbation V_d are given by

$$\begin{aligned} w_k&=\frac{u_\gamma}{5}\left[3-\frac{3k^2+m^2-1}{n^2}\right] , \\ p_k&=\frac{u_\gamma}{5}\left\{\left[\left[1-\frac{m}{n}\right]^2-\frac{(k-1)^2}{n^2}\right]\right. \\ &\quad\times\left.\left[\left[1+\frac{m}{n}\right]^2-\frac{(k-1)^2}{n^2}\right]\right\}^{1/2} . \end{aligned} \tag{1.3}$$

The value

$$u_\gamma\equiv\frac{5n^4}{16}\left[\frac{H}{c}\right]^2$$

is the natural unit of diamagnetic splitting (γ is the notation frequently used for the magnetic field measured in atomic units).

An alternative approach is to use a spherical basis set, which also leads to a TTR relation,

$$p_l C_{l-2}+(w_l-E')C_l+p_{l+2}C_{l+2}=0 \ . \tag{1.4}$$

The matrix elements

$$w_l=\langle nlm|V_d|nlm\rangle \ ,$$

$$p_l=\langle nl-2m|V_d|nlm\rangle$$

factor into products of their radial and angular parts:

$$\begin{aligned} & w_l=w_l^r w_l^\vartheta, \quad p_l=p_l^r p_l^\vartheta \ , \\ & w_l^r=u_\gamma\left[1+\frac{1-3l(l+1)}{5n^2}\right] , \\ & w_l^\vartheta=\frac{2(l^2+l-1+m^2)}{(2l-1)(2l+3)} , \\ & p_l^r=u_\gamma\left\{\left[1-\frac{l^2}{n^2}\right]\left[1-\frac{(l-1)^2}{n^2}\right]\right\}^{1/2} , \\ & p_l^\vartheta=-\left\{\frac{(l^2-m^2)[(l-1)^2-m^2]}{(2l+1)(2l-1)^2(2l-3)}\right\}^{1/2} . \end{aligned} \tag{1.5}$$

These equations were written long ago (Schiff and Snyder, 1939) in connection with the experiments of Jenkins and Segre (1939) on the Rydberg states of the alkali-metal atoms. However, there were no attempts to analyze their spectra until about 1980, when the following striking features of the quadratic Zeeman splitting were established (Clark and Taylor, 1980,1982; Zimmerman *et al.*, 1980; Clark, 1981; Delande and Gay, 1981a;1981b):

(a) If $|m|$ is not too large, the quadratic Zeeman multiplet consists of two parts with different properties (Fig. 1). The lower part contains extremely narrow doublets of levels of opposite parity. In the upper part the levels are locally equidistant. The relative size of the transition zone between the two parts is small (of the order n^{-1}).

(b) With the growth of $|m|$, the relative length of the doublet part decreases. When $m=0$ it constitutes 1/5 of the whole multiplet; it disappears altogether when $|m|$ is

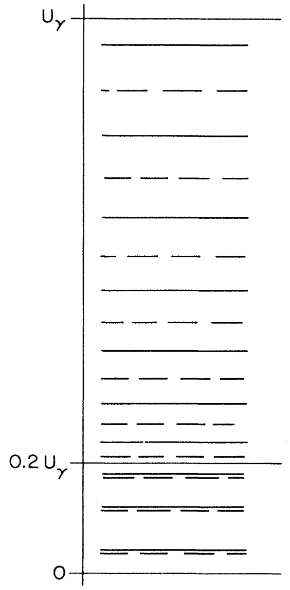

FIG. 1. Quadratic Zeeman multiplet in atomic hydrogen with $n=20$, $m=0$. Solid and dashed lines correspond to even and odd levels. The *g-u* splitting in the doublets is grossly exaggerated.

larger than a certain fraction of n ($n/\sqrt{5}$, as was established afterwards).

(c) If the magnetic field is increased, so that the quadratic Zeeman multiplets produced by splitting of the neighboring hydrogen atom levels begin to overlap (Fig. 2), then the width of the anticrossings between levels belonging to the upper part of the nth multiplet and to the lower part of the $(n+1)$th multiplet is extremely narrow, decreasing exponentially when n is increased (Fig. 3).

These properties of the quadratic Zeeman splitting were totally unexpected. Their explanation came soon and was based on classical perturbation theory (Solov'ev, 1981,1982). In the absence of an external magnetic field, the electron of a classical hydrogen atom would travel along a Kepler orbit, keeping constant its angular momentum **L** and the Runge-Lenz vector **A** (directed along the major semiaxis). These two vectors uniquely determine the form and orientation of the orbit. The external magnetic field leads to a slow change of **L** and **A** (with the exception of the component L_z, which is conserved due to the axial symmetry of the problem). Assuming that the period of the field-induced evolution is large compared with the Kepler period, it can be shown that the quantity

$$\Lambda = 4\mathbf{A}^2 - 5A_z^2 \tag{1.6}$$

remains constant, thus being an approximate integral of motion.

The existence of the integral Λ has significant implications, the most important of which is the division of the evolving Kepler orbits into classes with distinctly different properties. This can easily be shown by setting in Eq. (1.6) $A_z = A\sin\alpha$ where α is the angle between **A** and the plane orthogonal to the field. After that we obtain

$$\Lambda = \mathbf{A}^2(4-5\sin^2\alpha) = \text{const}\ . \tag{1.7}$$

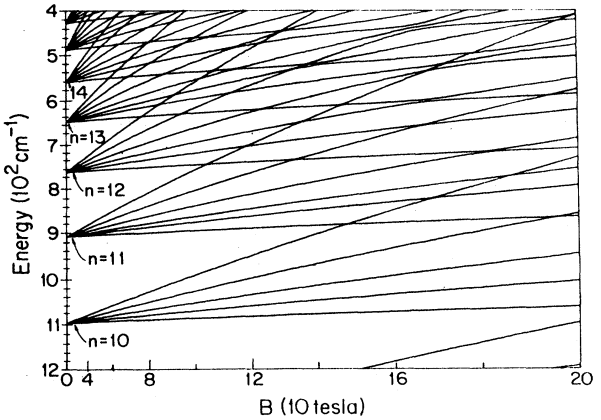

FIG. 2. Energy of hydrogen calculated as a function of magnetic field (plotted on a squared scale). Only even levels with $m=0$ in the range of $n=10-16$ are shown. What appear to be crossings of the levels (impossible, in view of the Wigner-Neuman rule) are in fact exceedingly narrow anticrossings. From Zimmerman *et al.* (1980).

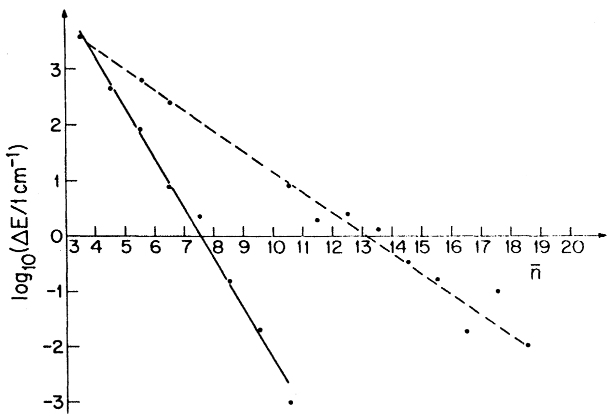

FIG. 3. Anticrossing size as a function of $\bar{n}$, the geometric mean of the principal quantum numbers of the adjacent manifolds. The solid line depicts the anticrossing size between the lowest-energy state of the $n+1$ manifold and the highest-energy state of the n manifold. The dashed line shows the anticrossing size between the lowest-energy state of the $n+1$ manifold and some "middle"-energy state of the n manifold. From Zimmerman *et al.* (1980).

The constant Λ can be of both signs. If $\Lambda > 0$ it follows from Eq. (1.7) that $-\alpha_0 < \alpha < \alpha_0$ where $\alpha_0 = \arcsin\sqrt{4/5} \sim 63°$. This means that the direction of the major semiaxis of the orbit of the atomic electron perturbed by the diagmagnetic interaction never leaves the belt delimited by the latitudes $\pm\alpha_0$. On the other hand, if $\Lambda < 0$, Eq. (1.7) leads to two inequalities, $\alpha > \alpha_0$ or $\alpha < -\alpha_0$. Thus in the case of negative Λ we have two symmetrical trajectories of the evolution of the orbit, its major semiaxis being limited to one of the two "polar regions."

These purely classical considerations can be used to interpret the spectra of highly excited atomic hydrogen in a magnetic field. In particular the existence of two symmetrical trajectories for each $\Lambda < 0$ is the cause of the doublet structure of the lower part of the quadratic Zeeman multiplets. The Bohr-Sommerfeld quantization condition for the energies of the perturbed atom can also be introduced (Solov'ev, 1981).

Conservation of Λ is a special case of the theorem of classical perturbation theory which, in a crude formulation, suggests that perturbation averaged over a period of the unperturbed motion is an approximate integral of motion. [A rigorous treatment of the subject is given by Arnold (1974).] The classical average of the diamagnetic interaction (1.1) over a period of the Kepler movement characterized by the vectors **L** and **A** is a function of these vectors equal to

$$E' = \langle V_d \rangle_{\text{class}} = \frac{H^2 n^2}{16c^2}(4\mathbf{A}^2 - 5A_z^2 + L_z^2 + n^2)\ . \tag{1.8}$$

Here, within the accuracy of semiclassical theory,

$$n=(-2E^{(0)})^{-1/2}=(\mathbf{L}^2+\mathbf{A}^2)^{1/2}\ ;$$

note that our definition of $\mathbf{A}$ differs by the factor n from that of Solov'ev (1981). The quantity (1.8) is bound to be an integral of motion; since L_z is conserved it leads to conservation of Λ.

There is also a rigorous quantum-mechanical relation similar to Eq. (1.8) between the matrices of the diamagnetic operator V_d and the operator corresponding to Λ in the manifold of a single hydrogen atom shell [see below, Eq. (3.41)]. This relation was used to investigate the zero-order eigenfunctions diagonalizing the diamagnetic perturbation V_d, which are the orbitals produced by separation of variables on Fock's sphere in the ellipsocylindrical coordinates in the momentum space (Solov'ev, 1981,1982; Herrick, 1982; Grozdanov and Solov'ev, 1984; Hasegawa and Adachi, 1988).

Further studies based on the classical perturbation theory revealed many other interesting properties of the quadratic Zeeman effect. Important contributions were made by Robnik (1981,1982), Delos *et al.* (1983a,1983b), Gay *et al.* (1983), Hasegawa *et al.* (1984), and other authors. This part of the theory of Rydberg atoms in external fields is extensively covered in many reviews; see Gay *et al.* (1985,1986), Nayfeh and Clark (1985), Lisitsa (1987), and Hasegawa *et al.* (1989).

In spite of these spectacular achievements, a sense of dissatisfaction still remains. Many decades ago the problem of the quadratic Zeeman effect was formulated in terms of the three-term recursion relations (1.2) and (1.4). The three-term recursion relations are actually very simple mathematical objects similar to ordinary second-order differential equations. However, for 40 years the TTR relations (1.2) and (1.4) were literally before the eyes of the investigators and no one guessed that there was anything interesting about their spectra.

It is obviously highly desirable to have a method allowing quick appraisal of the spectra of the recursion relations or, which is the same thing, of the tridiagonal matrices. Such a method and the results of its application to the spectra of Rydberg atoms in external fields is the topic of this review. In essence this is the WKB method adjusted to discrete representation.

The structure of the review is as follows. In Sec. II we describe the formalism of the discrete WKB method. In Sec. III the method is initially applied to the quadratic Zeeman effect in atomic hydrogen (Secs. III.A–III.C). We show that the properties of the splitting follow in a rather trivial way from the expressions of the matrix elements in Eqs. (1.2) and (1.4).

Imposition of the additional external electric field leads to complicated distortions of the diamagnetic multiplets. The pattern of the splitting is qualitatively different, depending on the relative strengths and orientation of the two fields. Its description for highly excited atomic hydrogen is given in Secs. III.D and III.E; the discrete WKB method was in this case the original means of investigation of the spectrum.

A new development in the theory of perturbed Rydberg atom spectra is the discovery of the relations between energy-level distribution and oscillator strengths in the quadratic Zeeman and the Stark-Zeeman multiplets. Section IV deals with these relations for the hydrogen atom.

Nonhydrogenic Rydberg atoms in external fields are considered in Sec. V.

Certain general aspects of the discrete WKB method are considered in the appendices. In particular, in Appendix C some applications of the method unconnected with the theory of the Rydberg atoms are briefly reviewed.

Throughout the paper we neglect the mixing of states from different shells, which corresponds to relatively weak external fields (the so-called l-mixing regime). The quantum-mechanical condition for this regime is that field-induced splitting ($\sim u_\gamma$) be small compared with the spacing between levels of the unperturbed atomic hydrogen (n^{-3}). In fact, many of the l-mixing regime laws remain in force even in considerably stronger fields (Wintgen and Friedrich, 1986a,1986b; Grozdanov and Taylor, 1986; Cacciani *et al.*, 1989). The reason behind this is that the properties of the highly excited states are fairly accurately described by classical perturbation theory, whose limitations on the perturbation strength are much more lenient, with n^{-3} replaced by n^{-2} (Landau and Lifshiftz, 1989).[1] The results referring to the domain of the classically chaotic movement are not considered here; they can be found in the reviews of Gay (1988), Friedrich and Wintgen (1989), and Hasegawa *et al.* (1989). See also the books by Taylor *et al.* (1988) and Bassani *et al.* (1989).

Atomic units are used. To go to the practical units of the fields one has to replace H/c by H/H_0 with $H_0=2.35\times10^5$ T and the electric field F by F/F_0 with $F_0=5.14\times10^9$ v/cm.

II. THE DISCRETE WKB METHOD

In view of the well-known similarity between the recursion relations and the differential equations, the idea of using semiclassical methods on TTR relations like (1.2)

---

[1] Here is a hint on how the limitations of quantum perturbation theory may be circumvented. Consider the nth level, $n \gg 1$, of a perturbed system with one degree of freedom. If the system is semiclassical, its levels $E_n^{(0)}$ are locally equidistant, and the matrix elements of the perturbation $\langle n|V|n+k\rangle$ change slowly with n,k being fixed. Therefore, in the expression for the second-order energy correction $E_n^{(2)}$, contributions from transitions up to $E_{n+k}^{(0)}$ and down to $E_{n-k}^{(0)}$ almost cancel each other. As a result the value of $E_n^{(2)}$ is greatly diminished. An expression for the perturbed wave function that is valid in the domain of classical perturbation theory may be found in Kazantsev and Pokrovsky (1983b).

or (1.4) is rather obvious. A rigorous mathematical study of the related problems can be found in the books of Maslov (1973) and Vasil'eva and Butuzov (1978). Physicists have derived the WKB solutions of the recursion relations mostly on their own. It was done many times in many different ways in papers dealing with the asymptotics of the $3nj$ symbols (Schulten and Gordon, 1975), the quasienergies of the anharmonic oscillator driven by the periodical force (Sazonov, 1978; Braun, 1978), and the quadratic Zeeman effect and Stark-Zeeman effect for atomic hydrogen (Braun, 1983a; Kazantsev, Pokrovsky, and Bergou, 1983; Delos *et al.*, 1988; Fano *et al.*, 1988). Connections with classical perturbation theory are traced by Kazantsev and Pokrovsky (1983a,1983b).

Apart from the papers cited above, the discrete WKB method has been applied to Rydberg atoms in external fields by Braun (1983b, 1986, 1989b, 1990a, 1990b, 1990c, 1991a), Braun and Solov'ev (1984), and Braun and Senyushkin (1991). Other applications include the rotational spectra of molecules of various types: the rigid asymmetric top (Braun and Kiselev, 1983; Bruev, 1986; Rau and Lijun Zhang, 1990), the nonrigid asymmetrical top (Braun, 1989a), the nonrigid spherical top (Braun *et al.*, 1985), the Lamb shift of an atom inside the resonator (Belov *et al.*, 1989), the microwave ionization of an atom (Ostrovsky and Telnov, 1987), and the three-body problem in the dipole approximation (Braun *et al.*, 1990).

Bruev (1986) used the method to study rotational relaxation in molecular gases. The semiclassical tridiagonal problems discussed in the papers of Rau (1989), Rau and Molina (1989), and Rau and Zhang (1990) also include the Edmonds-Pullen model (a two-dimensional isotropic oscillator perturbed by the interaction x^2y^2), angular correlation between highly excited electrons, and the problem of a two-nucleon system with quadrupole coupling. The paper of Leopold and Richards (1989) deals with a one-dimensional model of atomic hydrogen in a high-frequency electric field. A semiclassical approximation for a special type of recursion relation different from Eqs. (1.2) and (1.4) is considered by Bender *et al.* (1979).

Here we outline the method, beginning with a review of the classical problem, which is connected with the TTR relation through the correspondence relations (Sec. II.A). In Sec. II.B the analog of the potential energy for such problems is considered. WKB solutions of the TTR relations are introduced in Sec. II.C. The matching and quantization conditions are formulated in Sec. II.D. In Appendix A we list some of the typical errors connected with the application of the discrete WKB method. Appendix B contains explicit expressions for the lowest and highest eigenvalues of the TTR relation.

A. The classical Hamiltonian corresponding to a three-term recursion relation

Application of the WKB method in the discrete representation is based on two facts. (a) Linear recursion relations with constant coefficients are exactly soluble. (b) The coefficients of a recursion relation describing a physical system whose movement is semiclassical are locally almost constant, changing little on each step.

In the case of perturbed Rydberg atoms, the small parameter of the problem determining its semiclassical nature is n^{-1}. Accordingly the matrix elements (1.3) of Eq. (1.2) depend on the discrete variable k only in the combination k/n. This means that the derivatives of w_k and p_k by k are of the order n^{-1}, so that the change of coefficients in Eq. (1.2) on each step is indeed small; the same is true of Eq. (1.4). Using this property, one can obtain a formal asymptotic development of the solutions in powers of n^{-1}. We shall do this later, beginning with more physical considerations.

Let us consider a problem of classical mechanics connected with the TTR relation. It will be more convenient to begin with a relation that has a unit step in the index,

$$p_jC_{j-1}+(w_j-E')C_j+p_{j+1}C_{j+1}=0 \; . \tag{2.1}$$

It is supposed that j takes consecutive integer values. Now we suppose that w_j and p_j are smooth analytical functions known for all (not only integer) j. Both Eqs. (1.2) and (1.4) can be brought to this form. In the parabolic basis, one should take $k=2j$ or $k=2j+1$, depending on the parity of $n-m+1$; in the spherical basis, the substitutions $l=2j$ and $l=2j+1$ should be used for the even and odd parts of the spectrum, respectively.

For the moment let us regard j in Eq. (2.1) as a continuous variable, using notations like $C(j)$ along with C_j etc. Introducing the "momentum" operator

$$\varphi=-i\frac{\partial}{\partial j}$$

and considering that the operators $e^{\pm i\varphi}$ shift j by ± 1, we can write Eq. (2.1) as a Schrödinger equation for the function $C(j)$ with the eigenvalue E' and the Hamiltonian

$$\hat{H}=w(j)+p(j)e^{-i\varphi}+p(j+1)e^{i\varphi} \; . \tag{2.2}$$

In the classical limit j and φ turn into the canonically conjugate "coordinate" and "momentum." The operator $\hat{H}$ turns into a Hamiltonian function. Remembering that in the semiclassical situation $p(j)$ and $p(j+1)$ are only slightly different, and replacing them by their value at the midpoint, we obtain

$$H'(j,\varphi)=w(j)+2p(j+\tfrac{1}{2})\cos\varphi \; . \tag{2.3}$$

Later we shall use the notations w and p (without indicating the argument) for $w(j)$ and $p(j+\frac{1}{2})$.

When $n\rightarrow\infty$ the range of the discrete argument in the recursion relation runs to infinity so that, strictly speaking, it is not j but j/n which tends to a finite classical variable. If we consider j/n to be of the order n^0, we can develop the functions w and p into a series in n^{-1}. In accordance with the accuracy of the usual WKB treatment we shall keep two senior terms in these developments:

the purely classical limit plus the principal quantum correction. The terms of higher order are irrelevant,[2] so that expressions like $\sqrt{j(j+1)}/n$ can be replaced by $(j+\frac{1}{2})/n$ but not by j/n. The resulting Hamilton function (2.3) will be called the semiclassical Hamiltonian, as opposed to the purely classical one.

The classical variables j and φ obey the canonical equations

$$\frac{dj}{dt}=\frac{\partial H'}{\partial\varphi}=-2p\sin\varphi,\quad \frac{d\varphi}{dt}=-\frac{\partial H'}{\partial j}\ . \tag{2.4}$$

The physical meaning of j and φ depends on the representation. In the parabolic basis, $k=A_z$ so that the "coordinate" j is proportional to the z component of the Runge-Lenz vector, while in the spherical basis j is half the angular momentum value. For the meanings of the conjugate variable φ see Born (1960). In both cases Eq. (2.4) describes the slow evolution of the Kepler orbit of the atomic electron caused by diamagnetic perturbation.

B. Potential functions of the recursion relations

The Hamiltonian (2.3) depends on the canonical "momentum" via a cosine function. This is typical of problems in classical perturbation theory formulated in action-angle variables (Carruthers and Nieto, 1968). To deal with such problems it is convenient to introduce an equivalent of the potential-energy curve (Braun, 1978). This is the plot of the functions

$$\begin{aligned} U^+(j)&=H'(j,0)=w+2p\ ,\\ U^-(j)&=H'(j,\pi)=w-2p\ . \end{aligned} \tag{2.5}$$

Their role becomes clear from the following.

(a) According to Eq. (2.4) the classical "speed" becomes zero when $\varphi=0$ and π. Since the value of the Hamiltonian remains constant,

$$H'(j,\varphi)=E'\ , \tag{2.6}$$

this means that at the turning points of the variable j we have $E'=U^+$ and $E'=U^-$, respectively. Thus the turning points can be found crossing the curve of $U^\pm$ by the line of the constant energy E'.

(b) At each value of j the values of U^+ and U^- bound the Hamiltonian (2.3). Supposing that $p\geq 0$, we obtain

$$U^-(j)\leq E'\leq U^+(j)\ . \tag{2.7}$$

For a fixed E' these inequalities determine the classically allowed values of j. On the other hand, the extremal values of $U^\pm$ bound the interval of possible values of E',

$$\min U^-\leq E'\leq \max U^\pm\ . \tag{2.8}$$

Otherwise classical movement would not be possible anywhere. It can be proved that the extrema of $U^+(j)$ and $U^-(j)$ (if they exist) also give rigorous bounds to the eigenvalue spectrum of the quantum problem (2.1); see Braun (1978).

(c) Excluding φ from Eqs. (2.4) and (2.6), we obtain a differential equation for $j(t)$,

$$\frac{dj}{dt}=\pm\{[U^+(j)-E'][E'-U^-(j)]\}^{1/2}\ . \tag{2.9}$$

It can be seen that the evolution of j is an oscillation between the turning points, in which the right-hand side goes to zero. The period of oscillation is given by the integral

$$T(E')=2\int_{j_{t1}}^{j_{t2}}\frac{dj}{\sqrt{(U^+-E')(E'-U^-)}}\ . \tag{2.10}$$

(d) The two turning points j_{t1} and j_{t2} bounding the classically allowed interval can belong either to the same or to different potential curves. In the first case the variable φ oscillates in the vicinity of 0 or π, provided the turning points belong to U^+ or U^-, respectively. In the second case the evolution of φ is one of unlimited growth (rotation), with φ taking consecutive values $0,\pi,2\pi,3\pi,\ldots$ as the system reaches alternately U^+ and U^-.

Better understanding of what the functions $U^\pm$ mean can be achieved through a solid-state analogy. A TTR relation can be regarded as an equation describing a lattice in one dimension, in which interaction exists only between the closest neighbors. If the matrix elements w_j and p_j in the TTR relation were independent of j, the lattice would be periodic with the zone energy spectrum in the interval $(w-2p,w+2p)$. The semiclassical situation we are dealing with corresponds to a quasiperiodic lattice whose properties slowly change along its length. The lower and upper bounds of the zone can then be regarded as functions of the nodal number; remember, for example, the textbook picture of the inclined zones in the description of Zener tunneling in an electric field [Fig. 93 in Ziman (1964)]. These bounds are just the functions $U^\pm$.

Here are two simple mathematical examples.

(a) The recursion relation $(-\infty<j<\infty)$

$$C_{j-1}-(2j/a+E')C_j+C_{j+1}=0 \tag{2.11}$$

has the Bessel and Neuman functions of the argument a as its solutions, their index running the values $v=j+aE'/2$. The TTR (2.11) is semiclassical if $a\gg 1$. The corresponding classical Hamiltonian is

$$H'(j,\varphi)=-2j/a+2\cos\varphi\ . \tag{2.12}$$

Its potential functions are linear (Fig. 4),

$$U^\pm(j)=-2j/a\pm 2\ .$$

For all E' $(-\infty<E'<\infty)$ the movement of the system

---

[2] In some applications higher accuracy is needed. For example, in the theory of the microwave ionization of a particle in a short-range potential (Ostrovsky and Telnov, 1987), three orders of discrete WKB development were necessary to obtain nontrivial results.

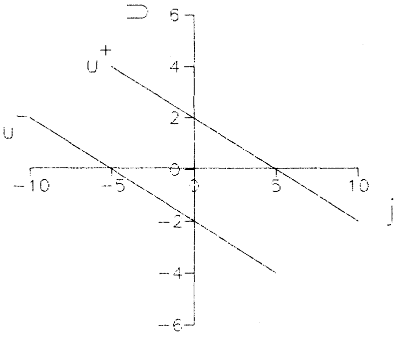

FIG. 4. Potential functions of the three-term recursion relation (2.11) for the Bessel functions ($a=5$).

with the Hamiltonian (2.12) is finite. Its turning points are $j_{t1}=-a-aE'/2$ and $j_{t2}=a-aE'/2$, belonging to U^- and U^+ respectively.

(b) Consider the solution of the Mathieu equation

$$\left[-\frac{1}{2}\frac{d^2}{dx^2}+F\cos x-E'\right]\psi=0 \tag{2.13}$$

corresponding to zero quasimomentum. Developing it into a Fourier series we obtain the recursion relation for the Fourier amplitudes ($-\infty<j<\infty$)

$$\frac{F}{2}(C_{j-1}+C_{j+1})+(j^2/2-E')C_j=0 \ . \tag{2.14}$$

The corresponding classical Hamiltonian following from Eq. (2.3),

$$H'(j,\varphi)=j^2/2+F\cos\varphi \ ,$$

is simply the Hamiltonian of the Schrödinger equation (2.13) with the coordinate and momentum interchanged (and renamed). The potential functions of the problem are parabolic (Fig. 5):

$$U^{\pm}(j)=j^2/2\pm F \ .$$

For all allowed $E'(-F<E'<\infty)$, the movement in j is finite. In the energy range $-F<E'<F$ there are two turning points belonging to U^- and a single classically allowed region of j. On the other hand, if $E'>F$ there are two symmetrical classically allowed regions of j divided by a forbidden area (where corresponding C_j are exponentially small). This fact reflects the difference in Fourier composition between eigenfunctions describing the "almost bound" and the "almost free" states in the potential $F\cos x$.

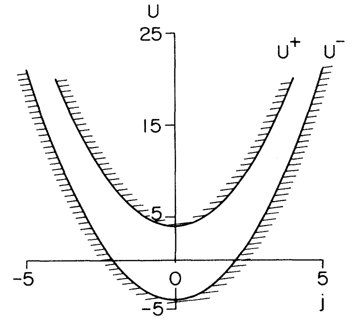

FIG. 5. Potential functions of the TTR relation (2.12) for the Fourier amplitudes of the solution of the Mathieu equation ($F=4$). Boundaries of the classically allowed region are hatched. From Braun (1978).

C. The semiclassical solutions

1. Physical arguments

From the energy conservation law we get the phase trajectory equation

$$\varphi=\arccos B(E',j) \ ,$$
$$B(E',j)\equiv\frac{E'-w}{2p} \ . \tag{2.15}$$

The action expressed through j is

$$S=\int\varphi dj$$

and the classical speed $v(j)=dj/dt$ is given by Eq. (2.9).

Now we can write the WKB solution of the recursion relation (2.1). It has the obvious form

$$C_j=\frac{A}{\sqrt{v(j)}}\cos[S(j)+\chi] \ , \tag{2.16}$$

with j taking integer values and A and χ constant.

The form (2.16) of the solution is convenient within the classically allowed interval of j where φ is real; this is where the inequalities (2.7) hold. If $E'>U^+$ we have $B>1$, and φ is purely imaginary. The two fundamental WKB solutions can then be written as

$$C_j=\frac{A}{\sqrt{|v(j)|}}\exp\left[\pm\int\operatorname{arccosh}B\,dj\right] \ . \tag{2.17}$$

One of them grows exponentially when j is increased, while the other one decreases exponentially. This is the usual behavior of WKB solutions outside the classically allowed region.

Now suppose that $E'<U^-$, which means that $B<-1$. Considering that $\varphi=\pi+i\operatorname{arccosh}(-B)$, the two solutions can then be written as

$$C_j=(-1)^j\frac{A}{\sqrt{|v(j)|}}\exp\left[\pm\int\operatorname{arccosh}(-B)dj\right] \ . \tag{2.18}$$

The absolute values of C_j increase and decrease exponentially. What is new is that the sign of C_j is changed on each step of the TTR relation.

Thus there are not two, but three different types of regions. These were named regions I ($U^-<E'<U^+$), II ($E'>U^+$), and III ($E'<U^-$) by Braun (1978). After the substitution $C_j=(-1)^j\tilde{C}_j$, the usual (II) classically forbidden region turns into the unusual one (III) and vice versa.

2. Formal derivation

Let us show how one can obtain the WKB solution (2.16) without appealing to physical considerations. We know that the matrix element p_j in Eq. (2.1) is a slowly changing function of j. In this section the dot over the function denotes its derivative by the variable j; thus

$$p_{j+1}-p_j \approx \dot{p}=O(n^{-1}) \, ,$$

and similarly for w_j. Each additional differentiation by j would introduce an additional power of n^{-1} into the estimate. Accordingly let us look for a solution of the TTR relation (2.1) that has the form

$$C_j=e^{i[\Phi_0(j)+\Phi_1(j)+\Phi_2(j)+\cdots]} \, ,$$

in which the unknown functions are ranged according to the speed with which they change:

$$\dot{\Phi}_0=O(n^0), \quad \dot{\Phi}_1=O(n^{-1}), \quad \dot{\Phi}_2=O(n^{-2})$$
$$\ddot{\Phi}_0=O(n^{-1}), \quad \ddot{\Phi}_1=O(n^{-2}), \ldots .$$

Dropping terms of order higher than n^{-1}, we can write

$$C_{j\pm 1}=C_j e^{\pm i\dot{\Phi}_0}\left[1+\frac{i}{2}\ddot{\Phi}_0 \pm i\dot{\Phi}_1+O(n^{-2})\right] .$$

Inserting this expression into Eq. (2.1), considering that

$$p_j=p-\tfrac{1}{2}\dot{p}+O(n^{-2}), \quad p_{j+1}=p+\tfrac{1}{2}\dot{p}+O(n^{-2}) \, ,$$

and comparing terms of the same order, we obtain the equations for Φ_0 and Φ_1,

$$2p\cos\dot{\Phi}_0=E'-w \, ,$$
$$2ip\dot{\Phi}_1\sin\dot{\Phi}_0=-\frac{d}{dj}(p\sin\dot{\Phi}_0) \, .$$

Their integration leads to two fundamental solutions:

$$C_j=\frac{A}{[4p^2-(E'-w)^2]^{1/4}} \times\exp\left[\pm i\int \arccos\frac{E'-w}{2p}dj\right]$$

whose real part is just Eq. (2.16).

D. Quantization rules for the recursion relations

1. Matching in the usual and unusual turning points

Suppose that the classically allowed region has at its left border the "usual" forbidden region so that $E'>U^+$ for $j<j_t$ and $E'<U^+$ for $j>j_t$. Here j_t is the root of the equation $E'=U^+(j)$ (not necessarily integer). Let us look for the solution that vanishes in the forbidden region. Then the matching condition has the customary form

$$\begin{aligned} C_j&=\frac{A}{2\sqrt{|v|}}\exp\left[-\int_j^{j_t}\operatorname{arccosh}B\,dj\right] , \quad j<j_t \, , \\ C_j&=\frac{A}{\sqrt{v}}\cos\left[\int_{j_t}^{j}\arccos B\,dj-\frac{\pi}{4}\right] , \quad j>j_t \, . \end{aligned} \tag{2.19}$$

Condition (2.19) can be derived by approximately reducing the TTR relation to a second-order differential equation (Schulten and Gordon, 1975; Sazonov, 1978). An alternative way is to use Eq. (2.11) for the Bessel functions as the reference equation in the vicinity of the turning point (Braun, 1978); this is analogous to Langer's (1937) method of matching the WKB solutions of the Schrödinger equation.

Next consider the turning point at the boundary of the unusual classically forbidden region, supposing that $E'<U^-$ when $j<j_t$ and $E'>U^-$ when $j>j_t$. Now j_t stands for the root of the equation $E'=U^-(j)$ (not necessarily integer). Surprisingly enough, the matching conditions in this case proved to be a stumbling block for many authors. In fact the problem is trivially reduced to the previous case by substituting $C_j=(-1)^j\tilde{C}_j$, applying Eq. (2.19) to $\tilde{C}_j$, and returning to the original sequence. The final result looks startlingly unlike Eq. (2.19):

$$\begin{aligned} C_j&=\frac{A}{2\sqrt{|v|}}(-1)^j\exp\left[-\int_j^{j_t}\operatorname{arccosh}(-B)dj\right] , \quad j<j_t \, , \\ C_j&=\frac{A}{\sqrt{v}}\cos\left[\int_{j_t}^{j}\arccos B\,dj+\pi j_t+\frac{\pi}{4}\right] , \quad j>j_t \end{aligned} \tag{2.20}$$

(Braun, 1978). Note the presence of the additional phase πj_t determined by the position of the turning point, which has important consequences in quantum-mechanical applications; note also the opposite sign of $\pi/4$.

The behavior of the TTR solution in the vicinity of usual and unusual turning points is shown in Fig. 6. Matching conditions similar to Eqs. (2.19) and (2.20) can be written for the case in which the classically forbidden region is situated to the right of the allowed one.

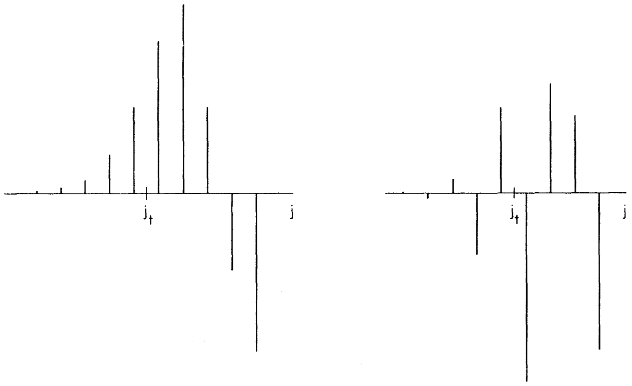

FIG. 6. Typical behavior of the solution C_j of a TTR relation in the vicinity of the turning point; (a) usual and (b) unusual turning points. [Solutions of the TTR relation (2.11) with $E'=\frac{1}{5}$, $a=5$ (case a) or $a=-5$ (case b) in the vicinity of the point $j=5$].

2. Quantization rules

Suppose that the three-term recursion relation under consideration has a classically allowed region bounded on both sides by forbidden regions. Requiring that the solution vanish beyond the allowed region and combining the matching conditions in the two turning points, we obtain a quantization rule for the eigenvalues of Eq. (2.1). Since each of the turning points can be of two types, the quantization rule can have four different forms (Braun, 1978),

$$\int_{j_{t1}}^{j_{t2}}\varphi(j)dj=N\pi+\begin{cases}\frac{\pi}{2}, & \text{both } j_{t1} \text{ and } j_{t2} \text{ on } U^+ ,\\ \frac{\pi}{2}+(j_{t2}-j_{t1})\pi, & j_{t1} \text{ and } j_{t2} \text{ on } U^- ,\\ -j_{t1}\pi, & j_{t1} \text{ on } U^- \text{ and } j_{t2} \text{ on } U^+ ,\\ j_{t2}\pi, & j_{t1} \text{ on } U^+ \text{ and } j_{t2} \text{ on } U^- .\end{cases} \tag{2.21}$$

Here N is an integer; the function φ is determined by Eq. (2.15). Since φ depends on the energy parameter E', the conditions (2.21) determine E' as a function of the quantum number N. Only the first of these formulas resembles the Bohr-Sommerfeld rule.

Equation (2.21) can be simplified by integration by parts in the left-hand side. In the turning points φ is equal either to zero (j_t belongs to U^+) or to π (j_t belongs to U^-). Therefore in all cases the extra-integral terms cancel the terms $\pm j_{t1}\pi$, $\pm j_{t2}\pi$ in the right-hand side. Redefining the quantum number N, we can bring Eq. (2.21) to just two types of conditions

$$\int_{j_{t1}}^{j_{t2}} j\frac{d\varphi}{dj}dj=\begin{cases}(N+\frac{1}{2})\pi, & j_{t1} \text{ and } j_{t2} \text{ on the same potential curve}\\ N\pi, & j_{t1} \text{ and } j_{t2} \text{ on different potential curves .}\end{cases} \tag{2.22}$$

According to Eq. (2.15)

$$\frac{d\varphi}{dj}=-\frac{1}{\sqrt{1-B^2}}\frac{dB}{dj} .$$

Quantization with half integers and integers in Eq. (2.22) is used when the canonical variable φ undergoes oscillation and rotation, respectively. This is formally identical with the rules of coordinate representation. The fundamental difference is that the left-hand side in Eq. (2.22) is not simply the classical action. It also contains the quantum corrections present in the matrix elements w and p entering the function $B(E',j)$.

One can of course obtain the quantization rule for the purely classical action by bringing the quantum corrections to the right-hand side. The result will be to destroy the simple rule "half integers for oscillation, integers for rotation" because the contribution of the quantum corrections is of the same order as $\pi/2$ in the right-hand side.

Instead of Eq. (2.22), a universal quantization rule can be introduced (Braun, 1978),

$$\int_{j_{t1}}^{j_{t2}}(j+\tfrac{1}{2})\frac{d\varphi}{dj}dj=(N+\tfrac{1}{2})\pi . \tag{2.23}$$

The contribution of $\frac{1}{2}$ in the left-hand side, which is equal to $[\varphi(j_{t2})-\varphi(j_{t1})]/2$, is 0 in the case of oscillation and $\pm\pi/2$ in the case of rotation, thereby automatically taking care of the proper quantization condition.

Each time we change the form of the quantization rule we also redefine the quantum number N. Therefore a level found from Eqs. (2.21), (2.22), and (2.23) can receive different quantum numbers. Note also that N is not necessarily positive and that larger N can correspond to smaller eigenvalues. These unconventional properties can be traced to the trigonometrical dependence of the Hamiltonian (2.3) on φ. Another frequent peculiarity is the discontinuity of the integrals in Eqs. (2.21)–(2.23) at some values of E', corresponding to the top of the barrier or quasibarrier (see below). However, this is a common property of most quantization rules used in the theory of Rydberg atom spectra, including Solov'ev's rule [see Cacciani *et al.* (1988a), Hasegawa *et al.* (1989)].

The quantization rules give the energies as the implicit functions of the quantum number N. Explicit expressions can be obtained for the highest and the lowest levels of the TTR relation. The reason for this is that when the energy parameter approaches its highest or lowest possible value, as determined by Eq. (2.8), the span of the classically allowed area in the associated classical mechanical problem shrinks to zero. The movement of the "coordinate" described by Eq. (2.9) then usually becomes a small-amplitude harmonic oscillation. Accordingly the extremal energy levels in the quantum problem will be approximately equidistant, with spacing equal to the classical frequency (Braun, 1983a; Braun and Solov'ev, 1984). This idea can be put on a purely quantum-mechanical footing. The resulting formulas are given in Appendix B.

III. THE ENERGY SPECTRA OF PERTURBED HIGHLY EXCITED ATOMIC HYDROGEN

A. The quadratic Zeeman effect (parabolic representation)

Following Braun (1983a) let us apply the theory of Sec. II to the recursion relation (1.2). It is brought into standard form with unit steps in the index by setting $k=2j$ or $k=2j+1$ if $n-m+1$ is even or odd, respectively. Bearing in mind the relation between k and j, we shall use k as an argument in the following semiclassical expressions. Thus, instead of $p_{j+1/2}$, the necessary off-diagonal matrix element in the intermediate point will be

$$p_{k+1}=\frac{u_\gamma}{5}\left\{\left[\left[1-\frac{m}{n}\right]^2-\frac{k^2}{n^2}\right]\left[\left[1+\frac{m}{n}\right]^2-\frac{k^2}{n^2}\right]\right\}^{1/2}$$

The potential functions of the problem expressed through k are $w_k \pm 2p_{k+1}$. Their plot is qualitatively different for different magnetic quantum numbers.

First consider the case $m=0$, when the potential functions written with the accuracy of the semiclassical approximation are

$$U^+(k)=u_\gamma\left[1-\frac{k^2}{n^2}\right],$$
$$U^-(k)=\frac{u_\gamma}{5}\left[1-\frac{k^2}{n^2}\right]. \tag{3.1}$$

The potential curves [Fig. 7(a)] are then a pair of parabolas crossing at the boundaries $\pm n$ of the discrete argument interval.[3] Studying them leads to the following conclusions.

(a) According to Eq. (2.8) the lowest and the highest points of the plot of the functions $U^\pm$ determine the span of the multiplet. Therefore all E' lie within the interval $(0,u_\gamma)$.

(b) The line of constant E', depending on its value, crosses the plot of $U^\pm$ in either two or four points. This means that there is either a single classically allowed region with its center at $k=0$ (in which case $E'>\max U^-=u_\gamma/5$) or, in the opposite case, two symmetrical classically allowed regions divided by the maximum of the function $U^-(k)$; see Fig. 7(a). In the second case, neglecting tunneling through the dividing forbidden region, there would be two sets of WKB solutions for the recursion relation (1.2), each localized in its respective classically allowed region. The energies corresponding to these solutions would be equal. Therefore the levels are approximately doubly degenerate in the lower part of the multiplet, where $E'<u_\gamma/5$, and nondegenerate if $(u_\gamma/5)<E'<u_\gamma$. This explains the 1/5:4/5 division of the quadratic Zeeman multiplet shown in Fig. 1.

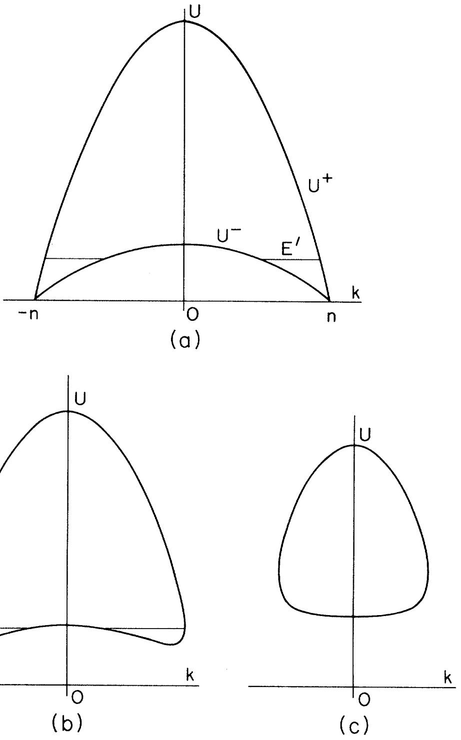

FIG. 7. Potential curves of the TTR relation (1.2) (parabolic representation): (a) $m=0$; (b) $0<|m|<n/\sqrt{5}$; (c) $|m|>n/\sqrt{5}$.

(c) Considering that the independent variable k is equal to the z component of the Runge-Lenz vector, it can be seen that the upper states of the multiplet are characterized by $A_z \approx 0$. The states at the bottom are restricted to $A_z \approx \pm n$.

Suppose that the field is increased until the highest level of the quadratic Zeeman multiplet arising from the nth shell anticrosses the lowest level of the multiplet from the $(n+1)$ shell. In the representation in which one of the independent variables is A_z, the wave functions of these states would not overlap. Consequently the width of the anticrossing is bound to be extremely small.

If m is different from zero but $|m|<n/\sqrt{5}$, the function U^- still has a maximum dividing two symmetrical allowed regions [Fig. 7(b)]. The same arguments show that at the energy correction interval $\min U^- < E' < \max U^-$ the spectrum consists of doublets, while at the interval $\max U^- < E' < \max U^+$ the levels are singlets. Here

$$\min U^-=u_\gamma\left[\frac{2}{\sqrt{5}}\frac{|m|}{n}-\frac{4}{5}\frac{m^2}{n^2}\right],$$
$$\max U^-=\frac{u_\gamma}{5}\left[1+\frac{m^2}{n^2}\right]=U^-(0), \tag{3.2}$$
$$\max U^+=u_\gamma\left[1-\frac{3}{5}\frac{m^2}{n^2}\right]=U^+(0).$$

---

[3] The problem of the quadratic Zeeman effect in atomic hydrogen when $m=0$ is closely related to the problem of a rigid asymmetrical top with the rotational constants 1, 5, and 0 (Braun, 1983a). In particular, the classical equation of motion (2.9) corresponding to the TTR relation (1.2) coincides with the equation for the projection of the angular momentum of the top on the axis with a zero rotational constant [Eq. (37.7) in Landau and Lifshitz (1988)]. This analogy has recently been rediscovered by Rau and Zhang (1990) and Uzer (1990). See also Appendix C on the discrete WKB treatment of rotational spectra.

The height of the potential barrier determining the span of the doublet part of the multiplet diminishes with the growth of $|m|$. If $|m|>n/\sqrt{5}$ the function $U^-(k)$ has a minimum rather than a maximum at the point $k=0$; see Fig. 7(c). Therefore all levels are then singlets and lie within the interval $U^-(0)<E'<U^+(0)$.

Thus, the peculiar properties of quadratic Zeeman splitting become obvious after a glance at the plot of the potential functions. This is rather amazing considering that to obtain $U^{\pm}$ one needs only the expressions (1.3) for the diagonal and the off-diagonal elements of the perturbation.

The connection between Solov'ev's integral Λ and the energy correction value following from Eqs. (1.6) and (1.8) can be written in the form

$$E'\approx U^-(0)+u_\gamma \Lambda/5n^2 \ . \tag{3.3}$$

Therefore the two types of classical trajectories, differing by the sign of Λ, which exist if $|m|<n/\sqrt{5}$ correspond to the levels above and below the potential barrier [Figs. 7(a) and 7(b)].

The quantization formulas (2.21)–(2.23) applied to the TTR relation (1.2) lead to exactly the same result as Solov'ev's (1981,1982) quantization rule. The equivalence of these approaches and the treatment using separation of variables on Fock's sphere is considered by Watanabe (1989).

A useful result of the semiclassical treatment is the expression for the spacings $\Delta E'$ in the quadratic Zeeman multiplet. It follows from Eq. (2.10) for the classical period $T(E')$ since $\Delta E'=2\pi/T$. An expression for the classical period containing the elliptic integrals is given in Braun (1983a,1990a) and Kazantsev and Pokrovsky (1983b,1983c).

The levels in the multiplet are strongly nonequidistant. This may readily be seen in the plot of $\Delta E'$ versus the diamagnetic shift E' (Fig. 8) scaled in such a way as to be independent of n and the field. If $|m|<n/\sqrt{5}$ there is a singularity in this plot reflecting the fact that the period turns logarithmically into infinity when E' approaches the barrier top. The function $\Delta E'(E')$ will be important in our treatment of the oscillator strength distributions (Sec. IV).

If tunneling is considered between the two classically allowed regions, the doubly degenerate levels in the lower part of the multiplet will split, forming g-u doublets. The value of the splitting was obtained by Braun (1983a),

$$E'_g-E'_u=(-1)^n e^{-W}/T \ . \tag{3.4}$$

Here

$$W=\int_{k'_t}^{k''_t} \operatorname{arccosh}\frac{w-E'}{2p}dk \tag{3.5}$$

is the classical action corresponding to tunneling through the forbidden region with the boundaries k'_t and k''_t; T is the classical period (2.10) of oscillation in one of the allowed regions. The important distinction between this equation and the well-known formula for splitting in the coordinate representation is that the lower level in each doublet is not always described by the even combination of the localized solutions of the TTR relation. [The combination is even only if k in Eq. (1.2) takes on even values, so that the symmetry point $k=0$ is among the points of the grid.]

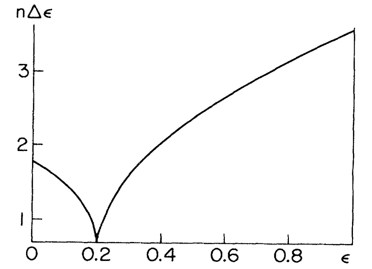

FIG. 8. The change of spacings $\Delta E'$ between adjacent levels along the quadratic Zeeman multiplet. The plot of $n\Delta\varepsilon=n\Delta E'/u_\gamma$ against the scaled diamagnetic shift $\varepsilon=E'/u_\gamma$.

An alternative expression to Eq. (3.4), valid for the splitting of the lowest doublets in the multiplet, was obtained by Grozdanov and Solov'ev (1984). Splitting in the opposite extreme (E' approaching the barrier top) is treated below (Sec. III.C).

B. The quadratic Zeeman effect (spherical representation)

It is instructive to consider the second-order Zeeman splitting in atomic hydrogen using a spherical basis set (Braun, 1983b; Fano *et al.*, 1988). The semiclassical approximations for the matrix elements (1.5), valid when l is not too close to the boundary points $|m|$ and $n-1$, are

$$\begin{aligned} w_l &\approx \frac{u_\gamma}{2}\left[1-\frac{3}{5}\frac{L^2}{n^2}\right]\left[1+\frac{m^2}{L^2}\right]\equiv \bar{w}(L) \ , \\ p_{l+1} &\approx -\frac{u_\gamma}{4}\left[1-\frac{L^2}{n^2}\right]\left[1-\frac{m^2}{L^2}\right]\equiv \bar{p}(L) \ , \end{aligned} \tag{3.6}$$

where $L\equiv l+\frac{1}{2}$.

A plot of the potential functions

$$\begin{aligned} U^-(L) &= \bar{w}-2\bar{p}=u_\gamma\left[1+\frac{m^2}{5n^2}-\frac{4}{5}\frac{L^2}{n^2}\right] \ , \\ U^+(L) &= \bar{w}+2\bar{p}=u_\gamma\left[-\frac{4}{5}\frac{m^2}{n^2}+\frac{L^2}{5n^2}+\frac{m^2}{L^2}\right] \end{aligned} \tag{3.7}$$

is shown in Fig. 9 (since $\bar{p}<0$, the lower potential curve is U^+). This figure helps to explain certain facts about the perturbed atomic states. In particular it can be seen that the lowest levels of the multiplet are associated with an angular momentum L whose value is almost fixed close to $(5)^{1/4}\sqrt{|m|n}$ (the minimum of the function U^+), if $|m|<n/\sqrt{5}$, and to n, in case of larger $|m|$. The upper

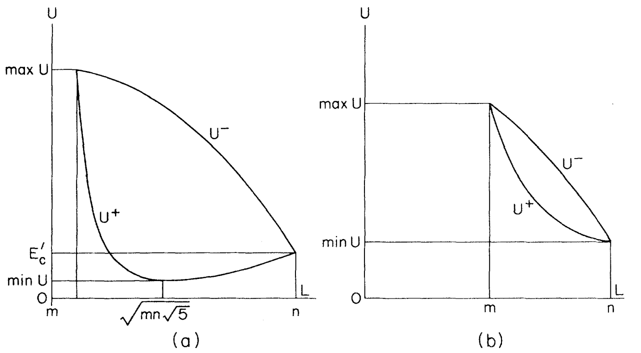

FIG. 9. Potential curves of the TTR relation (1.4) (spherical representation). (a) $0<|m|<n/\sqrt{5}$; (b) $|m|>n/\sqrt{5}$.

levels correspond to $L\approx|m|$.

If $|m|<n/\sqrt{5}$ and E' is close to the common value of the potential functions at the right point of their crossing

$$U^{\pm}(n)=\frac{u_\gamma}{5}\left[1+\frac{m^2}{n^2}\right]\equiv E_c' ,$$

the angular momentum of the classical electron periodically approaches n. The quantity E_c' is equal to $\max U^-$ of the parabolic representation given in Eq. (3.2). What may be puzzling is that there is nothing reminiscent of a symmetrical double-well potential, so we must look for an alternative explanation for the presence of doublets in the lower part of the multiplet.

The explanation follows from the property of the recursion relations that they change their eigenvalues when their independent variables are shifted. Consider the recursion relation

$$p(j+\Delta)C_{j-1}+[w(j+\Delta)-E']C_j+p(j+\Delta+1)C_{j+1}=0\ , \qquad (3.8)$$

where $p(x)$ and $w(x)$ are analytical functions and the shift Δ $(0<\Delta<1)$ is a parameter. The eigenvalues E' depend on Δ, and this dependence can take two very different forms. It can be evaluated by applying the quantization rule (2.22) to the TTR equation (3.8). The shift affects only the left-hand side in Eq. (2.22):

$$\int_{j_{t1}(\Delta)}^{j_{t2}(\Delta)} j\frac{d\varphi(j+\Delta)}{dj}dj=\int_{j_{t1}(0)}^{j_{t2}(0)} j\frac{d\varphi(j)}{dj}dj+\begin{cases}0, & \text{both } j_{t1} \text{ and } j_{t2} \text{ on the same potential curve,}\\ \Delta\pi, & j_{t1} \text{ on } U^- \text{ and } j_{t2} \text{ on } U^+\ ,\\ -\Delta\pi, & j_{t1} \text{ on } U^+ \text{ and } j_{t2} \text{ on } U^-\ .\end{cases} \qquad (3.9)$$

These results follow from φ being equal either to zero or to π in the turning points belonging to U^+ and U^-, respectively. Consequently, (a) if both of the turning points belong to the same potential curve, the eigenvalues of Eq. (3.8) are unchanged by the shift [in fact they do change, but this change is exponentially small; see Fig. 10(a)]; (b) if one of the turning points belongs to U^+ and the other one to U^-, the shift of the argument of the three-term recursion relation is equivalent to replacement of the quantum number N by $N+\Delta$ or $N-\Delta$. As a result, the eigenvalues are shifted by the spacing between two adjacent levels multiplied by Δ [Fig. 10(b)]. Note that case (a) is observed when the evolution of the classical angle φ conjugate to j is an oscillation, while case b is observed when the evolution of φ is a rotation.

The recursion relation in the spherical basis set (1.4) is brought into standard from with steps of unity by putting $l=2j$ or $l=2j+1$, depending on parity. The resulting TTR relations for the even and odd states differ by the shift $\Delta=\frac{1}{2}$. Consequently, if the turning points limiting the classically allowed region belong to the same potential curve, we shall observe approximate g-u degeneracy. As can be seen in Fig. 9(a), this is the case when the energy correction value is between

$$\min U^+=u_\gamma\left[\frac{2}{\sqrt{5}}\frac{|m|}{n}-\frac{4}{5}\frac{m^2}{n^2}\right]$$

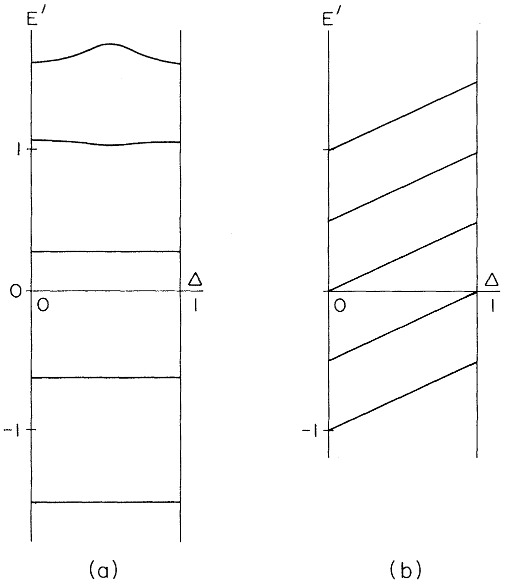

FIG. 10. Two types of dependence of the eigenvalues of a three-term recursion relation on the shift of the independent variable. (a) the TTR relation (3.8), with $p(x)=1$, $w(x)=x^2/4$ (five lowest eigenvalues are shown); (b) the TTR relation (3.8), with $p(x)=1$, $w(x)=x/2$.

and E_c'. In all other situations the even and odd levels are locally equidistant.

Thus the same peculiar structure of the quadratic Zeeman multiplet reemerges in the spherical representation. The quantization rules of the discrete WKB method applied to Eq. (1.4) lead to exactly the same eigenvalues as Solov'ev's (1981,1982) method and our treatment in the parabolic representation.

We shall reformulate the rules of Sec. II.D in order to obtain the quantization conditions for the purely classical action because this point has caused some controversy (Richards, 1983; Rath and Richards, 1988). As follows from Eq. (3.6), a semiclassical approximation for the matrix elements w_l and p_{l+1} that is correct up to second order in n^{-1} can be obtained from their purely classical limit expressions by the substitution $L=l+\frac{1}{2}$. This means that the semiclassical Hamiltonian in which L is taken as a canonical variable and $\theta=\varphi/2$ as the conjugate "momentum,"

$$H'(L,\theta)=\overline{w}(L)+2\overline{p}(L)\cos 2\theta \ ,$$

is identical with the classical Hamiltonian function describing perturbation of the Kepler movement in spherical coordinates. The variable θ is the angle between the major axis of the Kepler orbit and the line of nodes, minus $\pi/2$ (Delos *et al.*, 1983a,1983b; Richards, 1983).

Consider now the quantization rule (2.22). The connection between L and the standard integer variable j, with the step unity, is

$$\begin{aligned} j&=L/2-\tfrac{1}{4}, \quad \text{even states} \ ,\\ j&=L/2-\tfrac{3}{4}, \quad \text{odd states} \ . \end{aligned} \tag{3.10}$$

Substituting Eq. (3.10) and the relation $d\varphi=2\,d\theta$ into Eq. (2.22), we obtain quantization rules for the purely classical action in the variables L,θ. In the case of vibration (both of the turning points are on U^+), on the basis that $\theta(L_{t1})=\theta(L_{t2})=0$, we have

$$\int_{L_{t1}}^{L_{t2}} L\frac{d\theta}{dL}dL=\pi(N+\tfrac{1}{2}) \ . \tag{3.11}$$

In the case of rotation when $\theta(L_{t1})=0$, $\theta(L_{t2})=\pi/2$ we have

$$\int_{L_{t1}}^{L_{t2}} L\frac{d\theta}{dL}dL=\begin{cases}\pi(N+\frac{3}{4}), & \text{even states} \ ,\\ \pi(N+\frac{1}{4}), & \text{odd states} \ .\end{cases} \tag{3.12}$$

Let us rewrite these formulas extending the integral over the whole period of the field-induced evolution of the Kepler orbit. In the case of oscillation the integral in Eq. (3.11) is taken over half a period; consequently we can write

$$\oint L\,d\theta=2\pi(N+\tfrac{1}{2}) \ . \tag{3.13}$$

In the case of rotation the integral in Eq. (3.12) is taken over one-fourth of a period (corresponding to the change of θ by 2π). Extending integration over the whole period and combining the rules for the even and odd states so that the new quantum number is $N'=2N$ or $2N+1$, depending on parity, we again obtain Eq. (3.13).

The need to use half integers in the quantization condition (3.13), even in the case of rotation, is not self-evident. In the framework of the discrete WKB method it follows automatically from the general quantization rule and Eq. (3.10) connecting L with the integer variable j. The usual approach, based on the study of the caustics of the projection of the multidimensional phase trajectory onto the plane of L and θ (Maslov and Fedoryuk, 1976; Hasegawa *et al.*, 1989) leads to the same result but at a much greater effort.[4]

C. The treatment of singularities and quantization in the vicinity of the separatrix

Most recursion relations associated with physical problems have singularities close to which the WKB approximation becomes invalid. As regards the TTR equation (1.4) these are the boundary points $l=n-1$ and $l=|m|$. The way out is to find a solution in the vicinity of a singular point by some alternative method and then to match it with the WKB solution. However, such procedures are essential only if the singularity is not located deep in the classically forbidden region where the physical solution is vanishingly small.

1. The singularity at $l=n-1$

This singularity is important when the energy correction is close to E_c'. It reflects the presence of the separatrix dividing the classical trajectories, with $\Lambda<0$ and $\Lambda>0$. When $E'\to E_c'$ the period of oscillations of the angular momentum described by the classical equations (2.9) and (2.10) corresponding to the TTR equation (1.4) grows to infinity as $\ln|E'-E_c'|$.[5] This reminds us of the movement near the top of a potential barrier without, however, there being two separated classically allowed regions of the variable L. A similar peculiarity is found in many other problems expressed by TTR relations whose potential curves cross in such a way that the derivatives $(U^+)'$ and $(U^-)'$ have opposite signs at the crossing point. The term "quasibarrier" was suggested by Braun and Solov'ev (1984) to describe this situation.

---

[4] To quote Delos *et al.* (1983a), "The half-integer quantization condition is derived from a long argument that we cannot reproduce here." This argument is presented in Delos *et al.* (1983b).

[5] The logarithmic divergence of the classical period at $E'=E_c'$ is connected with the fact that both of the factors under the radical in the integrand of Eq. (2.10) go to zero at the upper integration limit.

To find a solution of the TTR equation (1.4) close to $l=n-1$, we introduce the following approximation for its coefficients ($n-l \ll n$):

$$w_l \approx u_\gamma \left[\frac{1}{5}\left[1+\frac{m^2}{n^2}\right] + \frac{n-l-1/2}{n}\left[\frac{m^2}{n^2}+\frac{3}{5}\right]\right] , \tag{3.14}$$

$$p_l \approx -\frac{u_\gamma}{2n}\left[1-\frac{m^2}{n^2}\right]\sqrt{(n-l)(n-l+1)} .$$

After that we obtain an exactly soluble TTR relation. Its solution C_l is given by the integral of overlap between the set of harmonic-oscillator eigenfunctions with the index $v=n-l-1$ and the parabolic cylinder function (Braun, 1983b). Matching it with the discrete WKB solution leads to a modified quantization rule. The result for the case $|m| \ll n$ will be discussed later, after the second singularity is considered.

2. The singularity at $l=|m|$

(The treatment in this section will be essential for the subsequent consideration of oscillator strength distributions in quadratic Zeeman multiplets and the spectra of the alkali-metal atoms.)

If $|m|$ is comparable to n there is no need to take special care of this singularity. Only the uppermost states of the quadratic Zeeman multiplet can feel it (see Fig. 9), and even for these levels the general WKB quantization rules give correct results.[6]

A much more important case, practically speaking, is $|m| \ll n$, where the terms in the semiclassical Hamiltonian that contain m are of the order n^{-2} and can be dropped. This is equivalent to complete neglect of the centrifugal terms in the equations of classical dynamics. In fact, if $|m| \ll n$ this can be done for all angular momenta large enough to justify the classical trajectory approach. After that we obtain

$$H'(L,\theta)=u_\gamma\left[\frac{1}{2}\left[1-\frac{3}{5}\frac{L^2}{n^2}\right]-\frac{1}{2}\left[1-\frac{L^2}{n^2}\right]\cos 2\theta\right] . \tag{3.15}$$

Note that in the case $|m| \ll n$ the "momentum" θ is simply the polar angle of the Runge-Lenz vector. The corresponding potential curves are two parabolas (Fig. 11),

$$U^+(L)=\frac{u_\gamma}{5}\frac{L^2}{n^2},\quad U^-(L)=u_\gamma\left[1-\frac{4}{5}\frac{L^2}{n^2}\right] . \tag{3.16}$$

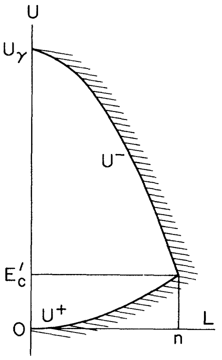

FIG. 11. Potential curves of the three-term recursion relation (1.4) (spherical representation), when $m=0$. Hatching marks the boundaries of the classically allowed region.

In this approximation the left turning point of L is zero, which corresponds to the Kepler orbit's periodically degenerating into a line; its angle with the magnetic field is then

$$\vartheta_0=\theta(L)|_{L=0}=\arccos\sqrt{1-\varepsilon} . \tag{3.17}$$

Here $\varepsilon=E'/u_\gamma$ is the energy correction measured in diamagnetic units. Equation (3.17) follows from the energy conservation law

$$H'(L,\theta)=E' , \tag{3.18}$$

with H' determined by Eq. (3.15).

The WKB solution of Eq. (1.4) can be written as

$$C_l=\frac{A^{\mathrm{WKB}}}{\sqrt{v(L)}}\cos\left[\int_0^L \theta(L)dL+\chi^{\mathrm{WKB}}\right]\Bigg|_{L=l+1/2} \tag{3.19}$$

where the "speed" $v=dL/dt$ and θ are determined with respect to the m-independent Hamiltonian (3.15); χ^{WKB} is the arbitrary phase. This solution is applicable if $l^2-m^2 \gg 1$.

For smaller l we need an alternative solution. It can be obtained by considering that when $l^2 \ll n^2$ the radial parts of both the diagonal (w_l^r) and the off-diagonal (p_l^r) matrix elements (1.5) can be approximated by the same constant u_γ. We obtain a recursion relation whose exact solution is

$$C_l=A\mathcal{P}_{lm}(\cos\vartheta_0) . \tag{3.20}$$

Here $\mathcal{P}_{lm}$ is the normalized Legendre function [the spherical function without the factor $\exp(im\varphi)/\sqrt{2\pi}$]. The angle ϑ_0 is the same as in Eq. (3.17).

If n is large, the domains where the WKB and Legendre solutions are valid overlap ($l^2-m^2 \gg 1$ and $l^2 \ll n^2$, respectively). The Legendre function can be replaced here by its asymptotical form

$$\mathcal{P}_{lm}(\cos\vartheta_0)\approx\left[\frac{2}{\pi\sin\vartheta_0}\right]^{1/2} \times\cos\left[\left[l+\frac{1}{2}\right]\vartheta_0-\frac{\pi}{4}+\frac{|m|\pi}{2}\right] . \tag{3.21}$$

---

[6] The matrix elements of the recursion relation entering the quantization rule should be taken in their semiclassical form (3.6), although the approximate equality in Eq. (3.6) is invalid for $l \approx m$. Compare with the quantization of the radial movement in the spherical potentials, where the replacement of $\sqrt{l(l+1)}$ by $l+\frac{1}{2}$ is used although this is not a valid approximation for l comparable with unity.

Comparison with Eq. (3.19) shows that the phase χ^{WKB} should be

$$\chi^{\mathrm{WKB}} = -\frac{\pi}{4} + \frac{|m|\pi}{2} \ . \tag{3.22}$$

This means that if $m=0$ the left singularity is formally equivalent to a usual turning point at $L=0$. For $m \neq 0$ there is an additional phase $|m|\pi/2$; this is the only term in the WKB solution (3.19) depending on m. Interestingly, the m-dependent phase is precisely the centrifugal phase induced in one-dimensional parabolic wave functions in the analogous electric-field problem.

Since the change of the phase χ^{WKB} by π is of no importance, levels with different m of the same parity are approximately degenerate provided $|m| \ll n$. This is a direct consequence of the fact that the solution C_l of the perturbation-theory equations in the domain $l \ll n$ is given by the Legendre functions. The same is true of a wide class of perturbations (Braun, 1991a); hence this degeneracy is a widespread phenomenon.

3. The quantization rule

Combining matching conditions that take into account both of the singularities, we obtain a quantization rule that preserves its validity even in the transition zone close to the critical-energy correction E_c' (Braun, 1983b). This energy range is of considerable interest, partly because it is here that the first signs of chaotic movement appear when the field is increased (Delande and Gay, 1987). After minor transformations this quantization rule can be brought into the form of an equation for the scaled diamagnetic energies

$$\begin{gathered} \varepsilon = E'/u_\gamma : \\ nz(\varepsilon) = \pi \left[N + \frac{|m|+1}{2} \right] \pm \gamma(n,\varepsilon) \ . \end{gathered} \tag{3.23}$$

Here ($\vartheta_0 \equiv \arccos\sqrt{1-\varepsilon}$),

$$\begin{gathered} z(\varepsilon) = \vartheta_0 + (\varepsilon - \tfrac{1}{5}) \int_0^{x_t} \frac{x\,dx}{(1+x)[(\varepsilon - x^2/5)(1-4x^2/5-\varepsilon)]^{1/2}} \\ \gamma(n,\varepsilon) = \frac{(-1)^n}{2} \arctan\exp\left[\frac{5}{4} n\pi \left[\varepsilon - \frac{1}{5} \right] \right] \ . \end{gathered} \tag{3.24}$$

The upper and lower signs in Eq. (3.23) refer to even and odd levels, respectively; $N = 0, 1, 2 \ldots$ is a quantum number. The complete elliptical integral $z(\varepsilon)$, whose upper limit is the smaller positive root of the expression under the radical, is connected with the action integral in Eqs. (3.11) and (3.12) by the relations ($L_t = nx_t$)

$$nz(\varepsilon) = \begin{cases} -\int_0^{L_t} L \dfrac{d\theta}{dL} dL, & \varepsilon < \frac{1}{5} \\ \dfrac{n\pi}{2} - \int_0^{L_t} L \dfrac{d\theta}{dL} dL, & \varepsilon > \frac{1}{5} \ . \end{cases} \tag{3.25}$$

Unlike the action integral, $z(\varepsilon)$ is a continuous function, monotonically growing from 0 to $\pi/2$ when ε changes from 0 to 1. A continuous function analogous to $z(\varepsilon)$ was introduced by Cacciani *et al.* (1988a); see also Hasegawa *et al.* (1989).

The angle $\gamma(n,\varepsilon)$ providing the smooth transition between the two parts of the quadratic Zeeman multiplet is close to 0 and $\pm\pi/4$ for levels lower and higher than the critical energy. If $n \gg 1$ this transition takes place in an almost steplike manner. Putting γ equal to 0 for $\varepsilon < \varepsilon_c = \frac{1}{5}$ and to $\pm\pi/4$ for $\varepsilon > \varepsilon_c$ we would return to Solov'ev's quantization rule. In particular, levels of opposite parity with $\varepsilon < \varepsilon_c$ would be doubly degenerate. The nonzero value of $\gamma(n,\varepsilon)$ leads to *g-u* splitting, whose size, according to Eq. (3.23), is

$$E_g' - E_u' = \frac{2\gamma(n,\varepsilon)}{\pi} \Delta E' \ . \tag{3.26}$$

Here $\Delta E'$ is the spacing between two adjacent levels of the same parity. For levels not too far below E_c' the splitting thus obtained is the same as that given by Eq. (3.4). For lower levels the approximation used in the derivation of the matching condition at $l = n-1$ becomes inaccurate and Eq. (3.4) is therefore preferable.

Let us now consider levels above the critical energy. If the limit values $\pm\pi/4$ are introduced instead of γ, the quantization rules (3.23) for even and odd levels can be combined into a single rule (a new quantum number equal to $2N$ and $2N+1$ for even and odd levels, respectively, has to be introduced). The resulting WKB eigenvalues would form a sequence of levels with alternating parity and smoothly changing spacings. The deviation of γ from $\pm\pi/4$ introduces irregularities into the behavior of the spacings. However, these irregularities can be observed only for the few levels closest to E_c'; see Fig. 12, where the spacings between the lowest three levels obviously do not fit the general pattern.

This effect is similar to the overbarrier reflection in problems with a double-well potential. As a matter of fact, rule (3.23) could also be obtained in the parabolic representation, where there does exist a double-well potential (Fig. 7). This is done by approximating Eq. (1.2) in the vicinity of the maximum of U^- by the differential equation for the functions of the parabolic cylinder and matching the result to the WKB solution.

As stated earlier, the WKB energy levels with different m of the same parity following from Eq. (3.23) are degenerate. This can readily be seen in Fig. 13, where the

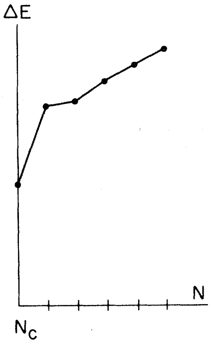

FIG. 12. Effects of reflection over the barrier in the quadratic Zeeman multiplet ($n=40, m=1$). Spacings $\Delta E'$ between the consecutive levels with energy higher than E_c' are shown. Note irregular change of $\Delta E'$ between the first three levels lying immediately over the top of the quasibarrier.

quadratic Zeeman levels of atomic hydrogen with $n=40$ and $m=0-3$ are depicted (compare the energies of these levels with $m=0$ and $m=2$). This approximate degeneracy holds throughout the multiplet, including the transition zone around E_c' where primitive WKB rules disregarding the barrier effects are inapplicable.

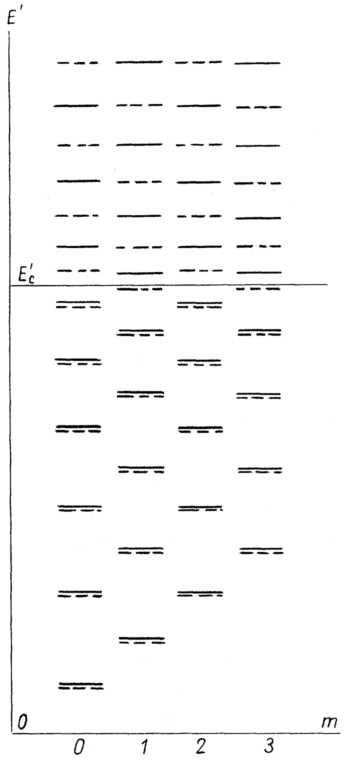

FIG. 13. The lower part of the quadratic Zeeman multiplet with $n=40$ and $m=0-3$. Below the barrier E_c': *g-u* degeneracy of levels with the same m; a much less exact degeneracy of levels with m differing by 2, which continues into the transition zone around E_c'. Above the barrier: no *g-u* degeneracy of levels with the same m; approximate degeneracy of levels with opposite parity and m differing by 1.

In the upper part of the multiplet the energies are observed to be totally independent of m, in line with the term "rotational levels" introduced by Herrick (1982). This can be explained by the fact that changing m by 1 and passing simultaneously to the states of opposite parity also leaves the quantization condition (3.23) intact, in the approximation $\gamma=\pm\pi/4$.

It should be noted that the m independence of the energies exists only for levels with $|m| \ll n$. It is far less rigorous than the *g-u* degeneracy of levels with the same m in the lower part of the multiplet [the respective splittings are proportional to m^2/n^2 and $\exp(-\text{const}\, n)$].

D. The hydrogen atom in parallel electric and magnetic fields

The combined effects of parallel electric and magnetic fields on the highly excited hydrogen atom were investigated by Braun (1983a) and Braun and Solov'ev (1984), using the discrete WKB method in the parabolic representation. The method earlier suggested by Sumetsky (1982) is applicable only for states localized in the direction of the fields; its advantage is that it remains valid in the n-mixing fields. Kazantsev and Pokrovsky (1983b) considered the limit of relatively weak electric fields. Cacciani *et al.* (1988b) used a semiclassical method analogous to Solov'ev's (1981,1982) approach to the quadratic Zeeman effect. A discrete WKB treatment in the spherical representation was carried out by Waterland *et al.* (1987) and Braun (1989b). Localization of the upper states of the Stark-Zeeman multiplet was discussed by Bivona *et al.* (1988). Extensive n-mixing calculations were carried out by Richter *et al.* (1987) and Zeller *et al.* (1989). Experimental results were reported for the hydrogenlike spectra of highly excited atomic lithium by Cacciani *et al.* (1988b,1988c).

Investigation of the combined Stark-Zeeman effect in parallel l-mixing fields is a simple extension of our treatment of the quadratic Zeeman effect in the parabolic representation (Sec. III.A). The additional perturbation operator $V_F=Fz$ is diagonal in the basis set of parabolic orbitals belonging to a single shell of the hydrogen atom. Consequently the set of equations for the coefficients of the zero-order eigenfunction will still be a TTR relation, differing from Eq. (1.2) only by the additional term $\frac{3}{2}Fnk$ in its diagonal coefficient w_k. The same additional term linear in k appears in the expressions for the potential functions of the TTR relation, and it is easy to establish the corresponding changes in their plots compared with Fig. 7.

In particular, consider the case $m=0$. The potential functions can be written as

$$\begin{aligned} U^+(k) &= u_\gamma \left[1-\frac{k^2}{n^2}+2\beta\frac{k}{n}\right], \\ U^-(k) &= u_\gamma \left[\frac{1}{5}\left[1-\frac{k^2}{n^2}\right]+2\beta\frac{k}{n}\right]. \end{aligned} \tag{3.27}$$

Here β stands for the parameter characterizing the relative value of the linear Stark and the quadratic Zeeman splitting

$$\beta=\frac{12F}{5n^2}\left[\frac{c}{H}\right]^2 . \tag{3.28}$$

The two potential curves are parabolas, even if $F\neq 0$, but their symmetry is lost. The plot of $U^{\pm}(k)$ is qualitatively different in the cases $\beta<\frac{1}{5}$, $\frac{1}{5}<\beta<1$, and $\beta>1$ (Fig. 14) and so is the spectrum of the problem (Braun, 1983a).

If $\beta<\frac{1}{5}$, then, inside the interval $(-n,n)$ of the allowed values of k, the lower potential function has a maximum dividing two classically allowed regions [Fig. 14(a)]. A similar problem in the coordinate representation would be the movement in the field of two nonequivalent potential wells. There are three different groups of states. The states with the energy correction lower than the top of the barrier [the maximum of U^-] can be localized either in the deeper potential well or in the shallower one. These are the states of groups I and II, respectively, according to classification introduced by Braun and Solov'ev (1984). The rest of the states have energies higher than the barrier top (group III).

The states of groups I and II are formed from the *g-u* doublets of the quadratic Zeeman multiplet. Even a very weak electric field is sufficient to overcome the exponentially small splittings between components of the doublets. As a result, a pair of states is formed from each doublet exhibiting a linear Stark shift of opposite sign (Kazantsev and Pokrovsky, 1983b); the states whose energy goes down and up belong to groups I and II, respectively. The classically allowed values of $k=A_z$ for these states are close to $-n$ (group I) and n (group II). This means that the classical image of these states is an almost linear Kepler orbit oscillating in the vicinity of the field's axis antiparallel or parallel to the electric field.

Changes in the opposite directions lead to numerous anticrossings between energy levels of the groups I and II. The condition of anticrossing was established by Braun and Solov'ev (1984) by comparing the values of the integral in the quantization rule of the discrete WKB method, taken over the left and right classically allowed regions of k. The result is remarkably simple:

$$\beta=\beta_N=\frac{N}{\sqrt{5}n}, N=1,2,3\ldots . \tag{3.29}$$

This means that if F is increased while H is kept constant, anticrossings occur repeatedly at equal intervals of F. A striking peculiarity of this phenomenon is that a whole series of anticrossings takes place simultaneously (all levels of group II go into anticrossings when β approaches β_N). See Fig. 15, in which the anticrossings are arranged in vertical equidistant columns.

The width of the anticrossings is determined by the tunneling through the classically forbidden region dividing the potential wells; it is exponentially small if $n\gg 1$. Consequently, if $\beta<\frac{1}{5}$, the spectrum of the Stark-Zeeman problem contains a part [the energy-correction interval $U^{\pm}(n)<E'<\max U^-$] in which all levels are grouped into extremely narrow doublets. This is obviously reminiscent of the pure quadratic Zeeman-effect spectrum. As a matter of fact, it was proved by Cacciani *et al.* (1988b) and Delande and Gay (1991) that when $\beta=\beta_N$ and $m=0$ the spectrum of the Stark-Zeeman problem in parallel fields (with the exception of the lower levels of group I, which do not take part in the anticrossings) is the same as in the pure quadratic Zeeman effect ($\beta=0$), but with $m=N$.

The levels of group III are formed from the upper levels of the quadratic Zeeman multiplet, which are far less sensitive to the electric field (if F is relatively weak, their Stark effect is quadratic). The value of the average A_z for these levels is determined by the position of the maximum of the function $U^+(k)$ and is close to zero when F is small. The classical image of the upper states of group III is an almost linear orbit, whose angle with the electric field is arccos β (Bivona *et al.*, 1988; Cacciani *et al.*, 1988b). A simple way to prove this is to analyze the potential curves of the five-term recursion relation for

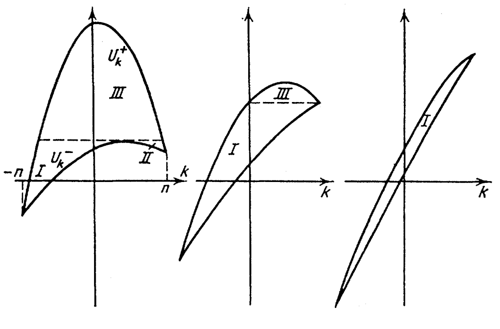

(a) (b) (c)

FIG. 14. Hydrogen atom in parallel electric and magnetic fields. Potential curves of the TTR equation in the parabolic representation. (a) $0<\beta<\frac{1}{5}$; (b) $\frac{1}{5}<\beta<1$; (c) $\beta>1$. From Braun and Solov'ev (1984).

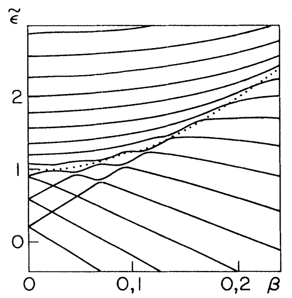

FIG. 15. Stark-Zeeman levels in parallel fields as functions of β (magnetic field fixed). $n=20$, $m=0$ ($\tilde{\varepsilon}\equiv 5E'/u_\gamma$). The fifteen lowest eigenvalues are shown. The dots indicate the position of the top of the barrier, which becomes a quasibarrier when $\beta>0.2$. From Braun and Solov'ev (1984).

coefficients of the zero-order eigenfunction in the spherical representation (Braun, 1989b,1991a).

With an increase of β, the number of states in group I increases, while that of groups II and III decreases. The relevant numbers are given in papers by Braun and Solov'ev (1984) and Cacciani *et al.* (1988b). When β exceeds $\frac{1}{5}$, the potential barrier and the right potential well disappear, and with them go the levels of group II and the anticrossings in the spectrum.

When $\frac{1}{5}<\beta<1$, instead of a potential barrier there exists a quasibarrier singularity with its abscissa at $k=n$ and its ordinate $E_c'=U^{\pm}(n)$; see Fig. 14(b). As explained above, the classical period (2.10) tends to infinity when E' tends to E_c' ["the quasibarrier top," to use the name introduced by Braun and Solov'ev (1984), although this is not a very appropriate term]. Therefore the presence of the quasibarrier means the existence of a separatrix dividing two types of classical trajectories. In the quantum problem these two trajectories correspond to the two groups of states (I and III) that remain when $\frac{1}{5}<\beta<1$.

The presence of the quasibarrier leads to a characteristic series of inflection points in the plot of the energies against β (Fig. 15). Diverse effects connected with the presence of the quasibarrier are discussed by Cacciani *et al.* (1988c) in connection with experimental observations on atomic lithium.

Finally, if $\beta>1$, the maximum of U^+ moves away from the allowed interval $-n<k<n$ [Fig. 14(c)]. The quasibarrier and group III states disappear. The spectrum becomes more primitive; it consists of the only group (I) of states, and with the growth of F it tends to linear Stark splitting.

When $m\neq 0$, the transformation of the quadratic Zeeman multiplet caused by the parallel electric field can be analyzed in a similar way. Spectacular changes in the spectrum, such as linear Stark splitting and anticrossings, can be observed if there are *g-u* doublets in the absence of the electric field, i.e., if $|m|<n/\sqrt{5}$.

E. The quadratic Stark-Zeeman effect in orthogonal fields

The first-order splitting of the hydrogen atom levels in crossed electric and magnetic fields is a famous quantum-mechanical problem solved by Epstein (1926) and Pauli (1926). However, if **F** and **H** are mutually orthogonal, there remains a residual degeneracy of atomic levels. Our topic here will be the lifting of this degeneracy under the influence of second-order effects. The problem was theoretically studied by Solov'ev (1983), Braun and Solov'ev (1984), and Belov *et al.* (1985). Later, second-order splitting was experimentally measured by the Bielefeld group (Wiebusch *et al.*, 1989); the results agreed well with the theoretical predictions.

1. The recursion relation describing second-order splitting

We begin by recapitulating the theory of Epstein and Pauli. The first-order operator describing the interaction of the hydrogen atom with the external fields is

$$V_1=\frac{\mathbf{H}\cdot\mathbf{L}}{2c}+\mathbf{F}\cdot\mathbf{r}\ . \tag{3.30}$$

Within the nth shell of atomic hydrogen the Pauli relation holds:

$$\mathbf{r}=\tfrac{3}{2}n\,\mathbf{A}\ .$$

The operators

$$\mathbf{J}_1=\frac{\mathbf{L}+\mathbf{A}}{2},\quad \mathbf{J}_2=\frac{\mathbf{L}-\mathbf{A}}{2} \tag{3.31}$$

possess the properties of the angular momentum operators of two independent pseudoparticles; their squares are constants,

$$\mathbf{J}_1^2=\mathbf{J}_2^2=j(j+1),\quad j\equiv(n-1)/2\ .$$

Written in terms of these operators, the perturbation V_1 is

$$V_1=\omega_1 J_{1,1}+\omega_2 J_{2,2}\ . \tag{3.32}$$

Here ω_1 and ω_2 are the absolute values of the vectors

$$\boldsymbol{\omega}_1=\frac{\mathbf{H}}{2c}+\frac{3}{2}n\mathbf{F},\quad \boldsymbol{\omega}_2=\frac{\mathbf{H}}{2c}-\tfrac{3}{2}n\mathbf{F}\ . \tag{3.33}$$

The commuting operators $J_{1,1}$ and $J_{2,2}$ are the components of $\mathbf{J}_1$ along $\boldsymbol{\omega}_1$ and of $\mathbf{J}_2$ along $\boldsymbol{\omega}_2$. Their eigenvalues k_1 and k_2 take integer or semi-integer values from $-j$ to j. Therefore the first-order energy-correction values equal to the eigenvalues of V_1 are given by the formula

$$E^{(1)}=\omega_1 k_1+\omega_2 k_2\ . \tag{3.34}$$

The zero-order eigenfunctions $\Psi^{(0)}_{k_1k_2}$ can also be found analytically (Demkov *et al.*, 1969). The common eigenfunctions $|k_1k_2\rangle$ of the components of $\mathbf{J}_1$ and $\mathbf{J}_2$ along the same vector $\boldsymbol{\omega}_1$ are parabolic orbitals quantized along the direction of $\boldsymbol{\omega}_1$; the parabolic quantum numbers are connected with k_1 and k_2 by the relations

$$k_1=\frac{n_1-n_2+m}{2},\quad k_2=\frac{n_2-n_1+m}{2}\ .$$

To obtain from $|k_1k_2\rangle$ the zero-order eigenfunctions in crossed fields, we must change the direction of quantization of the angular momentum $\mathbf{J}_2$ from $\boldsymbol{\omega}_1$ to $\boldsymbol{\omega}_2$. Denoting by δ the angle between $\boldsymbol{\omega}_1$ and $\boldsymbol{\omega}_2$, we can write the result as

$$\Psi^{(0)}_{k_1k_2}=\sum_{s=-j}^{j} d^{j}_{sk_2}(\delta)|k_1 s\rangle\ , \tag{3.35}$$

where $d^{j}_{sk_2}(\delta)$ are the Wigner functions.

In the case of orthogonal fields the two frequencies are equal: $\omega_1=\omega_2=\omega$. Therefore the first-order energies depend only on the sum of the quantum numbers $k_1+k_2\equiv q$:

$$E_q^{(1)}=\omega\cdot q, \quad -(n-1)\leq q\leq n-1 \ . \tag{3.36}$$

The integer quantum number q is an eigenvalue of the operator

$$\hat{Q}=J_{1,1}+J_{2,2} \ . \tag{3.37}$$

In the limit $F/H\to 0$ we have $\hat{Q}=L_z$, so that q becomes the usual magnetic quantum number m. In the opposite limit $H/F\to 0$ we have $\hat{Q}=A_z$ and $q=n_1-n_2$. The levels $E_q^{(1)}$ are $n-|q|$ times degenerate. The corresponding eigenfunctions are the functions (3.35) with a fixed sum k_1+k_2 and all possible $k=k_1-k_2$. From now on we shall denote these functions by $\Psi_{qk}^{(0)}$.

Degeneracy of the levels $E_q^{(1)}$ is lifted if we take into account the higher-order effects. These include the diamagnetic perturbation V_d given by Eq. (1.1). There are also the second-order effects of the perturbation V_1. These effects are characterized by the secular operator $\hat{W}$, whose matrix elements between states of the same (nth) shell are, by definition,

$$\langle n\alpha'|\hat{W}|n\alpha\rangle=\sum_{\substack{\alpha'',n''\\ n''\neq n}}\frac{\langle n\alpha'|V_1|n''\alpha''\rangle\langle n''\alpha''|V_1|n\alpha\rangle}{E_n^{(0)}-E_{n''}^{(0)}} \ . \tag{3.38}$$

Here $|n\alpha\rangle$ is an arbitrary complete set of unperturbed hydrogen atom orbitals, with α denoting all the quantum numbers but n. Actually, in this expression, only the electric part of V_1 is important because the operator $\mathbf{L}$ has only zero matrix elements between states with different principal quantum numbers.

If we choose as $|n\alpha\rangle$ the parabolic orbitals $|nn_1n_2\rangle$ quantized along the electric field direction, the matrix elements of $\hat{W}$ are expressed through values that are well known from the theory of the Stark effect in atomic hydrogen,

$$\begin{gathered}\langle nn_1n_2|\hat{W}|nn_1n_2\rangle=E_{nn_1n_2}^{(2)} \ , \\ \langle nn_1'n_2'|\hat{W}|nn_1n_2\rangle=\underset{(n_1\neq n_1')}{(E_{nn_1n_2}^{(1)}-E_{nn_1'n_2'}^{(1)})C_{n_1'n_2'}^{(1)}} \ .\end{gathered} \tag{3.39}$$

Here $E_{nn_1n_2}^{(1)}$ and $E_{nn_1n_2}^{(2)}$ are the first- and second-order energy corrections in the electric field; $C_{n_1'n_2'}^{(1)}$ is the coefficient at $|nn_1'n_2'\rangle$ in the development of the first-order correction to the zero-order eigenfunction $|nn_1n_2\rangle$. These values can be found in Adamov *et al.* (1964). Equations (3.39) follow from the equations for the perturbation theory for degenerate levels (Landau and Lifshitz, 1989).

The results of calculation in Eq. (3.39) can be summarized by the equivalence relation which holds within the nth shell (Solov'ev, 1983),

$$\hat{W}=\frac{n^4F^2}{16}(5n^2+31+24\mathbf{L}^2-21L_F^2+9A_F^2) \ . \tag{3.40}$$

The equivalence relation for the diamagnetic operator (Herrick, 1982; Solov'ev, 1982; Gay *et al.*, 1983) can also be written in a form that is independent of the choice of coordinate frame:

$$V_d=\frac{n^2H^2}{16c^2}(4\mathbf{A}^2-5A_H^2+L_H^2+n^2+3) \ . \tag{3.41}$$

Here, the subscripts F and H signify projections onto the direction of the electric and magnetic fields. By definition, Eqs. (3.40) and (3.41) mean equality of the matrix elements of the operators in the left- and right-hand sides between any functions belonging to the manifold of the orbitals of the nth shell of the unperturbed hydrogen atom.

To find the second-order splitting, one needs to diagonalize operator $\hat{W}+V_d$ in the basis set of the functions $\Psi_{qk}^{(0)}$ belonging to the degenerate level $E_q^{(1)}$; alternatively, one can diagonalize the sum of the operators in the right-hand side of Eqs. (3.40) and (3.41). Calculations are made easy if the operators $\mathbf{A}$ and $\mathbf{L}$ are expressed through components of the angular pseudomomentum $\mathbf{J}_1$ in the coordinate frame with the z axis along $\boldsymbol{\omega}_1$, and of $\mathbf{J}_2$ in the frame with the z axis along $\boldsymbol{\omega}_2$. The result is a TTR relation for coefficients of the zero-order eigenfunction,

$$p_kC_{k-2}+(w_k-E')C_k+p_{k+2}C_{k+2}=0 \tag{3.42}$$

with

$$\begin{aligned}p_k&=\frac{u_\gamma}{5}\left\{\left[\left[1-\frac{q}{n}\right]^2-\frac{(k-1)^2}{n^2}\right]\right.\\ &\qquad\times\left.\left[\left[1+\frac{q}{n}\right]^2-\frac{(k-1)^2}{n^2}\right]\right\}^{1/2} \ ,\\ w_k&=u_\gamma\frac{bk^2}{5n^2} \ .\end{aligned} \tag{3.43}$$

Here $u_\gamma=5n^4H^2/16c^2$; b is a parameter given by the formula ($\varkappa\equiv 3ncF/H$):

$$b=\varkappa^2-1-\frac{2}{1+\varkappa^2} \ . \tag{3.44}$$

It grows monotonically from -3 to infinity when the ratio F/H is increased from 0 to ∞.

The second-order energy corrections are equal to the eigenvalues E' of Eq. (3.42) plus a shift common to all levels of the multiplet obtained from $E_q^{(1)}$:

$$\begin{aligned}E^{(2)}&=E'+u_\gamma\left[\frac{3}{5}+\frac{1-q^2}{5n^2}\right]\\ &\quad+\frac{n^4F^2}{16}\left[3q^2-17n^2-19-\frac{6}{1-\varkappa^2}(n^2-3q^2-1)\right] \ .\end{aligned} \tag{3.45}$$

2. Investigation of the spectrum

Comparing the TTR relation (3.42) with Eq. (1.2) describing the quadratic Zeeman effect in the parabolic representation shows that the presence of an orthogonal electric field results only in modifying the coefficient of k^2 in the diagonal matrix element w_k (one also has to replace m by q). The potential functions of the Stark-Zeeman problem can now be obtained from those studied in Sec. III.A by adding $(b+3)k^2/5n^2$ to both $U^+(k)$ and $U^-(k)$. The resulting changes of the potential curves fully explain the complicated transformation of the spectrum accompanying changes in the relative strengths of the electric and magnetic fields.

In the simplest case $q=0$, corresponding to the central line in the first-order splitting pattern, the potential curves are two symmetrical parabolas:

$$
\begin{aligned}
U^+(k) &= \frac{u_\gamma}{5}\left[2-(2-b)\frac{k^2}{n^2}\right] , \\
U^-(k) &= \frac{u_\gamma}{5}\left[-2+(2+b)\frac{k^2}{n^2}\right] .
\end{aligned}
\tag{3.46}
$$

Depending on the value of b there are three possibilities.

(a) Let $-3<b<-2$ (weak electric fields). The potential curves are similar to those for the pure quadratic Zeeman effect [Fig. 16(a)]. The lower part of the quadratic Stark-Zeeman multiplet consists of exponentially close doublets. With the growth of b, the two symmetrical potential wells on both sides of the maximum of $U^-(k)$ grow shallower and the proportion of doublets diminishes.

(b) Let $-2<b<2$ (comparable fields). The potential curve U^- has a minimum instead of a maximum at the point $k=0$. There are no potential barriers in the plot of $U^\pm(k)$ [Fig. 16(b)], hence no doublets in the spectrum. Instead there are two symmetrical quasibarriers at $k=\pm n$. Their presence is manifested by a series of inflection points forming a typical crease in the plot of the eigenvalues against b (Fig. 17). A similar crease was observed by Herrick (1982) in a related problem.

(c) Let $b>2$ (weak magnetic field). The plot of the potential functions is turned upside down compared with the case $b<-2$ [Fig. 16(c)]. If the level E' is higher than the minimum of $U^+(k)$, there are two symmetrical classically allowed regions. These are divided by a classically forbidden region, which might be called an overturned potential barrier. The length of the classically forbidden interval grows when the energy correction is increased. This means that, in a strong enough transverse electric field, the doublet levels reemerge. However, this time they occupy the upper part of the quadratic multiplet, and the exponential splitting is smaller the higher (!) the energy of the doublet level.

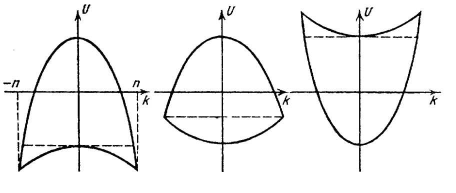

(a) (b) (c)

FIG. 16. Hydrogen atom in orthogonal fields. Potential curves of the TTR relation (3.42): (a) $b<-2$; (b) $-2<b<2$; (c) $b>2$. From Braun and Solov'ev (1984).

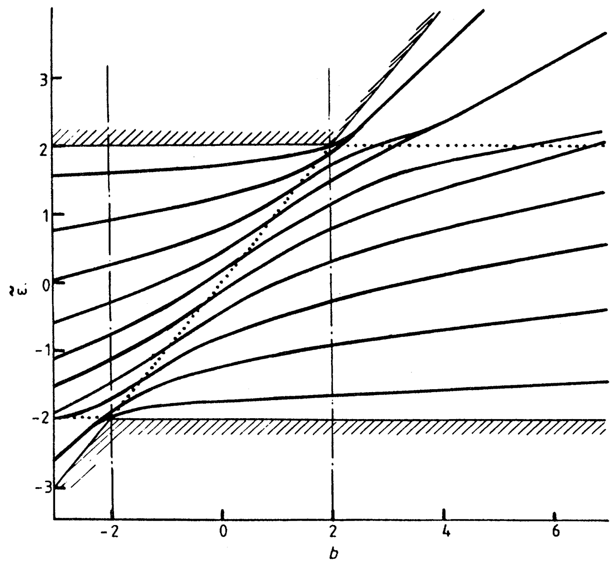

FIG. 17. Second-order splitting of the hydrogen atom levels in orthogonal fields ($\tilde{\varepsilon}\equiv 5E'/u_\gamma$), when $n=10$, $q=0$. From Braun and Solov'ev (1984).

The values $b=\pm 2$ are singled out because for these values one of the potential functions turns into a constant. In these cases the WKB theory integrals in Eqs. (2.10) and (2.21)–(2.23) become elementary instead of being elliptical. Now there seems to be a rule: if the semiclassical theory integrals are elementary, the corresponding quantum problem is likely to be exactly soluble. As a matter of fact, it was shown in Braun and Solov'ev (1984) that when $b=2$ the exact eigenvalues of Eq. (3.42) are

$$
\begin{aligned}
E' &= u_\gamma \frac{2}{5n^2}[q^2+n^2-1-2L(L+1)] , \\
L &= 0,1,\ldots,n-|q|-1 .
\end{aligned}
\tag{3.47}
$$

The case $b=-2$ is reduced to $b=2$ by the exact relation, which holds for all b,

$$
E'(-b) = -E'(b) . \tag{3.48}
$$

This can be proved by substituting $C_k=(-1)^{k/2}\tilde{C}_k$ in Eq. (3.42). Equation (3.48) means that there is a center of symmetry in the plot of the eigenvalues against b. Discussion of the case $q\neq 0$ can be found in Braun and Solov'ev (1984).

The pattern of quadratic Zeeman splitting is much less sensitive to the presence of a transverse electric field than to that of a parallel one. (The diamagnetic splitting should be compared with the second- and first-order Stark splittings, respectively). This means that in experiments on atomic hydrogen in orthogonal fields it is crucially important to establish the exact geometry of the fields. Even a slight deviation from 90° means that an additional parallel electric field is introduced, which can completely modify the spectrum, especially the doublet structure in the cases $b < -2$ and $b > 2$. This was indeed observed in the experiments of Wiebusch *et al.* (1989).

The problem of atomic hydrogen in approximately orthogonal electric and magnetic fields was considered by Belov *et al.* (1985) and Braun (1990a). Estimates in the latter paper show that in the experimental conditions of the work of Wiebusch *et al.* (1989) the doublet part of the quadratic multiplet is distorted beyond recognition if the angle between **F** and **H** differs from 90° by 15′.

3. Related problems. Splitting by the generalized van der Waals perturbation

Like the pure quadratic Zeeman effect, second-order Stark-Zeeman splitting of the central line with $q=0$ is related to the problem of a rigid asymmetrical top with the rotational constants

$$a_1=-b+2, \quad a_2=-b-2, \quad a_3=0 .$$

The exactly soluble cases correspond to the top's becoming symmetrical.

Another closely related problem is the first-order splitting of hydrogen atom levels by perturbations of the type

$$V(\alpha)=x^2+y^2+\alpha z^2 \tag{3.49}$$

(the so-called generalized van der Waals potential), which is considered by Gay and Delande (1983), Gay (1986), Gay *et al.* (1988), Alhassid *et al.* (1987), and Ganesan and Lakshmanan (1990). In addition to the case of the quadratic Zeeman effect ($\alpha=0$), the family $V(\alpha)$ includes the van der Waals interaction with the conducting surface ($\alpha=2$) and the hydrogen atom in a wave guide ($2<\alpha<\frac{8}{3}$); see Hinds (1990).

It can easily be checked that the equation for the zero-order eigenfunction corresponding to the perturbation $V(\alpha)$ in the parabolic basis set is essentially identical with Eq. (3.42) provided one chooses in this TTR relation

$$b=\frac{6(3\alpha-2)}{4-\alpha} \tag{3.50}$$

and replaces q by the magnetic quantum number m. Then the following relation holds between first-order energies $E^{(1)}$ corresponding to $V(\alpha)$ and eigenvalues of Eq. (3.42):

$$E^{(1)}=n^2\left[\frac{n^2}{4}(6+\alpha)+\frac{2+3\alpha}{4}-m^2\left(\frac{1}{2}+\frac{\alpha}{4}\right)\right.$$
$$\left.+\frac{5n^2(4-\alpha)}{8}\frac{E'}{u_\gamma}\right] . \tag{3.51}$$

TABLE I. The conjugate pairs of the parameter α in the operators $V(\alpha)$.

α	α'	Comment
0	$\frac{8}{7}$	The diamagnetic perturbation
$\frac{1}{4}$	1	Exactly soluble case
4	4	Exactly soluble case
$\frac{2}{3}$	$\frac{2}{3}$	Symmetrical spectrum

The exactly soluble cases $b=\pm 2$ correspond to $\alpha=\frac{1}{4}$ and $\alpha=1$; the limit of quadratic Stark splitting ($b\rightarrow\infty$) corresponds to $\alpha=4$. As regards splitting by $V(\alpha)$, the exact solubility of these cases is well known (see the papers cited above). In general the second-order splitting of the hydrogen atom in orthogonal electric and magnetic fields $0<F/H<\infty$ is equivalent, up to a scaling factor and a shift, to the first-order splitting by $V(\alpha)$ with $0<\alpha<4$.

An interesting result follows from the symmetry relation (3.48) (we do not know whether it was earlier reported). The replacement of b by $b'=-b$ means, according to Eq. (3.50), the replacement of α by

$$\alpha'=\frac{7\alpha-8}{3\alpha-7} . \tag{3.52}$$

Using Eq. (3.51), it is easy to prove that the first-order splitting produced by two different operators $V(\alpha)$ and $V(\alpha')$ is essentially equivalent, with the first-order energies connected by the following exact relation:

$$E^{(1)}(\alpha')=\frac{5}{3\alpha-7}E^{(1)}(\alpha)+\frac{5n^4(\alpha-4)}{3\alpha-7}\left(1+\frac{2m^2-3}{5n^2}\right) . \tag{3.53}$$

Some of the conjugate values of α and α' are listed in Table I. The diamagnetic splitting ($\alpha=0$) is equivalent to the splitting produced by the operator $V(\frac{8}{7})$. In the case $\alpha=\frac{2}{3}$ we have $\alpha=\alpha'$, which means that Eq. (3.53) connects different eigenvalues of the same perturbation matrix.

IV. INTENSITY DISTRIBUTION IN THE SPECTRA OF HIGHLY EXCITED ATOMIC HYDROGEN IN EXTERNAL FIELDS

Calculations of the spectrum of excited atomic hydrogen in an external magnetic field (Clark and Taylor, 1980,1982; Wintgen and Friedrich, 1987; Zeller *et al.*, 1989) have revealed that the oscillator strength distribution in this spectrum has a highly characteristic appear-

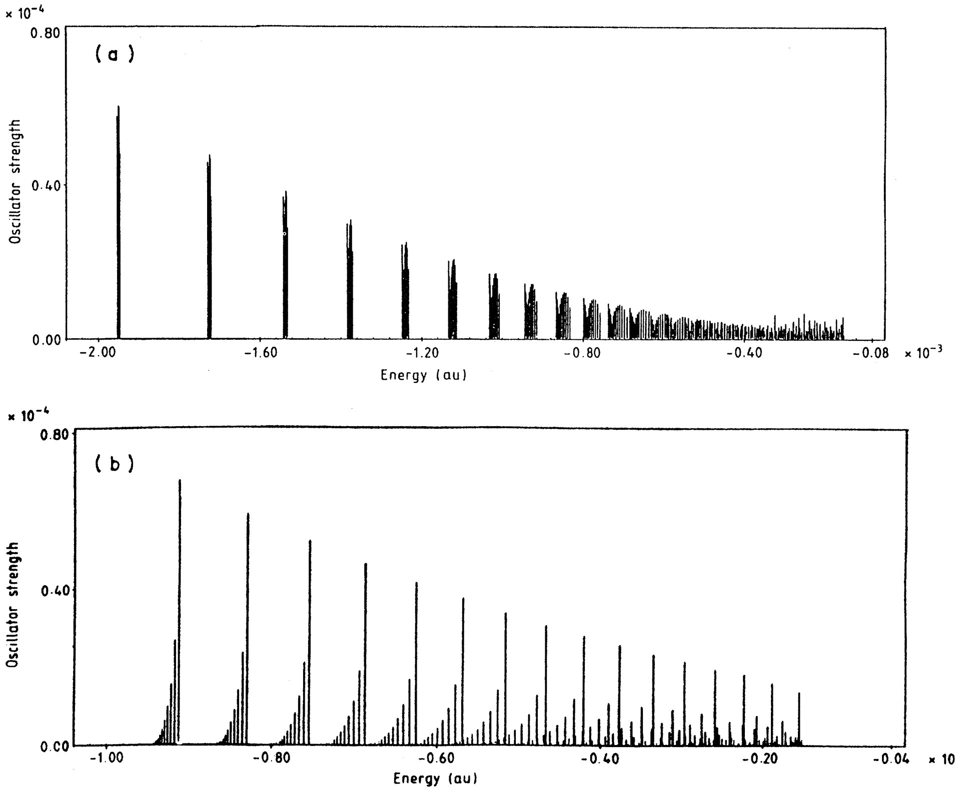

FIG. 18. Lyman series oscillator strengths of the hydrogen atom in the magnetic field $H = 4.7$ T: (a) $m = 0$; (b) $m = 1$. From Clark and Taylor (1980).

ance (Fig. 18). The following properties may be singled out.

(a) As long as quadratic Zeeman multiplets with different n do not overlap, the oscillator strength distribution within each multiplet has a peculiar profile practically independent of n (apart from the scaling factors). This profile can also be reproduced in the l-mixing approach when the intensity distribution within a single multiplet with n fixed is calculated (Grozdanov and Taylor, 1986; Wunner, 1986); see Fig. 19.

(b) The form of the intensity envelopes in the spectra of the Lyman series transitions with $\Delta m = 0$ and $\Delta m = 1$ is totally different. It is also absolutely unlike the intensity distribution in the Balmer series transitions from the $2p$ state [see Fig. 20(c,d) below]. There are two types of behavior at the high-frequency edge of each multiplet, with intensity either going to zero or rocketing upward.

(c) There are details in the intensity plots obviously connected with properties of the classical evolution of the orbit of an atomic electron. In particular, the minimum in the intensity which divides the span of each multiplet in the ratio 1:4 is obviously connected with the presence of a separatrix corresponding to the critical diamagnetic energy shift $E_0' = u_\gamma / 5$ (or $\Lambda = 0$).

It is usually assumed that reliable prediction of the oscillator strengths is a far more difficult task than calculation of the energy levels. It will be shown that, in the case of perturbed Rydberg atoms, the real situation is just the opposite: provided the energy-level distribution is known, the oscillator strengths of transition to the low-lying atomic states can be obtained by simple algebraic formulae. We shall also see that the intensity distributions with different Δm in the spectra of the Lyman and Balmer series, which look so different, are in fact connected by elementary relations. Apart from the quadratic Zeeman effect (Sec. IV.A), we consider the oscillator strengths of atomic hydrogen perturbed by the van der Waals interaction with a conducting wall (IV.B) and by parallel (IV.C) and crossed (IV.D) electric and magnetic fields.

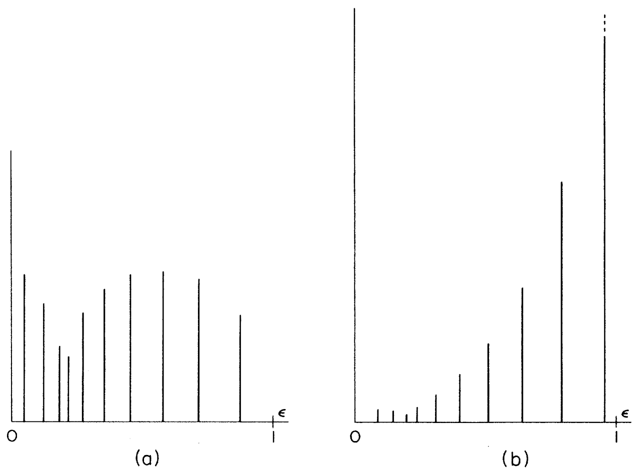

FIG. 19. Lyman series oscillator strengths in a separate quadratic Zeeman multiplet with $n = 20$: (a) $m = 0$. (b) $m = 1$.

A. Oscillator strengths in quadratic Zeeman-effect spectra

In comparatively weak l-mixing external magnetic fields, the low-lying atomic states remain virtually unchanged. The oscillator strengths of transitions from these states to the levels of the quadratic Zeeman multiplet with $n \gg 1$ can be expressed through the coefficients C_l of the zero-order eigenfunction in a spherical basis set. For example, in the case of transitions from the 1s state (the Lyman series), the oscillator strength is the weight C_1^2 with which the np orbital enters the Zeeman state in question times the oscillator strength of the 1s-np transition in unperturbed atomic hydrogen.

Thus all we need to calculate the oscillator strength distribution is the formula for the coefficients C_l with $l \ll n$. It has already been obtained in the form of Eq. (3.20), which expresses C_l through the Legendre functions. The fact that it matches the WKB solution (3.19) establishes the relation between the normalizing constants A and A^{WKB}. On the other hand, the latter constant can, as usual, be expressed through the classical oscillation frequency of the "coordinate" L, which in its turn is equal to the spacing $\Delta E'$ between quadratic Zeeman levels of the same parity:

$$A^{\mathrm{WKB}} = 2\left[\frac{\Delta E'}{\pi}\right]^{1/2} . \tag{4.1}$$

Finally we obtain the formula (Braun, 1990c)

$$C_l = \frac{\sqrt{\Delta\varepsilon}}{[1-\varepsilon]^{1/4}} \mathcal{P}_{lm}(\sqrt{1-\varepsilon}), \quad l \ll n . \tag{4.2}$$

Here $\varepsilon = E'/u_\gamma$. This value $\Delta\varepsilon = \Delta E'/u_\gamma$ is the scaled

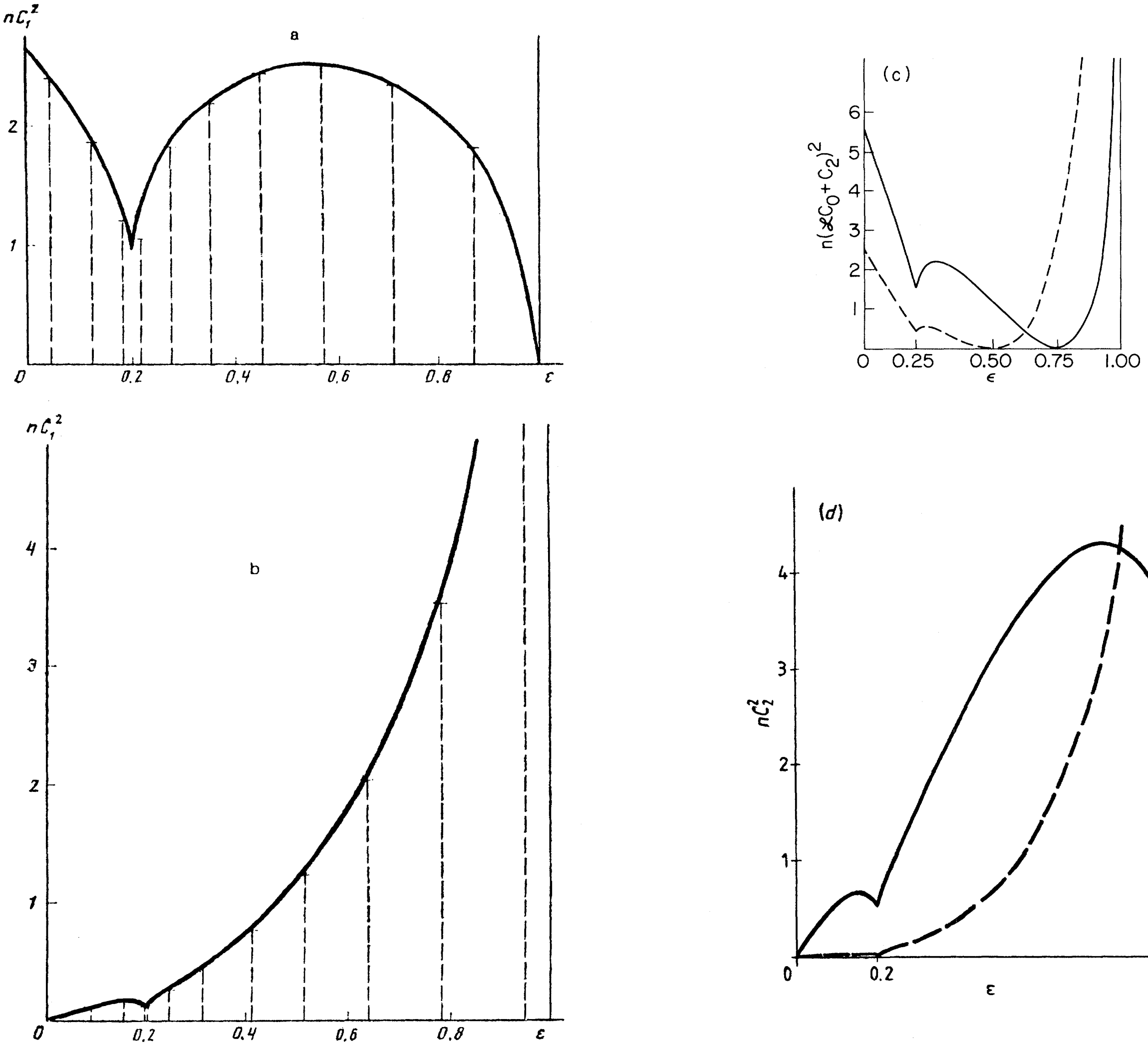

FIG. 20. Analytical oscillator strength distribution profiles in the quadratic Zeeman effect: (a) Transitions 1s $-nm$, $m=0$. (b) Transitions 1s $-nm$, $m=1$. (c) Transitions 2p $-nm$, $m=0$ with $\Delta m=0$ (solid curve) and $\Delta m=1$ (dashed curve). Here $\mathcal{L} \equiv \sqrt{5}/8$ ($\Delta m=0$) or $-\sqrt{5}/4$ ($\Delta m=1$). (d) Transitions 2p $-nm$, $m=1$ (solid curve) and $m=2$ (dashed curve). From Braun (1990c).

spacing. It is the reciprocal of the density of levels in the quadratic Zeeman multiplet and is different in its different parts. The plot of $\Delta\varepsilon$ against ε was shown in Fig. 8 (Sec. III.A). It can either be regarded as an empirical quantity or expressed through the classical period (2.10).

In some cases it is more convenient to use the angle $\vartheta_0 = \arccos\sqrt{1-\varepsilon}$ instead of ε as the independent variable in the expression for C_l:

$$C_l = \sqrt{2\sin\vartheta_0 \Delta\vartheta_0}\, \mathcal{P}_{lm}(\cos\vartheta_0) \tag{4.3}$$

where

$$\Delta\vartheta_0 = \frac{d\vartheta_0}{d\varepsilon}\Delta\varepsilon$$

is the difference in the value of ϑ_0 for two adjacent levels.

It follows from Eq. (4.2) that in the Lyman series the oscillator strength distributions in quadratic Zeeman multiplets are proportional to

$$\begin{aligned} C_1^2 &= \frac{3}{2}\sqrt{1-\varepsilon}\,\Delta\varepsilon(\varepsilon), \quad \Delta m = 0\ , \\ C_1^2 &= \frac{3}{4}\frac{\varepsilon}{\sqrt{1-\varepsilon}}\Delta\varepsilon(\varepsilon), \quad \Delta m = 1 \end{aligned} \tag{4.4}$$

[see Figs. 20(a) and 20(b)].

In Balmer series transitions from the $2p$ state, the magnetic quantum number m of the upper state can be ± 2, ± 1, and 0. If $m \neq 0$ the oscillator strengths are proportional to the weight of the nd orbital in the Zeeman states [Fig. 20(c)],

$$\begin{aligned} C_2^2 &= \frac{15}{4}\varepsilon\sqrt{1-\varepsilon}\,\Delta\varepsilon(\varepsilon), |m| = 1\ , \\ C_2^2 &= \frac{15}{16}\frac{\varepsilon^2}{\sqrt{1-\varepsilon}}\Delta\varepsilon(\varepsilon), |m| = 2\ . \end{aligned} \tag{4.5}$$

If $m = 0$ both the ns and the nd components contribute to the transition amplitude. Using the relation between the amplitudes of the $2p$-ns and $2p$-nd dipole transitions (Bethe and Salpeter, 1957) it is easy to show that the oscillator strengths are proportional to [Fig. 20(d)]

$$\begin{aligned} \left[\frac{\sqrt{5}}{8}C_0 + C_2\right]^2 &= \frac{(\varepsilon-\frac{3}{4})^2}{\sqrt{1-\varepsilon}}\Delta\varepsilon(\varepsilon), \quad \Delta m = 0\ , \\ \left[-\frac{\sqrt{5}}{4}C_0 + C_2\right]^2 &= \frac{(\varepsilon-\frac{1}{2})^2}{\sqrt{1-\varepsilon}}\Delta\varepsilon(\varepsilon), \quad \Delta m = 1\ . \end{aligned} \tag{4.6}$$

Thus all the oscillator strength profiles can be obtained from the plot of the spacings $\Delta\varepsilon$ versus ε (Fig. 8) by multiplying the curve of spacings by the appropriate elementary function of ε. This means, by the way, that these profiles are connected by simple relations. For example, the Lyman series distribution with $\Delta m = 1$ differs from that with $\Delta m = 0$ only by the factor $\varepsilon/(1-\varepsilon)$.

Various peculiarities in the oscillator strength distributions can be traced to different factors in Eqs. (4.4)–(4.6). The minimum in the intensity at $\varepsilon = \frac{1}{5}$ is due to a singularity in $\Delta\varepsilon$ caused by the classical period's logarithmically tending to infinity. The well-known steep rise in intensity at the high-frequency edge (Clark and Taylor, 1980,1982; Gay, 1986) is connected with the denominator $\sqrt{1-\varepsilon}$; it is absent if the sum of the indices of the relevant Legendre function is odd, because this function then turns into zero at the point $\varepsilon = 1$.

The analytical expressions (4.3)–(4.6) agree, to within an accuracy usually far exceeding practical demands, with the results of the numerical calculations in the cited papers. They are also in complete agreement with the experimental findings of the Bielefeld group (Holle *et al.*, 1985; Wintgen, Holle *et al.*, 1986). Comparison with the experimental spectra of nonhydrogenic Rydberg atoms in a magnetic field (Gay *et al.*, 1980; Delande and Gay, 1981b; Cacciani *et al.*, 1986a;1988a; van der Veldt *et al.*, 1990;1992) shows that, in situations where core effects could be neglected, the theoretical and the experimental intensity distributions are almost identical.

A predictable fall in accuracy is observed for the levels in the immediate vicinity of the critical energy E_c'; the reason for this is failure of the normalizing condition (4.1) for levels close to the barrier or quasibarrier top. The results are also slightly less accurate than average for the transitions to the highest level of the multiplet. In this case higher accuracy is provided by the expression for C_l given in Fano *et al.* (1988); see the discussion and numerical examples in Braun (1990c).

B. Oscillator strengths of a hydrogen atom perturbed by the van der Waals interaction with the conducting wall

The problem of a Rydberg atom inside a resonator attracts much attention because of its connection with the fundamental problems of quantum electrodynamics as well as because of its possible practical implications; see the reviews of Haroche (1986), Beterov and Lerner (1989), and Hinds (1990). A related topic is the problem of transformation of the Rydberg atom spectrum caused by interaction with the conducting wall of the resonator (Barton, 1987,1988). The principal term in the interaction is usually the van der Waals attraction of the atomic dipole to its electrostatic image. The operator of the interaction is proportional to

$$V(2) = x^2 + y^2 + 2z^2 \tag{4.7}$$

and belongs to the family of operators considered in Sec. III.E.3.

Let E' be the first-order energy correction due to $V(2)$ and $\varepsilon = 2E'/5n^4$ be the scaled quantity. Suppose that $|m| \ll n$. In this case the spectrum is limited to the interval $\frac{3}{5} < \varepsilon < 2$. It turns out that in the part of the van der Waals multiplet where $1 < \varepsilon < 2$ the spectrum consists of extremely close doublets. In the part of the multiplet where $\frac{3}{5} < \varepsilon < 1$ the levels are singlets. Thus, if the sign of the perturbation operator were changed, the splitting would be similar to quadratic Zeeman splitting. The dependence of the scaled energy spacings $\Delta\varepsilon$ on ε has the

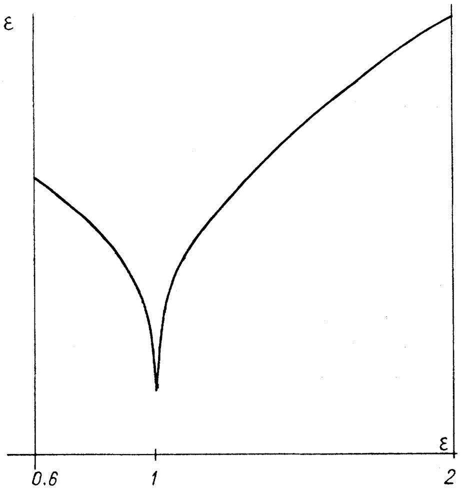

FIG. 21. Spacings in the van der Waals multiplets.

same birdlike appearance (Fig. 21) as in the case of the quadratic Zeeman effect (Fig. 8). However, the oscillator strength distribution is totally different (Fig. 22). Almost all of the intensity goes to the spectral interval $1<\varepsilon<2$, whereas at the interval $\frac{3}{5}<\varepsilon<1$ the oscillator strengths are negligible, quickly decreasing exponentially when we move down the multiplet away from the critical point $\varepsilon=1$.

A qualitative explanation of these effects, based on a study of the operator equivalent to $V(2)$ within the nth shell, is given by Alhassid *et al.* (1987). The discrete WKB method provides an alternative explanation and analytical expressions for the oscillator strengths (Braun and Senyushkin, 1991).

In the spherical basis set the perturbation theory equation corresponding to $V(2)$ is a TTR relation. It differs from Eq. (1.4) in that the angular parts of the matrix elements of Eq. (1.5) are modified in the following way:

$$w_l^\vartheta \to 2-w_l^\vartheta ,\quad p_l^\vartheta \to -p_l^\vartheta \tag{4.8}$$

and that we set $H^2/8c^2=1$. The corresponding semiclassical Hamiltonian, from which we have dropped the terms depending on m, for the same reasons as in Sec. III.C.2, is $(L=l+\frac{1}{2})$

$$H'(L,\theta)=\frac{5}{2}n^4\left[\frac{3}{2}\left[1-\frac{3}{5}\frac{L^2}{n^2}\right]+\frac{1}{2}\left[1-\frac{L^2}{n^2}\right]\cos 2\theta\right] .$$

The angle θ canonically conjugate to L is the polar angle of the Runge-Lenz vector of the classical hydrogen atom. The canonical variables slowly change because of the interaction described by $V(2)$. The equation for the evolution $\theta=\theta(L)$ follows from the energy conservation law $E'=H'(L,\theta)$.

The potential curves are parabolic (Fig. 23),

$$\begin{aligned} U^+(L)&=\frac{5}{2}n^4\left[2-\frac{7}{5}\frac{L^2}{n^2}\right] ,\\ U^-(L)&=\frac{5}{2}n^4\left[1-\frac{2}{5}\frac{L^2}{n^2}\right] . \end{aligned} \tag{4.9}$$

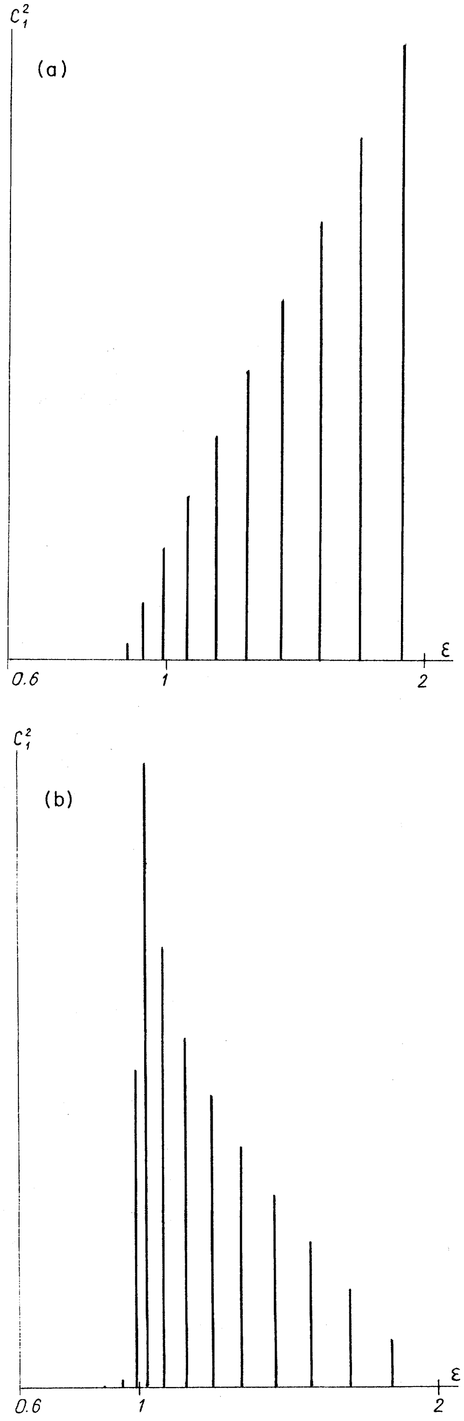

FIG. 22. Oscillator strengths of the Lyman series transitions to the levels of the van der Waals multiplet with $n=30$: (a) $m=0$; (b) $m=1$.

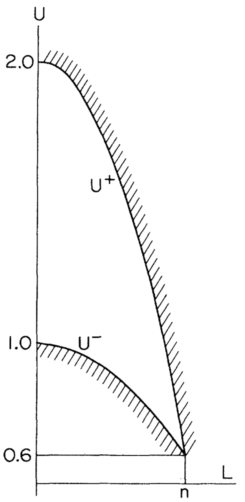

FIG. 23. Potential curves of the three-term recursion relation describing the van der Waals splitting of atomic hydrogen (spherical representation), when $m=0$. The boundaries of the classically allowed region are hatched.

The plot of $U^{\pm}$ immediately shows that if $\varepsilon<1$, small values of L lie in the classically forbidden region. This means that the coefficients C_l with $l \ll n$ of the eigenfunction in the spherical basis set will be extremely small. Hence the oscillator strengths of transitions to the low-lying levels will also be extremely small; this completes the qualitative explanation.

The analytical treatment of the intensities is based on the fact that if $l \ll n$ the coefficients C_l are given by the same Eq. (3.20) as in the case of the quadratic Zeeman effect, but with a different relation between the argument of the Legendre functions and the energy correction, which follows from the formula

$$\varepsilon=\tfrac{3}{2}+\tfrac{1}{2}\cos 2\vartheta_0 \, . \tag{4.10}$$

It can be seen that ϑ_0 is equal to the value of $\theta(L)$ at $L=0$. [The reason for the universal validity of Eq. (3.20) will be considered later.]

The same arguments as in the preceding section show that at the energy-correction interval $1<\varepsilon<2$ the coefficients C_l are still expressed through ϑ_0 and $\Delta\vartheta_0$ by Eq. (4.3). By means of Eq. (4.10) they can be expressed through ε and $\Delta\varepsilon$. It follows that, in the case of the Lyman series, the intensity distribution at the interval $1<\varepsilon<2$ is proportional to

$$C_1^2=\frac{3}{2}\sqrt{\varepsilon-1}\,\Delta\varepsilon(\varepsilon), \quad \Delta m=0 \, ,$$

$$C_1^2=\frac{3}{4}\frac{(2-\varepsilon)}{\sqrt{\varepsilon-1}}\Delta\varepsilon(\varepsilon), \quad \Delta m=1 \, .$$

In the energy-correction interval $\frac{3}{5}<\varepsilon<1$, the normalizing constant of the Legendre solution (3.20) is found by matching it to the WKB solution of the TTR relation in the classically forbidden region. The latter solution is then matched by means of Eq. (2.20) to the WKB solution in the allowed region, and is normalized in the usual way. The resulting expression is

$$\begin{aligned} C_l &= \sqrt{2\sin\vartheta_0\Delta\vartheta_0}\,\mathcal{P}_{lm}(\cos\vartheta_0)e^{-S} \, , \\ S &= \int_0^{L_t} |\pi-\theta(L)|\,dL \, . \end{aligned} \tag{4.11}$$

Compared with Eq. (4.3), the result includes the additional factor, which gives the probability amplitude of tunneling of the atomic electron into a state with $L=0$ in which its Kepler orbit is a line. The integral is taken over the classically forbidden region. The function $\pi-\theta(L)$ in the integrand is purely imaginary. The presence of the factor e^{-S} leads to the rapid vanishing of C_l when ε becomes significantly smaller than unity. A check of Eq. (4.11) shows that it leads to values of the oscillator strengths that agree almost perfectly with the numerical results, despite the fact that the intensities in different parts of the interval $\frac{3}{5}<\varepsilon<1$ differ by many orders of magnitude.

C. Intensities in parallel electric and magnetic fields

Introduction of an electric field parallel to the magnetic field leads to a marked complication of the oscillator strength distribution; see the numerical calculations of Richter *et al.* (1987), Bivona *et al.* (1988), Grozdanov and Racović (1988), Zeller *et al.* (1989). If the electric field is not too strong, the pattern of line intensities looks like the plot in Fig. 24. At the bottom of the multiplet the oscillator strengths form a smooth sequence resembling the pure Stark effect. The intensities of lines with higher frequency change in a complicated fashion so that

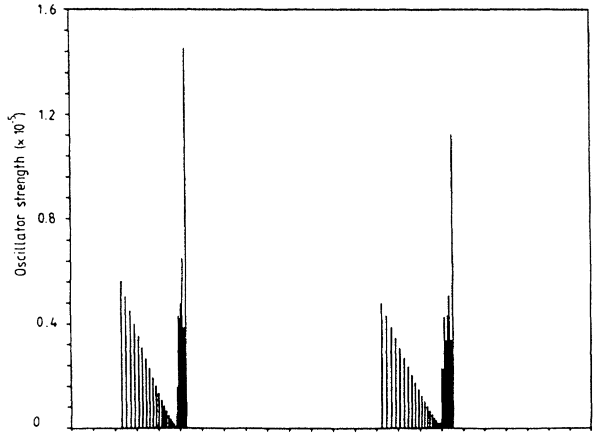

FIG. 24. Lyman series oscillator strengths of the hydrogen atom in parallel electric and magnetic fields, $H=4.7$ T, $F=25$ V/cm, when $m=0$. The multiplets with $n=27$ and 28 are shown. From Bivona *et al.* (1988).

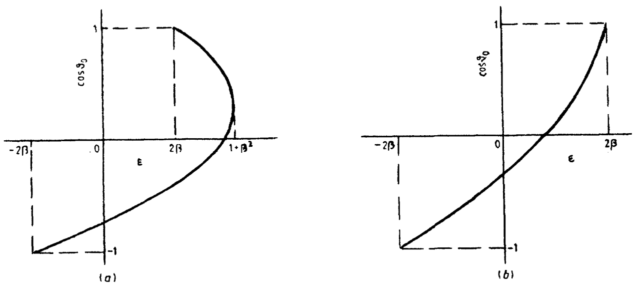

FIG. 25. The Stark-Zeeman effect in parallel fields. Dependence of cos ϑ_0 on the scaled energy correction ε: (a) $\beta < 1$, two ϑ_0 for each E' in the upper part of the multiplet; (b) $\beta > 1$. From Braun (1991a).

the oscillator strength distribution has nothing resembling a smooth envelope. A similar picture is observed in experiments on atomic lithium (Cacciani *et al.*, 1988c). Following Braun (1991a), we shall explain the peculiarities in the intensity distribution in Stark-Zeeman multiplets and give analytical expressions for the transition amplitudes.

To find the oscillator strengths, we have to determine the coefficients of the zero-order eigenfunctions in the spherical basis set. These coefficients obey a five-term recursion relation,

$$p_lC_{l-2}+q_lC_{l-1}+(w_l-E')C_l+q_{l+1}C_{l+1}+p_{l+2}C_{l+2}=0\ . \qquad (4.12)$$

Here p_l and w_l are the matrix elements (1.5) of the diamagnetic operator, while

$$q_l=\langle nl-1m|Fz|nlm\rangle=q_l^rq_l^\vartheta\ ,\qquad q_l^r=\frac{3}{2}Fn^2\left[1-\frac{l^2}{n^2}\right]^{1/2},\quad q_l^\vartheta=\left[\frac{l^2-m^2}{4l^2-1}\right]^{1/2}\ . \qquad (4.13)$$

When $l \ll n$ the radial parts of the matrix elements in Eq. (4.12) can be replaced by constants,

$$w_l^r\approx p_l^r\approx u_\gamma,\quad q_l^r\approx\tfrac{3}{2}Fn^2\ .$$

If these approximations are made, Eq. (4.12) reduces to the equation for the eigenfunctions of the operator

$$\tilde V(\vartheta)=u_\gamma(\sin^2\vartheta+2\beta\cos\vartheta)$$

in a basis set of spherical functions. Here β is the parameter (3.28) introduced when the problem was considered in the parabolic representation.

The operator $\tilde V$ is simply a function of the polar angle. Therefore its eigenfunctions with a definite m are $\delta(\vartheta-\vartheta_0)e^{im\varphi}$, where ϑ_0 is any angle in the interval $(0,\pi)$, the respective eigenvalues being

$$E'=u_\gamma(\sin^2\vartheta_0+2\beta\cos\vartheta_0)\ . \qquad (4.14)$$

Projecting these eigenfunctions onto the basis set of the spherical functions, we find that in the domain of small l the solution of the problem (4.12) corresponding to a certain eigenvalue E' has the form

$$C_l=AY_{lm}(\vartheta_0,0),\quad l\ll n\ . \qquad (4.15)$$

Here A is a normalizing constant, while E' and ϑ_0 are assumed to be connected by Eq. (4.14). Since

$$Y_{lm}(\vartheta_0,0)=\mathcal{P}_{lm}(\cos\vartheta_0)/\sqrt{2\pi}\ ,$$

this solution is identical to the Legendre solution (3.20).

It is important that, if $\beta<1$, a part of the spectrum of the operator $\tilde V$ is doubly degenerate (Fig. 25), so that there are two angles (ϑ_0^{I} and $\vartheta_0^{\mathrm{II}}$) corresponding to a fixed value of the energy correction E'. Consequently, in general, the solution is a sum of two partial solutions for Eq. (4.15) with different ϑ_0 and A.

The unknown normalizing constant (or constants) can be found by matching the Legendre solution of the five-term recursion relation with the semiclassical one. The discrete WKB method for the five-term recursion can be developed in much the same way as for the three-term relation (Waterland *et al.*, 1987; Braun, 1989b). It is based on an expression of the semiclassical Hamiltonian corresponding to Eq. (4.12) in the case $|m| \ll n$:

$$H'(L,\theta)=u_\gamma\left[\frac{1}{2}\left[1-\frac{3}{5}\frac{L^2}{n^2}\right]+2\beta\left[1-\frac{L^2}{n^2}\right]^{1/2}\cos\theta-\frac{1}{2}\left[1-\frac{L^2}{n^2}\right]\cos2\theta\right]\ . \qquad (4.16)$$

The terms containing m are dropped for the reasons given in Sec. III.C. The phase trajectory equation follows from the energy conservation law

$$H'(L,\theta)=E'\ . \qquad (4.17)$$

The fundamental WKB solutions have the same form (3.19) as for the case of the quadratic Zeeman effect, with $\theta(L)$ fixed by Eq. (4.17).

The formalism of the discrete WKB method in the case of the five-term recursion relation is more complicated. Most importantly, there are in general two independent solutions of the type (3.19). This is because Eq. (4.17) is quadratic with respect to $\cos\theta$, so that the phase trajectory consists, generally, of two branches, $\theta^{\mathrm{I}}(L)$ and $\theta^{\mathrm{II}}(L)$. There are now three potential functions and three types of matching conditions. However, the final expression for C_l with $l \ll n$ is remarkably simple. The result can be better understood in terms of a classical model describing the radiative transition to and from the perturbed Rydberg levels. (The role of this model is purely illustrative; the results themselves are obtained by a step-by-step quantum treatment.)

The field-induced evolution of the angular momentum described by the Hamiltonian (4.16) is an oscillation of L between 0 and some maximal value. This means that the perturbed Kepler orbit periodically turns into a line whose angle $\theta(0)$ with the direction of the field depends on E' and is equal to ϑ_0 as determined by Eq. (4.14).

Consider the optical transition from one of the low-lying atomic states to a Rydberg Stark-Zeeman state. Prior to the transition the atomic angular momentum was close to zero; hence immediately after it L is also almost zero. This means that the "newborn" Kepler orbit modeling the Rydberg state is in its linear phase. Its polar angle is connected with the energy of the Stark-Zeeman level by Eq. (4.14); its azimuth is completely undetermined. Therefore possible positions of the orbits immediately after the transition form a cone around the direction of the fields.

We can now state the results, which can take three different forms.

(a) In the lower part of the multiplet, the angle ϑ_0 is uniquely determined by the energy correction E'. (In terms of our treatment in the parabolic representation in Sec. III.D, this is the part of the spectrum where only the levels of group I are present.) Let $\Delta E'$ be the energy spacing in the multiplet so that

$$\Delta\Omega = 2\pi \sin\vartheta_0 \left| \frac{d\vartheta_0}{dE'} \right| \Delta E' \tag{4.18}$$

is the solid angle between the two close cones of the linear Kepler orbit directions corresponding to two adjacent quantum levels. Then the coefficients of the Rydberg state eigenfunction in the spherical basis set are

$$C_l = \sqrt{\Delta\Omega}\, Y_{lm}(\vartheta_0, 0), \quad l \ll n . \tag{4.19}$$

By means of Eq. (4.14) we can express C_l in terms of E' and $\Delta E'$.

If there are two ϑ_0 corresponding to a given E' there are two possibilities.

(b) The angles ϑ_0^{I} and $\vartheta_0^{\mathrm{II}}$ are connected with two isolated phase trajectories $\theta^{\mathrm{I}}(L)$ and $\theta^{\mathrm{II}}(L)$. Remembering our treatment in the parabolic representation, we can see that this is the intermediate-energy range in which the levels of groups I and II overlap. (This situation occurs only if $\beta < \frac{1}{5}$). The two isolated trajectories correspond to oscillation of the point representing the system to the left and to the right of the potential barrier in Fig. 14(a), Sec. III.D.

In this case the spectrum is composed of two overlayed partial spectra obtained by independent quantization of the movement along the two trajectories. In each spectrum the solution is given by Eq. (4.19), the dependence of C_l on E' and $\Delta E'$ following from the equation $\vartheta_0 = \vartheta_0^s(E')$, where $s = \mathrm{I,II}$.

(c) If $\beta < 1$, then in the upper part of the multiplet (the energy domain of the levels of group III) there is a single phase trajectory for each E'. However, in a period of the field-induced evolution, the classical orbit twice becomes a line, its polar angle at first time being ϑ_0^{I} and at the second time $\vartheta_0^{\mathrm{II}}$. The probability amplitudes connected with these events are coherent and may interfere. Accordingly the solution is

$$C_l = C_l^{\mathrm{I}} \pm C_l^{\mathrm{II}} , \tag{4.20}$$

where the summands are the expressions obtained by substituting $\vartheta_0^{\mathrm{I}}(E')$ and $\vartheta_0^{\mathrm{II}}(E')$ into Eq. (4.19). The spacing $\Delta E'$ in both of the partial amplitudes is the same. The signs in Eq. (4.20) alternate from level to level (for the uppermost level of the multiplet the sign is plus).

Knowing C_l, one can calculate the oscillator transition strengths. In particular, in the Lyman series they are proportional to C_l^2. The pattern of spectral lines in the parts of the multiplet where the situations (a), (b), and (c) are realized is quite different. If there is a single ϑ_0 for each E' [case (a)], the positions and intensities of the lines change smoothly (this is the Stark-effect-like part we spoke about).

Otherwise the spectrum is much more complicated. If there are two isolated phase trajectories [case (b)], overlaying of two independent spectra results in an alternation both of the energy spacings and of the line intensities. Finally, if there is a united phase trajectory, the interference of two probability amplitudes expressed by Eq. (4.20) leads to alternation of the line intensities while the energy spacings change smoothly.

All or some of these situations are observed simultaneously in the same multiplet, depending on the value of β. For example, the multiplets shown in Fig. 24 corresponding to $\beta = 0.4$ consist of two parts in which cases (a) and (c) are realized.

The results of this section provide, as simple limiting cases, the oscillator strength distributions of the linear Stark effect ($\beta \to \infty$) and, in the opposite limit ($\beta = 0$), the quadratic Zeeman effect.[7] On the other hand, the treatment can be extended to other perturbations of the type

$$v(r,\vartheta) = \sum_{i,k} \alpha_{ik} r^i (\cos\vartheta)^k , \tag{4.21}$$

where α_{ik} are some constants and the maximal powers of i and k are small compared with n. The results are again expressed through the function connecting the polar angle of a linear Kepler orbit and the corresponding energy-correction value (Braun, 1991a).

The role of the classical orbits passing through the nucleus was earlier stressed in works on the averaged photoabsorption close to the ionization threshold of atomic hydrogen in a magnetic field (Reinhardt, 1983; Delos and Du, 1988; Du and Delos, 1988; Holle *et al.*, 1988 and reference therein; Bogomolny, 1989). We deal with a much simpler situation of a completely regular classical motion (and hence have no need to use the heavy guns of the Gutzwiller theory). On the other hand, we obtain a much more detailed description of the spectrum, including the oscillator strengths of individual lines, given as

---

[7] Note that in Sec. IV.A $\Delta E'$ meant the spacing between levels of the same parity. In the case of levels of group III this spacing is twice as large as $\Delta E'$ in Eq. (4.18). The effect of alternation of intensities of the lines of group III in the limit $\beta = 0$ goes to the extreme (every second line disappears because of parity considerations). In this case $\vartheta_0^{\mathrm{I}} = \pi - \vartheta_0^{\mathrm{II}}$.

functions of the quantities that can be measured in the experiment (the line positions and the energy spacings).

D. Intensities in crossed electric and magnetic fields

If the electric and magnetic fields acting on a highly excited hydrogen atom are not orthogonal, complete lifting of degeneracy occurs in the first order of perturbation theory. The zero-order eigenfunction of a state with the quantum numbers k_1 and k_2 is then given by Eq. (3.35). Its development in the spherical basis set necessary for oscillator strength calculations is given by the formula

$$\begin{aligned} C_{lm} &= \langle nlm | \Psi^{(0)}_{k_1 k} \rangle \\ &= \langle jjk_1 m - k_1 | lm \rangle d^{j}_{m-k_1 k_2}(\delta) , \end{aligned} \tag{4.22}$$

where $j=(n-1)/2$. It is assumed that the spherical orbitals are quantized along the direction of the vector $\boldsymbol{\omega}_1$ (Sec. III.E).

The right-hand side in Eq. (4.22) is a product of the Clebsch-Gordan coefficient and the Wigner function. It depends in a complicated way on the quantum numbers and the angle δ between the vectors $\boldsymbol{\omega}_1$ and $\boldsymbol{\omega}_2$ determined by Eq. (3.33). The explicit expression for δ is

$$\delta = \arctan \left[\frac{2\varkappa \sin\alpha_{\mathrm{FH}}}{1-\varkappa^2} \right] ,$$

where $\varkappa \equiv 3ncF/H$ and α_{FH} is the angle between the two fields.

We shall use the semiclassical approximation to analyze the dependence of the oscillator strengths on k_1, k_2, and δ. This will be easy because the WKB approximations for the Clebsch-Gordan coefficients (Edmonds, 1960) and the Wigner functions (Brussard and Tolhoek, 1957; Ponzano and Regge, 1968) are well known. The result can be brought into a physically meaningful form closely tied to the semiclassical model of the problem.

Before we formulate the result, let us consider the behavior of the classical hydrogen atom in crossed nonorthogonal fields (Born, 1960). The classical first-order Hamiltonian can be written as

$$H' = \boldsymbol{\omega}_1 \cdot \mathbf{J}_1 + \boldsymbol{\omega}_2 \cdot \mathbf{J}_2 .$$

It describes rotation of the two independent angular momenta $\mathbf{J}_1$ and $\mathbf{J}_2$ with the constant length $j+\frac{1}{2}$ around the vectors $\boldsymbol{\omega}_1$ and $\boldsymbol{\omega}_2$, respectively. Their projections,

$$\begin{aligned} J_{1,1} &= (\mathbf{J}_1 \cdot \boldsymbol{\omega}_1)/\omega_1 , \\ J_{2,2} &= (\mathbf{J}_2 \cdot \boldsymbol{\omega}_2)/\omega_2 , \end{aligned}$$

are integrals of motion. In the quantum-mechanical approach these integrals can take either integer or half-integer values equal to the quantum numbers of the Stark-Zeeman state:

$$J_{1,1} = k_1 , \quad J_{2,2} = k_2 .$$

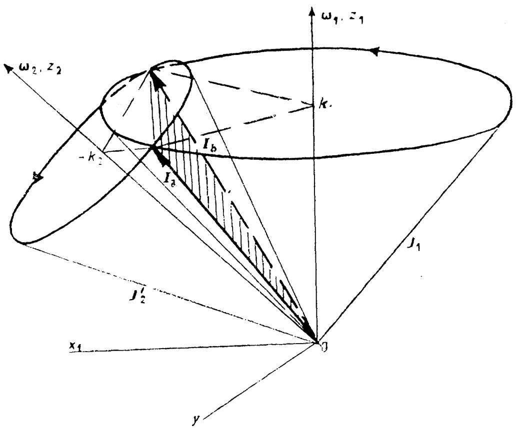

FIG. 26. The vector model of radiation of the hydrogen atom in crossed electric and magnetic fields. From Braun (1991b).

It is convenient to introduce the vector $\mathbf{J}_2' = -\mathbf{J}_2$, which also rotates around $\boldsymbol{\omega}_2$; its projection on $\boldsymbol{\omega}_2$ is $-k_2$. The two cones described by $\mathbf{J}_1$ and $\mathbf{J}_2'$ are shown in Fig. 26.

Consider the light emission of a highly excited hydrogen atom in crossed fields leading to a transition to a low-lying state. Because of the angular momentum selection rules, the transition can take place only if the Kepler orbit modeling the perturbed Rydberg state is in the linear phase of its field-induced evolution, i.e., when $\mathbf{L}=0$ or $\mathbf{J}_1 = \mathbf{J}_2'$. Denoting the common value of $\mathbf{J}_1$ and $\mathbf{J}_2'$ by $\mathbf{I}$, we see that there are two such vectors, $\mathbf{I}_a$ and $\mathbf{I}_b$, directed along the lines showing the crossing of the two cones in Fig. 26; they are symmetrically placed with respect to the plane of the fields.

Thus when we study transitions to the low-lying levels we get a "stroboscopic" picture of the upper state, observing it when the corresponding Kepler orbit is linear and directed either along $\mathbf{I}_a$ or along $\mathbf{I}_b$. We obtain a model of two identical radiating linear vibrators directed along $\mathbf{I}_a$ and $\mathbf{I}_b$, with equal amplitudes but shifted phase. For a given level $E^{(1)}_{k_1 k_2}$ the orientation of the two corresponding vectors is fixed by their projections on $\boldsymbol{\omega}_1$ and $\boldsymbol{\omega}_2$:

$$I_{a,1} = I_{b,1} = k_1 , \quad I_{a,2} = I_{b,2} = -k_2 .$$

Once this model is adopted it leads to important conclusions.

(a) The cones in Fig. 26 may cross or not, depending on the value of k_1, k_2, and δ. The noncrossing of the cones means that the angular momentum of the Rydberg state never approaches zero. Consequently the transition to the low-lying levels will be classically forbidden; if $n \gg 1$ its probability will be extremely small.[8]

---

[8] Similar arguments were used by Penent *et al.* (1988) in estimates of the quantum defect shifts of nonhydrogenic Rydberg atoms in orthogonal fields.

Let us depict the Stark-Zeeman states of the nth shell by the integer or half-integer points in the k_1k_2 plane. These points fill an $n \times n$ square whose sides are parallel to the coordinate axes (Fig. 27). It may be shown that the cones in the vector diagram Fig. 26 cross, provided the following inequality is fulfilled:

$$\left[\frac{k_1+k_2}{\sin(\delta/2)}\right]^2+\left[\frac{k_1-k_2}{\cos(\delta/2)}\right]^2<n^2 . \qquad (4.23)$$

This is the equation of an ellipse inscribed into the square in Fig. 27, the axes of the ellipse being the diagonals of the square. The points outside the ellipse correspond to the levels $E^{(1)}_{k_1k_2}$ of the multiplet classically inaccessible by radiative transitions from the low-lying atomic levels.

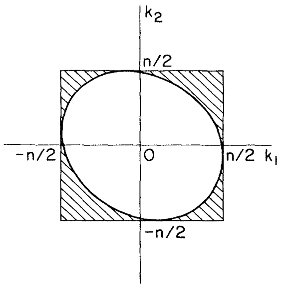

FIG. 27. The ellipse of classically allowed values of the quantum numbers k_1,k_2 in the radiative transitions between the Rydberg Stark-Zeeman levels $E^{(1)}_{k_1k_2}$ and the low-lying levels. The spectral lines with the upper-state quantum numbers depicted by a point in one of the hatched areas have exponentially low intensity if $n \gg 1$. From Braun (1991b).

As an example in Table II we present the relative oscillator strengths $f_{1s-nk_1k_2}/f^{(0)}_{1s-np}$ of the Lyman series transitions to the Stark-Zeeman levels, for the case in which $n=21$ and $\delta=80°$ (here $f^{(0)}_{1s-np}$ is the oscillator strength of the $1s-np$ transition in the unperturbed hydrogen). Results are given for the non-negative k_1 and k_2, i.e., the first quadrant in the square in Fig. 27. The dashed curve indicates the position of the elliptic boundary following from Eq. (4.23). Note the rise in intensity near the inner side of this boundary, in accordance with its role of a caustic, and rapid extinction beyond it.

(b) The radiation emitted by the atom is symmetrical with respect to the plane containing the vectors $\mathbf{I}_a$ and $\mathbf{I}_b$. If the line of observation lies in this plane, the light is

TABLE II. Relative intensities for the Lyman series ($\times 10^4$) of transitions to the levels with non-negative k_1,k_2 of atomic hydrogen in crossed fields, when $\delta=80°$, $n=21$. The dashed curve indicates the boundary of the classically allowed area of the quantum numbers; the underlined values mark the strongest transition in each row.

k_2 k_1	0	1	2	3	4	5	6	7	8	9	10
0	83	6.0	83	10	81	24	72	56	59	105	179
1	6.0	86	4.8	82	22	65	54	59	59	148	124
2	83	4.8	81	27	53	63	48	60	90	156	73
3	10	82	27	48	69	40	61	68	131	124	36
4	81	22	53	69	39	59	63	106	137	76	15
5	24	65	63	40	59	63	95	134	99	35	4.7
6	72	54	48	61	63	95	132	108	50	12	1.2
7	56	59	60	68	106	134	108	55	17	3.0	0.23
8	59	59	90	131	137	99	50	17	3.8	0.51	0.031
9	105	148	156	124	76	35	12	3.0	0.51	0.054	0.0026
10	179	124	73	36	15	4.7	1.2	0.23	0.031	0.0026	0.0001

linearly polarized, otherwise it is elliptically polarized.

The semiclassical approximation for the coefficients C_{lm} following from the well-known asymptotic expressions for the factors in Eq. (4.22) turns out to be full agreement with our vector model. It is an obvious extension of Eqs. (4.10) and (4.20) of the previous section to the axially nonsymmetric case:

$$C_{lm}=\sqrt{\Delta\Omega}[\,Y^*_{lm}(\vartheta_a,\varphi_a)e^{iS}+Y^*_{lm}(\vartheta_b,\varphi_b)e^{-iS}] \, . \tag{4.24}$$

The arguments of the spherical functions are the spherical angles of the vectors $\mathbf{I}_a$ and $\mathbf{I}_b$; S is the semiclassical phase. The quantity $\Delta\Omega$ is expressed through the Jacobian of ϑ_a, φ_a by k_1 and k_2:

$$\Delta\Omega=\sin\vartheta_a\frac{\partial(\vartheta_a,\varphi_a)}{\partial(k_1,k_2)} \, .$$

This is the solid angle of the directions of the vector $\mathbf{I}_a$ corresponding to a unit area in the k_1k_2 plane, i.e., to a single state of the Stark-Zeeman multiplet of the nth shell [compare with Eq. (4.19)]. The quantities S and $\Delta\Omega$ are functions of k_1, k_2, and δ; their expressions can be found in Braun (1991b).

Equation (4.24) represents C_{lm} as a sum of two probability amplitudes, created by the multipoles determined with respect to the directions $\mathbf{I}_a$ and $\mathbf{I}_b$. The oscillator strengths, which are proportional to $|C_{lm}|^2$, contain, apart from the (a) and (b) contributions, an interference term depending on the large phase difference $2S$. The changes of the quantum numbers k_1 and k_2 by 1, or of the angle δ between the vectors ω_1 and ω_2 by a small quantity of the order π/n lead to changes comparable to π of this phase difference.

Interference between the two vibrators is the obvious reason for the violent oscillations of intensities accompanying even small variations in the relative strength and geometry of the crossed fields (Fig. 28); it is also responsible for large variations in the probability of transitions from states with close k_1 and k_2 (Table II). Certain polarization properties of the light emitted by the atom are independent of S; these properties are much less sensitive to variations of k_1, k_2, and the fields.

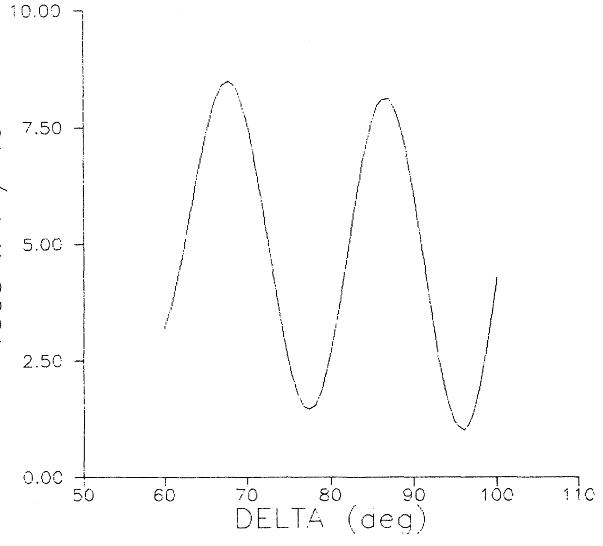

FIG. 28. Relative intensity of the Lyman series spectral line $1s-\Psi_{nk_1k_2}$ in crossed fields, $n=21$, $k_1=3$, $k_2=2$, as a function of the angle δ. From Braun (1991b).

When the fields are orthogonal we have to take second-order perturbations into account if we want to determine the zero-order eigenfunctions and the oscillator strengths. An analytical description of the intensity distribution in this case has not yet been reported. Simple results have been obtained (Braun, 1991b) for the total transition probability connected with quasidegenerate first-order levels.

V. NONHYDROGENIC RYDBERG ATOMS IN EXTERNAL FIELDS

The analytical studies of Rydberg atoms in external fields have concentrated mainly on the hydrogen atom. On the other hand most of the experiments have been carried out on the nonhydrogenic Rydberg atoms. The presence of a core leads to serious changes in the pattern of field-induced splitting and in the intensity distribution.

One of the merits of the discrete WKB method is the ease with which core effects can be taken into account. In doing so there is no need to introduce any specific model for the core potential, since the results are expressed in terms of the quantum defects of the unperturbed atom.

A. The quadratic Zeeman effect in highly excited alkali-metal atoms

The quantum defects δ_l of alkali-metal atoms, which are comparable to unity when l is small, quickly subside with the growth of l [see Table III, where their values corresponding to $n\to\infty$ and reduced to the interval $(-\frac{1}{2},\frac{1}{2})$ are given]. In a comparatively weak magnetic field the levels with small l can be considered isolated. Their diamagnetic shift is found by averaging the operator Eq. (1.1) over the unperturbed atomic orbital. The states of a free atom with larger l are almost degenerate

TABLE III. Quantum defects of alkali-metal atoms reduced to the interval $(-0.5,0.5)$ [after Lindgard and Nielsen (1977)].

			δ_l		
	s	p	d	f	g
Li	0.40	0.05	0.002	0	0
Na	0.35	−0.14	0.015	0.002	0
K	0.18	−0.28	0.26	0.009	0
Rb	0.14	−0.35	0.34	0.015	0
Cs	0.06	−0.44	0.48	0.032	0.005

and are heavily mixed by the external field. The numerical methods for calculating the quadratic Zeeman energies are considered by O'Mahony and Taylor (1986a,1986b); see also the review of O'Mahony (1988). We shall describe here the semiclassical treatment of the problem (Braun, 1983b,1990b).

Let us use the perturbation theory for a group of close levels and suppose that $|m| \ll n$ (otherwise the spectrum is exactly like that of hydrogen). Developing the zero-order eigenfunctions in the basis set of orbitals of the free atom, we obtain the three-term recursion relation

$$p_l C_{l-2} + (w_l + E_{nl}^{(0)} - E')C_l + p_{l+2} C_{l+2} = 0 \ . \tag{5.1}$$

Its difference from Eq. (1.4) is in the core-induced shifts $E_{nl}^{(0)} = -\delta_l / n^3$ present in the diagonal terms.[9]

Only a tiny fraction of the equations of the three-term recursion relation (5.1) is spoilt by the presence of phase shifts. Indeed, for $l > l_0$ where $l_0 = 1-3$ depending on the atom, the quantum defects δ_l and the energies $E_{nl}^{(0)}$ are practically zero. Therefore the hydrogenic WKB solution (3.19), which is valid only if l is large enough, remains valid for the nonhydrogenic atoms; what differs is the value of the phase χ^{WKB}.

Further treatment is best demonstrated by a specific example. Consider the lithium atom's diamagnetic splitting in the case $m = 0$, beginning with the even part of the spectrum. The quantum defect of the *ns* state is so large (0.4) that in the *l*-mixing magnetic field it is not appreciably intermixed with the rest of the manifold; its diamagnetic shift is found as the average of the diamagnetic operator. On the other hand, states with $l \geq 2$ are almost perfectly hydrogenic. Therefore the corresponding even eigenvalues can be found by diagonalizing the diamagnetic operator in the incomplete manifold of orbitals of the *n*th shell of the hydrogen atom with the *ns* orbital excluded. This "truncated basis set" approximation has been extensively used in the theory of perturbed Rydberg atoms (Braun, 1983b; Fabre *et al.*, 1984; Penent *et al.*, 1988). In this approximation the coefficients C_l can be found from the purely hydrogenic TTR relation (1.4), starting with the equation with $l = 2$, in which one should set $C_0 = 0$.

In the case of hydrogen the analytical solution of Eq. (1.4) with small l was given by the Legendre solution (3.20). However, this TTR relation also has a second, irregular, solution proportional to the functions ($\cos\vartheta_0 = \sqrt{1-\varepsilon}$, $\varepsilon = E'/u_\gamma$),

$$\mathcal{Q}_{lm} = \frac{2}{\pi}\left[\frac{2l+1}{2}\,\frac{(l-|m|)!}{(l+|m|)!}\right]^{1/2} Q_{lm}(\cos\vartheta_0) \ , \tag{5.2}$$

where Q_{lm} are the second-order Legendre functions. Normalization is carried out in such a way that the asymptotic expression for $\mathcal{Q}_{lm}$ differs from that of $\mathcal{P}_{lm}$ given by Eq. (3.21) only by an additional phase shift $\pi/2$ in the cosine argument. The sequence $\mathcal{Q}_{lm}$ satisfies the equations of the TTR relation (1.4) with $l \ll n$ except for the initial one, with $l = |m|$. In the case of nonhydrogenic atoms this initial equation is either absent or distorted. Therefore we have to include $\mathcal{Q}_{lm}$ in the general solution, writing it as

$$C_l = A\,[\cos\chi\,\mathcal{P}_{lm}(\cos\vartheta_0) + \sin\chi\,\mathcal{Q}_{lm}(\cos\vartheta_0)] \ . \tag{5.3}$$

The constant phase χ determines the contents of the irregular solution.

Considering the even states of Li with $m = 0$, we obtain the value of χ from the condition $C_0 = 0$, which gives

$$\cot\chi = -\frac{\mathcal{Q}_{00}}{\mathcal{P}_{00}} = -\frac{2}{\pi}\operatorname{arctanh}\sqrt{1-\varepsilon} \ . \tag{5.4}$$

After χ is fixed, matching the solution of Eq. (5.3) with the WKB solution (3.19) provides the WKB phase

$$\chi^{\mathrm{WKB}} = -\frac{\pi}{4} + \frac{|m|\pi}{2} + \chi \ . \tag{5.5}$$

The remaining steps are the same as in the case of atomic hydrogen (Sec. III.C). The phase χ finds its way into the quantization condition for the eigenvalues, which differs from the hydrogenic rule [Eq. (3.23), upper sign] by an additional term, $-\chi(\varepsilon)$, in its right-hand side. Its presence leads to a shift of the even levels, compared with the respective quadratic Zeeman levels of atomic hydrogen, by

$$E'_{\mathrm{Li}} - E'_{\mathrm{H}} = -\frac{\chi}{\pi}\Delta E' \ , \tag{5.6}$$

where $\Delta E'$ is the spacing between even levels in hydrogen. The shift (5.6) varies from 0 to $\Delta E'/2$ as we move from the bottom to the top of the multiplet. Note that in the truncated basis approximation the splitting pattern does not depend on the field strength.

The behavior of the odd levels is more complicated, due to the small but significant quantum defect of the *np* state ($\delta_1 = 0.053$). In very weak fields the *np* level can be considered to be isolated and not taking part in the *l* mixing; the rest of the levels formed from the odd states with $l \geq 3$ can be found in the truncated basis approximation. At the other extreme (fields strong enough to be on the verge of the *n*-mixing regime), the energy gap between the *np* level and the rest of the odd levels becomes insignificant compared with the diamagnetic splitting, and the spectrum becomes almost hydrogenlike. Core effects can then be considered as small perturbations (Komarov *et al.*, 1980).

In intermediate fields the solution has to be sought in the form (5.3). The angle χ is a function of E'; it is fixed by the requirement that Eq. (5.3) satisfy the equation of the TTR relation (5.1) with $l = 1$. The result is

$$\cot\chi = -\frac{E_{n1}^{(0)}\mathcal{P}_{10}}{(w_1 + E_{n1}^{(0)} - E')\mathcal{Q}_{10} + p_3\mathcal{Q}_{30}} \ . \tag{5.7}$$

---

[9] The matrix elements of the diamagnetic operator are also slightly different from those given in Eq. (1.5), but this distinction is of secondary importance.

The quantization condition is the same as for the odd states of atomic hydrogen [Eq. (3.23), lower sign] except for the additional term $-\chi$ in the right-hand side. The energy shifts of the Zeeman levels with respect to those of atomic hydrogen are given by Eq. (5.6).

The emerging picture of quadratic Zeeman splitting in atomic lithium with $m=0$ is heavily distorted compared with atomic hydrogen (Fig. 29; compare with Fig. 1). A particularly striking feature is the presence of *g-u* doublets in the upper part of the multiplet instead of the local equidistance of the levels characteristic of atomic hydrogen. The reason for this is that the core-induced shift of the even levels is much greater because it is connected with the huge quantum defect of the *ns* states. More formally, it follows from the fact that the phase χ of the even and odd solutions with close energies differs by about 90° (Braun, 1983b). According to Eq. (5.6) this means that the shifts of the even and odd levels differ by $\Delta E'/2$. This value is equal to the spacing between levels of opposite parity in the upper part of the quadratic Zeeman multiplet in atomic hydrogen, hence the formation of the doublets.

This approximate pairwise degeneracy of the quadratic Zeeman levels in the upper part of the multiplet was experimentally confirmed by Cacciani *et al.* (1986a,1988a). It was also demonstrated in experiments showing the avoided crossings of levels originating in adjacent shells of the lithium atom, when the atoms were subjected to a magnetic field strong enough to cause n mixing and a weak parallel electric field (Cacciani *et al.*, 1989).

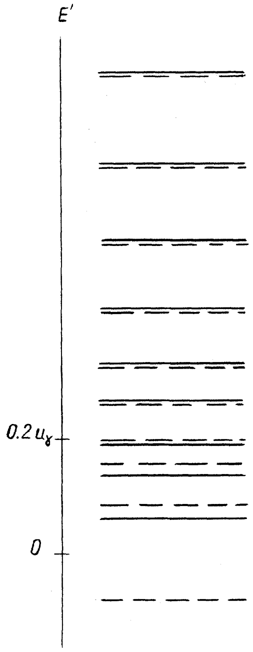

FIG. 29. Quadratic Zeeman splitting of the levels of atomic lithium with $n=20$, $m=0$ in a magnetic field $H=4.7$ T ($E_{n1}^{(0)}/u_\gamma=-0.33$). Solid and dashed lines correspond to even and odd levels.

The situation described for the lithium atom is typical of other alkali-metal atoms. The quantum defects δ_l become small beginning with a certain l_0, so that δ_{l_0+1} is practically zero while δ_{l_0-1} is comparable to unity ($l_0=1$ for Li, 2 for Na, and 3 for the rest of the alkali-metal atoms). Levels with the same parity as l_0+1 can be found in the truncated hydrogen-atom basis approximation from which the orbitals with $l<l_0+1$ have been dropped. The phase χ in Eq. (5.3) for these states is found from the condition $C_{l_0-1}=0$ (supposing that $|m|\le l_0$; otherwise the spectrum is exactly hydrogenic).

States of the same parity as l_0 are practically hydrogenic if the diamagnetic splitting is large compared with $E_{nl_0}^{(0)}$. Otherwise the phase χ is obtained by inserting Eq. (5.3) into the equation of the TTR relation (5.1) with $l=l_0$ in which case C_{l_0-2} should be set to zero.

Our treatment has been based exclusively on the approximation of a single shell. In a strong enough field, n-mixing effects tend to smooth out the nonhydrogenic features of the spectrum (Cacciani *et al.*, 1988a). In order to appreciate the impact of this n mixing, it might be useful to explore the effective operator giving the higher-order corrections associated with the diamagnetic perturbation (Delande and Gay, 1984).

B. Intensities in the quadratic Zeeman splitting of alkali-metal atoms

In the preceding section we obtained Eq. (5.3) for the coefficients of the zero-order eigenfunctions in the basis set of the unperturbed orbitals of the valence electron. The normalizing constant A in this equation is determined by matching with the WKB solution (3.19), whose normalizing constant is expressed through the energy spacings $\Delta E'$. The result is the same as for atomic hydrogen,

$$A=\frac{(\Delta\varepsilon)^{1/2}}{(1-\varepsilon)^{1/4}}\ ,$$

$$\varepsilon=E'/u_\gamma,\quad \Delta\varepsilon=\Delta E'/u_\gamma\ .$$

Inserting A and χ into Eq. (5.3) gives C_l as a function of ε, which can be used to obtain the oscillator strengths of transitions to the low-lying levels.

An analytical study of intensities in the quadratic Zeeman effect of atomic lithium was made by Braun (1990b). The lower state was assumed to be the ground $1s^22s$ state, so that only the odd sublevels of the Zeeman multiplet were important. The oscillator strengths within each multiplet were proportional to the contents of the *np* orbital in the wave functions of the levels. Using Eq. (5.7) and the similar result for the case $|m|=1$, Braun obtained the following expressions. They give the oscillator strength distribution in the interval

$$(-1/2n^2+mH/2c,\,-1/2n^2+mH/2c+u_\gamma)$$

of energies of the upper level or, in terms of the reduced energy correction, in the interval $0<\varepsilon<1$:

$$(C_1^2)_{\mathrm{Li}}=(C_1^2)_{\mathrm{H}}M_m(\varepsilon)\ . \tag{5.8}$$

Here $(C_1^2)_{\mathrm{H}}$ are the Eqs. (4.4) for the intensities in the Lyman series of atomic hydrogen. The factor M_m reflects the impact of the quantum defect of the np state. If we denote

$$x=\sqrt{1-\varepsilon},\quad \varepsilon_1^{(0)}=E_{n1}^{(0)}/u_\gamma\ ,$$

the factors M_m for $m=0$ and 1 can be written

$$\begin{aligned} M_0&=\left\{[1+3\varepsilon_1^{(0)}(x\ \mathrm{arctanh}x-1)]^2+\left[\frac{3\pi x}{2}\varepsilon_1^0\right]^2\right\}^{-1},\\ M_1&=\left\{\left[1+\frac{3}{2}\varepsilon_1^{(0)}\left[\frac{\varepsilon}{x}\mathrm{arctanh}x+1\right]\right]^2+\left[\frac{3\pi\varepsilon}{4x}\varepsilon_1^{(0)}\right]^2\right\}^{-1}. \end{aligned} \tag{5.9}$$

Equations (5.8) and (5.9) describe the transformation of the oscillator strengths with changes in the magnetic field. In very weak fields, the parameter $\varepsilon_1^{(0)}$ is large and M_0 and M_1 are small. Indeed, in weak fields almost all of the spectral intensity goes to the perturbed np level, while the rest of the quadratic Zeeman lines have very low intensity.

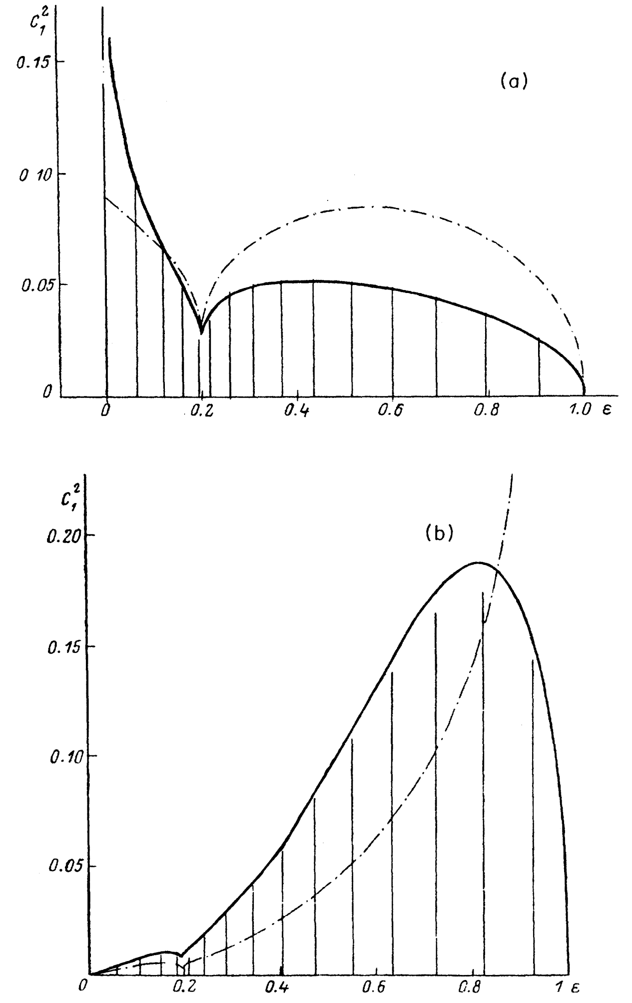

FIG. 30. Analytical oscillator strength profiles in the quadratic Zeeman multiplet of atomic lithium (solid line) compared with those of the Lyman series transitions of atomic hydrogen, (dashed line) $n=30$, $H=1.65$ T: (a) $m=0$; (b) $m=1$. From Braun (1990b).

In stronger fields the intensity is more evenly distributed along the multiplet, and the oscillator strength profile becomes more hydrogenlike. However, there are important differences. First the bulk of the intensity is shifted to lower energies (Fig. 30). Then there are specific changes in the form of the intensity plots. The most obvious of these is observed in the σ spectra $(m=\pm1)$ close to the high-energy edge of the multiplet $(\varepsilon\rightarrow1)$: instead of the hydrogenic monotonic growth as $(1-\varepsilon)^{-1/2}$, the oscillator strengths reach maximum and then go down as $(1-\varepsilon)^{1/2}$. On the other hand, the behavior of the intensi-

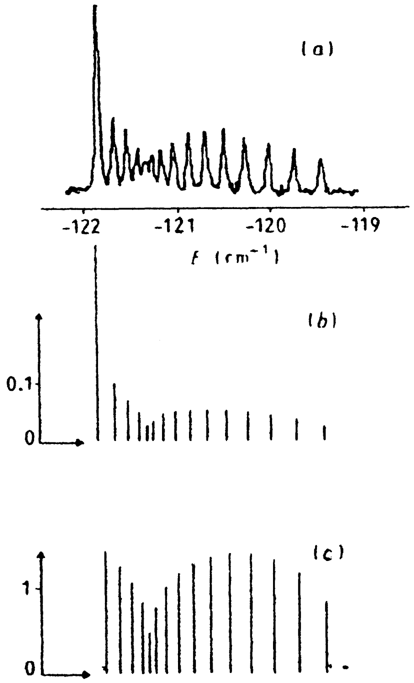

FIG. 31. Excitation spectrum for the $n=30$, $m=0$ odd diamagnetic spectrum of lithium, $H=1.65$ T: (a) experimental recording for lithium; (b) numerically calculated spectrum for lithium; (c) calculated spectrum for hydrogen. From Cacciani *et al.* (1988a).

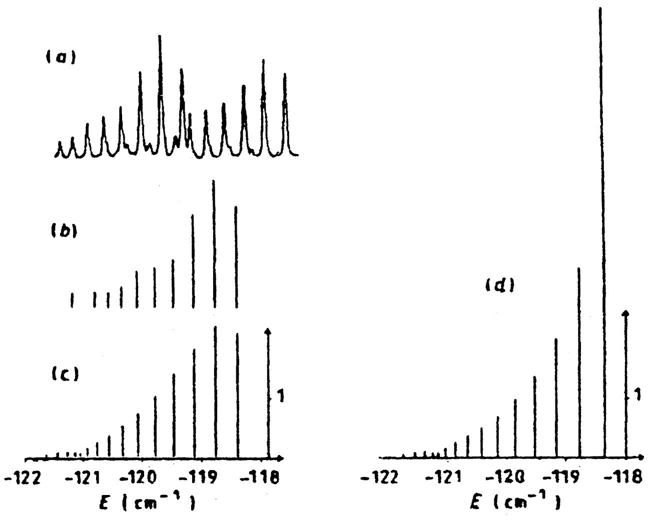

FIG. 32. The $n=30$, $m=1$ odd diamagnetic manifold: (a) Experimental spectrum for lithium at $H=1.94$ T composed of two spectra shifted by double the Larmor frequency. (b) Experimental spectrum for lithium obtained by eliminating in (a) the contribution of the paramagnetic interaction. (c) Theoretical spectrum numerically calculated for lithium by disregarding the paramagnetic term. (d) Theoretical spectrum calculated for hydrogen by disregarding the paramagnetic term. From Cacciani *et al.* (1988a).

ties close to the singularity $\varepsilon=0.2$ ($\Lambda=0$) remains unchanged, because this singularity, associated with near-maximal l components of the wave function, does not feel the presence of the core.

Our results are in good agreement with the experimental findings of Cacciani *et al.* (1986a,1988a). In these studies atomic lithium was optically excited to states with n close to 30. The fields were about 1.6–2.5 T, which corresponds to values of the parameter $\varepsilon_1^{(0)}$ in the range -0.16 to -0.08. The observed intensity profiles were indeed characterized by the nonhydrogenic peculiarities mentioned here; see Figs. 31 and 32.

In more complex atoms, deviations from the hydrogenic pattern of intensity distribution may be more pronounced. It can be seen in the results of Rinneberg *et al.* (1987), who measured the spectra of highly excited atomic barium with $n=78$, $m=0$ in the l-mixing magnetic field (Fig. 33). The oscillator strength distribution strongly differed from its hydrogenic prototype [the Balmer series transitions with $m=0$; see Eq. (4.6) and Fig. 20(c)]. In particular, the intensity went to zero at the high-frequency edge. Interestingly, some of the hydrogenic peculiarities remained, including the minimum at $\varepsilon=0.2$ and the zero value of the intensity inside the multiplet; the latter is characteristic of the Balmer series transitions to the Rydberg states with $m=0$.

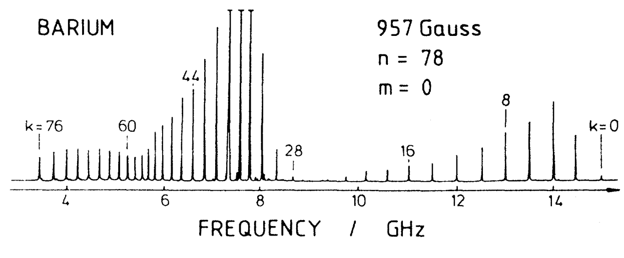

FIG. 33. Spectrum of the $n=78$, $m=0$ diamagnetic manifold of barium. $H=957$ Gauss. From Rinneberg *et al.* (1987). (The label k denotes the quadratic Zeeman levels in order of decreasing energy, beginning with $k=0$ for the level at the top.)

C. Alkali-metal Rydberg atoms in an electric field and in combined electric and magnetic fields

1. Electric field only

The Stark effect in the nonhydrogenic Rydberg atoms has been extensively studied both theoretically and experimentally (Zimmerman *et al.*, 1979; Fabre *et al.*, 1984; Mur and Popov, 1988; O'Mahony, 1988; Chardonnet *et al.*, 1989). The analytical theory of the effect (Harmin, 1984) uses separation of variables in the parabolic coordinates in the problem of atomic hydrogen in an electric field. Here for the sake of completeness we describe the discrete WKB approach to the problem (Braun, 1986).

Once more we use the fact that there is a number l_0 dividing orbitals of the free atom with huge quantum defects ($l<l_0$) from those which are practically hydrogenlike ($l>l_0$). The zero-order eigenfunction contains the components with $l\geq l_0$. The coefficients in its development satisfy the recursion relation whose first equation is

$$(E_{nl_0}^{(0)}-E')C_{l_0}+q_{l_0+1}C_{l_0+1}=0\ . \tag{5.10}$$

Other equations are totally hydrogenlike:

$$q_lC_{l-1}-E'C_l+q_{l+1}C_{l+1}=0\ .$$

Here q_l are the matrix elements of the operator Fz given by Eq. (4.13).

The coefficients C_l with $l_0\leq l\ll n$ are given by a combination of Legendre functions (5.3). The phase χ is obtained by substituting Eq. (5.3) into Eq. (5.10). After that the Legendre solution should be matched to the WKB solution (3.19), in which one should set

$$\theta=\arccos\frac{E'}{2q_{l+\frac{1}{2}}}\ .$$

The matching determines the value of the WKB phase and leads to the quantization rule. Denoting $e=2E'/3nF$, we have

$$ne=\frac{2}{\pi}\chi(\varepsilon)+\begin{cases}2N, & n+m\ \text{odd}\ ,\\ 2N+1, & n+m\ \text{even}\ .\end{cases} \tag{5.11}$$

In the case of hydrogen $\chi=0$. The shift of the Stark levels of the alkali-metal atom compared with the corresponding levels of atomic hydrogen is approximately equal to

$$E'-E'_H=\frac{3\chi F}{\pi} .$$

An expression for the phase χ through the Legendre functions of the scaled energy e is given by Braun (1986). The oscillator strengths can be calculated using Eq. (5.3), in which the normalizing constant is now equal to $A=n^{-1/2}$.

2. Parallel electric and magnetic fields

Experiments on Rydberg atoms in parallel electric and magnetic fields were carried out on atomic barium by Rinneberg *et al.* (1986) and König *et al.* (1988) and on atomic lithium by Cacciani *et al.* (1986c,1988c,1989). Generally the spectra were similar to that of atomic hydrogen. In particular, anticrossings were observed in the part of the multiplet where groups I and II of levels overlapped. The positions of the anticrossings were almost exactly as given by our Eq. (3.29). However, their width was much greater than in hydrogen, indicating strong coupling between the states of groups I and II caused by the presence of the core.

[The tendency of the core field to couple states connected with isolated classical phase trajectories was also obvious in the observations of anticrossings between the quadratic Zeeman levels of atomic lithium belonging to adjacent shells (Cacciani *et al.*, 1986c). Instead of the exponentially small anticrossing widths characteristic of atomic hydrogen, the widths in the case of lithium were much larger and decreased according to a power law when n was increased.]

The semiclassical theory of the Stark-Zeeman effect in the alkali-metal atoms is laid down in Braun (1989b). The object studied is the five-term recursion relation for the coefficients C_l of the zero-order eigenfunction. It differs from Eq. (4.12) by the presence of quantum defect shifts in the diagonal matrix elements. The form of the solution depends on the energy correction range. In the lower part of the multiplet, where only the levels of group I are present (cf. Sec. III.D), the coefficients C_l with $l \ll n$ are given by Eq. (5.3). This treatment led to a formula for the energy levels and the oscillator strengths similar to the pure Stark-effect case.

In the intermediate part of the multiplet, where groups I and II of levels overlap, the situation is more complicated. In the case of hydrogen this was the energy range where two isolated phase trajectories $\theta(L)$ existed. Because of the presence of the core it is now inadmissible to quantize the movement along these trajectories independently. Accordingly the solution of the five-term recursion relation in the range $l \ll n$ should be sought in the form

$$C_l=\sum_{s=\mathrm{I,II}} A^{(s)}[\cos\chi^{(s)}\mathcal{P}_{lm}(\cos\vartheta_0^{(s)})+\sin\chi^{(s)}\mathcal{Q}_{lm}(\cos\vartheta_0^{(s)})] . \tag{5.12}$$

Here ϑ_0^{I} and $\vartheta_0^{\mathrm{II}}$ are the two roots of Eq. (4.14), giving the polar angles of the Kepler orbit of the atomic electron at the moments when it degenerates into a line.

The constants A^{I} and A^{II} determine the probability amplitudes of the system moving along the respective phase trajectories, i.e., localized in the left or the right potential well in Fig. 14(a). These constants are obtained simultaneously with the energy spectrum by matching Eq. (5.12) with the WKB solution and using the second matching condition as the right turning point of the angular momentum.

Here are some of the results obtained for atomic lithium with $m=0$ in the truncated basis approximation (the *ns* orbital is dropped from the basis set, while the orbitals with $l \geq 1$ are considered to be exactly hydrogenic). Let us introduce notations for the functions of the reduced energy correction and the parameter β determined by Eq. (3.28):

$$\Phi=\frac{1}{\pi}\ln\frac{(\sqrt{1+\beta^2-\varepsilon}+1)^2-\beta^2}{(\sqrt{1+\beta^2-\varepsilon}-1)^2-\beta^2} ,$$

$$y=\Phi\sin\sqrt{5}\pi n\beta .$$

The equation for the probabilities $(A^{\mathrm{I}})^2$ and $(A^{\mathrm{II}})^2$ has the form

$$\frac{(A^{\mathrm{I}})^2-(A^{\mathrm{II}})^2}{(A^{\mathrm{I}})^2+(A^{\mathrm{II}})^2}=\pm\frac{y}{\sqrt{1+y^2}} . \tag{5.13}$$

The function y rapidly oscillates when β is increased, due to the presence of the large factor n in the argument of the sine. As a result, the ratio of components I and II in the wave function oscillates with the period $2/n\sqrt{5}$ when β is increased. Consequently the atomic properties should also oscillate when the electric field is increased. In particular, there should be oscillations of the line intensities, which indeed were observed by Cacciani *et al.* (1988c).

At the avoided crossing ($\sqrt{5}\beta n=1,2,3,\ldots$), one of the participating states has $A^{\mathrm{I}}=A^{\mathrm{II}}$ while for the other $A^{\mathrm{I}}=-A^{\mathrm{II}}$. This means that at the anticrossing one of the spectral lines attains maximal intensity while the other one disappears.

The distance between the levels at the anticrossing is

$$\Delta E_{nl}=\frac{\arctan\Phi}{\pi}\Delta E' , \tag{5.14}$$

where $\Delta E'$ is the spacing in one of the two overlapping spectra in the case of atomic hydrogen. When β is small, ΔE_{nl} becomes equal to the shift of the Li-atom even quadratic Zeeman levels compared with the corresponding levels of atomic hydrogen.

Provided $\beta<1$, the states of group III occupying the upper part of the multiplet are described by Eq. (5.12) with $A^{\mathrm{I}}=\pm A^{\mathrm{II}}$, the signs alternating from level to level. There is no oscillation of the atomic properties with growth of the electric field; instead these properties alternate when we move from level to level down the multiplet.

A plot of the eigenvalues calculated in the truncated basis approximation as functions of β is shown in Fig. 34; it closely resembles the experimental plots of the energies versus the electric field obtained by Rinneberg *et al.* (1986) and Cacciani *et al.* (1988c).

An interesting peculiarity connected with group-III levels of atomic lithium was observed by Cacciani *et al.* (1988c). Every second level of this group was virtually unmoved by the presence of the core, occupying almost exactly the same position as the corresponding Stark-Zeeman level of atomic hydrogen. That would be understandable if the magnetic field alone were present, because the odd levels would not feel the huge quantum defect of the *ns* state. However, it is not immediately clear why this situation persists even in the presence of a strong parity-breaking electric field.

The explanation lies in the peculiar property of the hydrogen atom states in parallel electric and magnetic fields (Braun, 1991a): every second state of group III is almost exactly orthogonal to the *ns* orbital. This follows from Eq. (4.20) in the case $l=0$, when the two terms in this equation cancel each other (provided the sign in it is minus).

This property has nothing to do with the approximate parity conservation. In the example given by Braun (1991a; $\beta=0.5$, $n=30$, $m=0$), the hydrogenic eigenfunction of one of the Stark-Zeeman levels had the following coefficients at the *ns*, *np*, and *nd* orbitals, respectively:

$$C_0=0.11\times 10^{-5},\quad C_1=-0.220,\quad C_2=-0.426\ ,$$

with the amplitudes of the *s* and *d* components differing by five orders of magnitude.

It follows that every second level of group III cannot react to the quantum defect of the *ns* state. Its energy would have been exactly the same as that of the corresponding level of atomic hydrogen had there not been the small quantum defect in the *np* state. The same situation holds, for the same reasons, at the anticrossings in the lower part of the multiplet: the energy of one of the participating levels is almost the same as that of the corresponding level in atomic hydrogen, while the other level takes the whole of the phase shift (5.14).

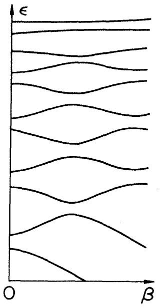

FIG. 34. Calculated Stark-Zeeman levels of atomic lithium in parallel electric and magnetic fields as functions of the scaled electric field. $n=30$, $m=0$. From Braun (1989b).

3. Orthogonal fields

The nonhydrogenic atoms in *l*-mixing orthogonal electric and magnetic field were experimentally studied by Korevaar and Littman (1983; sodium in the state with $n=12$) and Penent *et al.* (1984,1988; rubidium with *n* up to 40). Other experiments on atoms in crossed fields involved either low-excited atoms (Windholz, 1990) or atoms far into the *n*-mixing regime (Fauth *et al.*, 1987; Raithel *et al.*, 1991).

In the case of atomic hydrogen, first-order splitting in orthogonal fields led to $2n+1$ equidistant levels $E_q^{(1)}$, $q=-(n-1),-(n-2),\ldots,n-1$, each of which was $n-|q|$ times degenerate. The origin of this degeneracy was the special symmetry of the problem (Nikitin and Ostrovsky, 1982; Gay, 1986). In the nonhydrogenic atoms the Coulomb field is distorted by the presence of the core, and this symmetry is lost. Therefore one might expect that even first-order splitting in a crossed field would bring about complete lifting of degeneracy. This, however, is not true. As shown by Braun (1985), when $n\gg 1$ the overwhelming majority of the Stark-Zeeman states have the same energy as the corresponding states of atomic hydrogen in orthogonal fields; the degeneracy of the first-order levels is diminished but does not disappear.

The reason behind this is that the quantum defects of nonhydrogenic atoms differ from zero only for a limited number of states with $l\le l_0$, where l_0 is of the order of unity and depends on the atom. Indeed, consider some level $E_q^{(1)}$ of atomic hydrogen in orthogonal fields. Transforming the manifold of the degenerate eigenfunctions belonging to $E_q^{(1)}$, we can separate the subspace orthogonal to all the unperturbed spherical orbitals with $l\le l_0$. Obviously none of the states in this subspace would react to the introduction of the quantum defects δ_l for $l\le l_0$. Therefore they will not feel the presence of the core and will have the same energy as in hydrogen. The degeneracy of the level will be lessened by $2l_0+1$ [not, by the way, by the total number $(l_0+1)^2$ of the orbitals $|nlm\rangle$ with nonzero quantum defects. See the explanation in Braun (1985)].

Therefore first-order splitting of the levels of a nonhydrogenic Rydberg atom leads to a spectrum consisting of degenerate levels whose energy is exactly the same as in the case of atomic hydrogen and a number of nondegenerate levels. The positions of the hydrogenic levels depend on the strength of the fields only through ω, where

$$\omega=\sqrt{\omega_L^2+\omega_S^2},\quad \omega_L=\frac{H}{2c},\quad \omega_S=\frac{3}{2}nF\ .$$

The positions of the nonhydrogenic levels, on the other hand, depends not only on ω but also on the relative strength of the fields.

The plot of the splitting of the levels of atomic rubidium, calculated in the truncated basis approximation as a function of the angle $\alpha=\arctan(\omega_S/\omega_L)$, with ω kept constant, is shown in Fig. 35. The hydrogenic levels in-

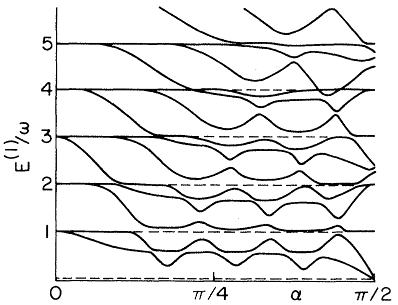

FIG. 35. Calculated first-order energies of the rubidium atom in orthogonal fields as functions of the angle $\alpha=\arctan(\omega_S/\omega_L)$. The nonhydrogenic and hydrogenic parts of the spectrum are shown by the solid curves and dashed horizontal lines, respectively.

dependent of α are depicted by dashed horizontal lines. The nonhydrogenic levels behave in a complicated way, with a number of avoided crossings and other peculiarities. The experimentally measured energies of the Rb atom in orthogonal fields behave in a closely similar manner (Penent *et al.*, 1988).

The hydrogenic levels $E_q^{(1)}$ should in fact be split due to second-order field effects in the same way as was observed for the hydrogen atom (Sec. III.E). This splitting for the nonhydrogenic Rydberg atoms has not yet been analyzed. Experimental studies are likely to be hampered by the fact that the respective eigenfunctions are orthogonal to all states with $l \le l_0$. Therefore optical one-photon excitation of the atoms can be achieved only via a level with a sufficiently large angular momentum.

VI. CONCLUSIONS

The discrete WKB method provides a unified approach to the effects connected with level splitting of Rydberg atoms in l-mixing external fields. In many cases alternative methods could also be used; however, they have a narrower scope of application. In particular, separation of variables in the ellipsocylindrical coordinates on Fock's sphere is a useful method in the case of atomic hydrogen in a magnetic field and in orthogonal electric and magnetic fields, but not in parallel fields; in the framework of the equivalent operator method, it is difficult to take into account the effect of the core; Harmin's treatment of the Stark effect in nonhydrogenic atoms relies on separation of variables in parabolic coordinates in the absence of the core and cannot be generalized to diamagnetic perturbation.

The main subjects of our study have been the three-term recursion relations for coefficients of the zero-order eigenfunctions of the Rydberg atoms. In the semiclassical limit their spectra could be analyzed by a simple set of rules similar to those used in the case of the Schrödinger equation in one dimension. The similarity between the two types of problems goes far; it includes the possibility of introducing in both cases meaningful potential-energy functions, which are highly useful in visualizing the movement of the physical system. Considering how often one encounters TTR relations and tridiagonal matrices in various applications of quantum mechanics, we believe that the formalism of the discrete WKB method deserves to be widely popularized.

ACKNOWLEDGMENTS

The author is indebted to his colleagues in the Department of Theoretical Physics of St. Petersburg University for many fruitful discussions, in particular to Yu. N. Demkov, A. K. Kazansky, V. N. Ostrovsky, T. K. Rebane, and E. A. Solov'ev.

APPENDIX A: TYPICAL ERRORS IN APPLICATIONS OF THE DISCRETE WKB METHOD

There are a surprising number of errors in papers devoted to the semiclassical solution of the recursion relations; we shall name the most widespread.

(a) Uncritical use of the replacement

$$C_{j\pm 1} \rightarrow C_j \pm \frac{dC_j}{dj} + \frac{1}{2}\frac{d^2C_j}{dj^2} , \tag{A1}$$

which amounts to the truncation of the finite shift operators $\exp(\pm i\varphi)$ in the Hamiltonian (2.2). This can be justified only if the function $\varphi(j)$ determined by Eq. (2.15) is close to zero for all relevant values of j. The reader may check it using Eq. (A1) on a three-term recursion relation with constant coefficients whose exact solutions are known (they have the form μ^j where μ is a constant).

(b) Improper treatment of the unusual turning points. Specific errors can be different. For example, Schulten and Gordon (1975) use the substitution

$$C_j = \left[\frac{\varphi(j)}{\sin\varphi(j)} \right]^{1/2} f(j)$$

and obtain an approximate differential equation for the function $f(j)$. However, in the vicinity of the unusual turning points, when φ tends to π, this substitution becomes singular and the connection between the solutions of the TTR relation and the differential equation is lost.

(c) Stereotyped use of the Bohr-Sommerfeld quantization rule with half-integers for the action

$$S_{12} = \int_{j_{t1}}^{j_{t2}} \varphi dj \ .$$

As can be seen from Eq. (2.21), this leads, statistically, to correct results only in one case out of four.

(d) Omission of the principal quantum corrections in the expression for the action S_{12}. In fact, if these corrections are not taken into account, the calculated eigenvalues can fall anywhere between the real ones; thus no information whatsoever is obtained about the position of the levels.

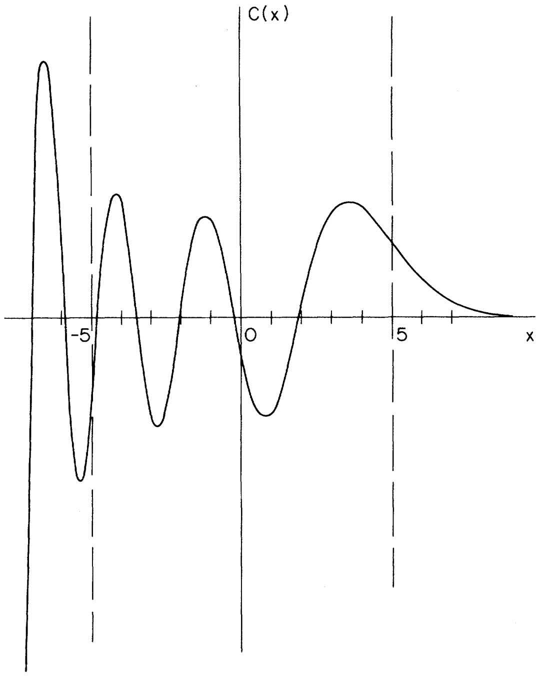

FIG. 36. Solution of the difference equation (A2) with $a=5$ vanishing at $x\rightarrow\infty$. Note oscillations with a rapidly growing amplitude at $x\rightarrow-\infty$ which cannot be eliminated by the choice of the parameter E.

(e) Confusion of the properties of the differential and the finite difference equations. Some authors obviously do not realize that there is no such thing as a "smooth eigenfunction of the finite difference operator." In fact, an eigenfunction of such an operator has the form of a sequence of δ pulses,[10]

$$f(x)=\sum_j C_j\delta(x-j-\Delta),\quad 0<\Delta<1\ .$$

Therefore the eigenvalue problem always reduces to a recursion relation for the coefficients C_j.

Here is a typical example. Consider the difference equation

$$C(x-1)-\left[\frac{2x}{a}+E\right]C(x)+C(x+1)=0 \tag{A2}$$

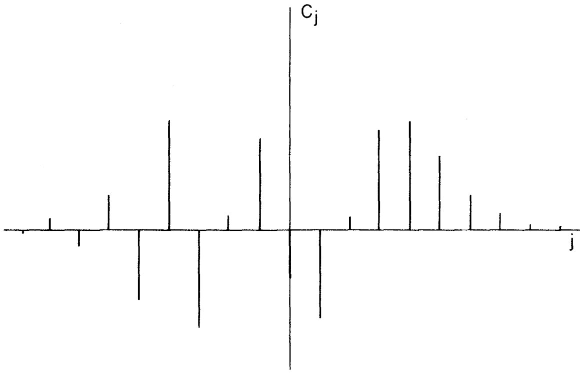

FIG. 37. The same function as in Fig. 36, in integer points ($E=0$).

with the parameter a fixed and $-\infty<x<\infty$. If $a\gg1$ this equation is semiclassical, with the classically allowed region at $-a<x<a$ and the classically forbidden usual and unusual regions at $x>a$ and $x<-a$, respectively. It has no continuous eigenfunctions. Its smooth solution, which is well-behaved when $x\rightarrow\infty$ [the Bessel function $J_{x+Ea/2}(a)$ multiplied by an arbitrary periodical function with the period unity], exhibits oscillations with a quicker than exponentially growing amplitude when $x\rightarrow-\infty$ (Fig. 36).

On the other hand, if the argument in Eq. (A2) is allowed to take only the integer values $x=j$, the result is the recursion relation (2.11). The latter has a complete set of well-behaved orthogonal eigenvectors $C_j^{[k]}=J_{j+k}(a),k$ integer (Fig. 37), corresponding to the equidistant eigenvalues $E^{[k]}=2k/a$.

APPENDIX B: EXPLICIT EXPRESSIONS FOR THE HIGHEST AND LOWEST EIGENVALUES OF THE TRIDIAGONAL MATRICES

Suppose that the potential function U^+ of the recursion relation (2.1) determined by Eq. (2.5) has a maximum at some point j_0. Then the spectrum is bounded from above by the value $U^+(j_0)\equiv a_0$, and the levels close to a_0 are given by the following explicit expression ($N=0,1,2,\ldots$):

$$\begin{aligned}E_N\approx{}& a_0-(N+\tfrac{1}{2})\sqrt{(-a_2)(a_0-b_0)}+(N^2+N+\tfrac{1}{2})\left[\frac{b_2}{8}-\frac{a_2}{4}-\frac{3a_4(a_0-b_0)}{8a_2}+\frac{3b_1^2}{32(a_0-b_0)}\right]\\&+(N^2+N+\tfrac{11}{30})\frac{15a_3^2(a_0-b_0)}{32a_2^2}-(N^2+N+\tfrac{1}{6})\frac{3a_3b_1}{16a_2}\ ,\end{aligned}\tag{B1}$$

where a_s,b_s are the coefficients of the Taylor expansion of the potential functions in the vicinity of j_0:

$$\begin{aligned}U^+(j)&=a_0+\sum_{s\geq2}a_s(j-j_0)^s\\U^-(j)&=\sum_{s\geq0}b_s(j-j_0)^s\ .\end{aligned}\tag{B2}$$

---

[10] There are rare exceptions connected with difference operators whose eigenvalues are infinitely degenerate, like those studied in the theory of incommensurable lattices (Sokoloff, 1983).

This formula was obtained (Braun, 1989a) by developing the quantum Hamiltonian (2.2) of the TTR relation in powers of the operators $\varphi = -i\partial/\partial j$ and $j - j_0$. Treating the harmonic-oscillator part of the Hamiltonian as the zero-order problem and the rest of the terms as perturbations, we obtain Eq. (B1). This is analogous to the expression for the lower energy levels in a potential well through the Taylor coefficients of the potential energy at the minimum. A similar approximation can be obtained for the lower levels of the TTR equation (2.1) adjacent to the minimum point of the function U^-; the problem is brought to the preceding one by the substitution $C_j = (-1)^j \tilde{C}_j$.

The accuracy of Eq. (B1) is higher than that of the usual semiclassical approach because terms of relative order n^{-2} are taken into account. The similar, but less accurate, expression given in Braun (1983a) was obtained by an approximate solution of the quantization rules of the discrete WKB method with respect to the eigenvalue E'; its difference from Eq. (B1) was that it contained $(N+\frac{1}{2})^2$ instead of the three different quadratic polynomials in N.

To give an example of the use of Eq. (B1), consider the upper levels of the quadratic Zeeman multiplet of atomic hydrogen in the case $m=0$. The potential functions of the TTR relation (1.2) are

$$U^+ = u_\gamma \left[1 + \frac{1}{5n^2} - \frac{k^2}{n^2}\right], \quad U^- = \frac{u_\gamma}{5}\left[1 + \frac{1}{n^2} - \frac{k^2}{n^2}\right].$$

In contrast to Eq. (2.1) we retain the term $(5n^2)^{-1}$ because Eq. (B1) goes beyond the WKB level of accuracy. The argument k is either $2j$ or $2j+1$, depending on the parity of $n-1$ where j is the integer variable with a step equal to unity.

The upper levels are adjacent to the maximum of U^+, which is at $k=0$, i.e., at $j_0 = 0$ or $-\frac{1}{2}$. Expressing $U^\pm$ through j and developing in powers of $j - j_0$, we get

$$a_0 = \left[1 + \frac{1}{5n^2}\right] u_\gamma, \quad a_2 = -\frac{4}{n^2} u_\gamma, \tag{B3}$$

$$b_0 = \left[\frac{1}{5} + \frac{1}{5n^2}\right] u_\gamma, \quad b_2 = -\frac{4}{5n^2} u_\gamma. \tag{B4}$$

The rest of the Taylor coefficients are zero. Consequently we get from Eq. (B1), replacing u_γ by $5n^4H^2/16c^2$,

$$E'_N = \left[\frac{nH}{2c}\right]^2 \left[\frac{5n^2}{4} - n\sqrt{5}\left[N + \frac{1}{2}\right] + \frac{9}{8}(N^2+N) + \frac{13}{16}\right]. \tag{B5}$$

A somewhat different approach is described by Rau (1990). He uses the replacement (A1) to transform the TTR relation into a differential equation for the spheroidal functions. The eigenvalues of this equation provide an approximation for the upper eigenvalues of the TTR relation. In their development in powers in n^{-1} the first two terms coincide with those of Eq. (B1). The rest of the terms describing deviations of the levels from exact equidistance are meaningless. This is because the replacement (A1) does not take into account the third and the fourth powers of the "momentum" operator $-i\partial/\partial j$ in the development of the finite shift operators (corresponding, one may say, to the "dependence of mass on speed").

TABLE IV. The upper levels of the quadratic Zeeman multiplet in atomic hydrogen, $n=50$, $m=0$.

	$E'_N \Big/ \left[\frac{nH}{2c}\right]^2$		
N	Approximation (B6)	Approximation (B5)	Numerical
0	3069.848	3069.910	3069.910
1	2959.044	2960.357	2960.356
2	2849.241	2853.054	2853.053
3	2740.438	2748.000	2748.003
4	2632.634	2645.197	2645.206

With respect to the upper levels of the quadratic Zeeman multiplet, an approach based on the spheroidal equation provides the approximation (Rau, 1990)

$$E'_N = \left[\frac{nH}{2c}\right]^2 \left[\frac{5n^2}{4} - n\sqrt{5}\left[N + \frac{1}{2}\right] + \frac{1}{2}(N^2+N) + \frac{3}{4}\right]. \tag{B6}$$

This is fairly accurate if N is small; however, with the growth of N the accuracy quickly decreases due to the wrong coefficient at (N^2+N) ($\frac{1}{2}$ instead of $\frac{9}{8}$). See the numerical example in Table IV.

Other approximations introduced for the upper levels of the quadratic Zeeman multiplet also provide lower accuracy than Eq. (B5). The expression given in Braun (1983a) contains a small shift independent of N ($\frac{17}{32}$ in the formula for E'_N instead of the correct value $\frac{13}{16}$). Solov'ev's (1982) approximations have the same order of accuracy as Eq. (B6). The formula given by Herrick (1982) differs from Eq. (B5) by slightly changed coefficients at $N+\frac{1}{2}$ (2 instead of the correct $\sqrt{5}$) and N^2 (1 instead of $\frac{9}{8}$).

Approximate formulas for the lower levels of the quadratic Zeeman multiplets were established by Herrick (1982) for the case $|m| \ll n$ and by Braun (1983a) for the general case.

APPENDIX C: SOME ALTERNATIVE APPLICATIONS OF THE DISCRETE WKB METHOD

The discrete WKB method can be used in numerous physical problems leading to three-term recursion relations and tridiagonal (Jacobian) matrices. We shall give here a brief account of several alternative applications of the method unconnected with the theory of the Rydberg atoms.

1. Floquet spectra of vibrational systems in external resonant fields

Consider a weakly nonlinear quantum oscillator driven by a resonant external force with the Hamiltonian

$$H=-\frac{\hbar^2}{2m}\frac{d^2}{dx^2}+\frac{m\omega^2x^2}{2}+\alpha x^3+\beta x^4+Fx\cos\Omega t\ . \tag{C1}$$

This system is used to model the excitation of nondegenerate molecular vibrations in a laser field (Makarov and Fedorov, 1976).

In dealing with quantum systems whose Hamiltonian is time-periodic, it is essential to know their Floquet, or quasienergy, spectrum (Baz *et al.*, 1971). Developing the Floquet solution of the time-dependent Schrödinger equation with the Hamiltonian (C1) in the basis set of stationary oscillator eigenfunctions $|v\rangle$ and applying the rotating-wave approximation, we obtain a TTR relation (Kravchenko and Prostnev, 1973; Fedorov, 1977). Neglecting small corrections, this relation can be written as

$$f(\sqrt{v}\,C_{v-1}+\sqrt{v+1}\,C_{v+1})+(\gamma v^2+\delta v-E)C_v=0\ . \tag{C2}$$

Here $v=0,1,2,\ldots$ is the vibrational quantum number, E is the quasienergy of the Floquet state, $f=(\hbar/8m\omega)^{1/2}F$ is the scaled amplitude of the periodic force, $\delta=\hbar(\omega-\Omega)$ is the detuning, and

$$\gamma=\frac{\hbar^2}{(m\omega)^2}\left[\frac{3}{2}\beta-\frac{15}{4}\frac{\alpha^2}{m\omega^2}\right]$$

is the effective anharmonicity. Equation (C2) was examined by semiclassical methods by Sazonov (1978) and Braun (1978). This study revealed interesting parallels between the classical and quantum pictures of nonlinear resonance.

Depending on the detuning δ the potential curves of the TTR relation (C2) can have one of the two forms shown in Fig. 38(a), the case in which $\delta<\delta_{\rm crit}$, and Fig. 38(b), the case in which $\delta>\delta_{\rm crit}$, where

$$\delta_{\rm crit}=-3(f^2\gamma/2)^{1/3}\ .$$

(It is assumed that $\gamma<0$; this can be done without loss of generality.) Using the expressions for γ, f, and δ, one can see that the inequalities $\delta<\delta_{\rm crit}$ and $\delta>\delta_{\rm crit}$ coincide with the well-known conditions for the existence of one or two stable resonant amplitudes, respectively, of a classical nonlinear oscillator with zero damping (Landau and Lifshitz, 1988).

In the classical bistable case [Fig. 38(b)] the lower potential function is nonmonotonic. As a result there is an interval of E in which there are two classically allowed regions of the variable v for each E (a situation similar to the nonsymmetrical double-well potential of the coordinate representation). In this interval the quasienergy spectrum consists of two overlapping spectra obtained by independent quantization in the left and right allowed regions of v.

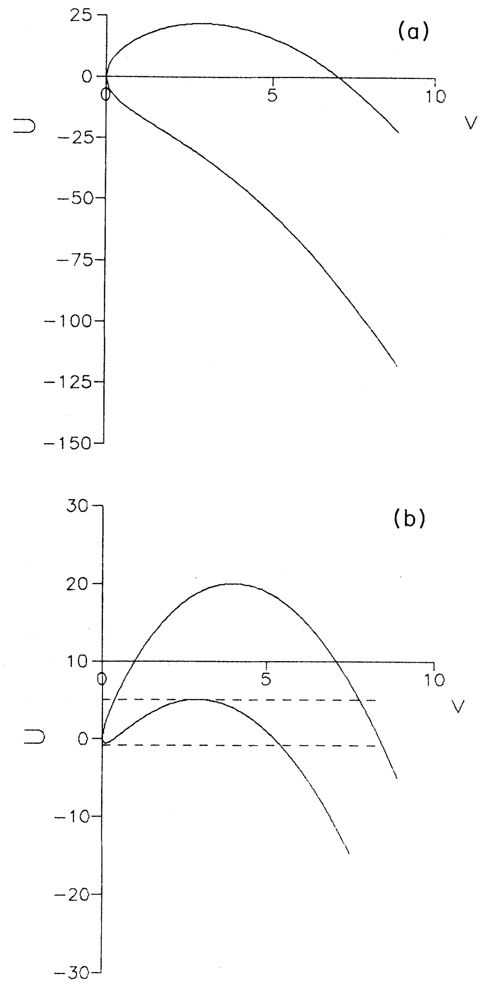

FIG. 38. The potential curves of the three-term recursion relation (C2) describing the resonant properties of a nonlinear quantum oscillator (a) $\delta<\delta_{\rm crit}$; (b) $\delta>\delta_{\rm crit}$ (classically bistable case). The dashed lines mark at the ordinate axis the quasienergy interval in which there is an overlay of two independent Floquet spectra. From Braun (1978).

The plots of the potential functions of Eq. (C2) are particularly helpful in studying the effects of adiabatic variations of the external field parameters on the quantum oscillator. For example, when $\delta>\delta_{\rm crit}$ the two groups of Floquet levels localized in the left and right classically allowed regions of v anticross when the detuning is changed. If this change is slow enough, the oscillator tunnels from the left to the right "potential well," which means a sharp increase of the average vibrational energy $\hbar\omega(\bar{v}+\frac{1}{2})$.

Other examples of the nonlinear resonance situations considered by discrete semiclassical methods can be found in Braun (1979; the parametric excitation of a nonlinear oscillator) and Braun and Microshnichenko (1980; excitation of the deformational vibration of the linear triatomics).

2. Rotational spectra of rigid and nonrigid molecules

In the rigid-rotor approximation, the rotational Hamiltonian of a molecule with the rotational constants A_x, A_y, A_z is expressed through the components of the angular momentum **J** on the principal molecular axes of inertia as

$$H=A_xJ_x^2+A_yJ_y^2+A_zJ_z^2\ . \tag{C3}$$

The problem of finding the eigenvalues of H becomes difficult only if all the rotational constants are different (the asymmetric top case). The rotational eigenstate is then a combination of generalized spherical functions corresponding to the same total angular momentum $J(J+1)$ but different angular momentum projections $K=J_z$ on the molecular axis z. The coefficients of the combination obey the TTR relation $(-J\le K\le J)$

$$p_KC_{K-2}+(w_K-E)C_K+p_{K+2}C_{K+2}=0 \tag{C4}$$

with

$$p_K=\frac{A_x-A_y}{4}[(J+K)(J-K+1)(J+K-1)\times(J-K+2)]^{1/2}\ ,$$

$$w_K=\frac{A_x+A_y}{2}J(J+1)+\left[A_z-\frac{A_x+A_y}{2}\right]K^2\ .$$

If J is large, the problem represented by the recursion relation (C4) is semiclassical and can be treated by the discrete WKB method (Braun and Kiselev, 1983; Braun, 1984). Its potential functions are parabolic:

$$U^+(K)\approx A_xJ^2+(A_z-A_x)K^2\ ,$$

$$U^-(K)\approx A_yJ^2+(A_z-A_y)K^2\ .$$

Depending on the choice of z axis of the molecular-fixed frame (along the axis of inertia with the largest, intermediate, or smallest rotational constant), the plot of the potential functions can have one of three forms (Fig. 39).

The quantization rules of Sec. II.D applied to the rigid-rotor problem lead to the same energy levels as other more conventional semiclassical methods (Colwell *et al.*, 1978). Among the advantages of the discrete WKB approach is that it makes obvious the behavior of the amplitudes C_K, which may sometimes be important. For example, suppose that the generalized spherical functions are quantized on the axis with the smallest rotational constant [Fig. 39(c)] and consider the lower levels of the rotational multiplet with a given J. There are two symmetrical classically allowed regions of K divided by a barrier. Therefore the coefficients C_K will be significantly nonzero only if their subscript belongs to one of these regions, whereas C_K with small $|K|$ will be exponentially small. It is also clear that the rotational levels are doublets with the splitting determined by the probability of tunneling through the potential barrier. Calculation of this splitting in the framework of the discrete WKB method is described in Braun (1981).

A less hackneyed problem is calculation of the rota-

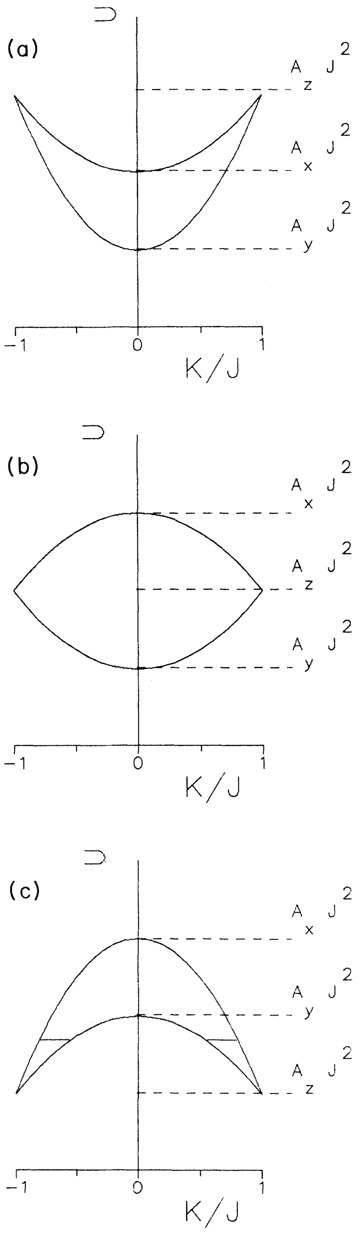

FIG. 39. The potential curves of the TTR relation (C4) for a rigid asymmetric top. There are three ways of choosing the quantization axis Z of the generalized spherical functions: (a) $A_z>A_x>A_y$; (b) $A_x>A_z>A_y$; (c) $A_x>A_y>A_z$.

tional spectra when centrifugal deformation of the molecule has to be taken into account ("nonrigid rotation"). The model Hamiltonian commonly used in this case is the so-called Watson tridiagonal form (Watson, 1967,1977),

$$H=(J_x^2-J_y^2)\Phi(\mathbf{J}^2,J_Z^2)+\mathrm{H.c}+F(\mathbf{J}^2,J_Z^2)\ . \tag{C5}$$

Here Φ and F are functions (usually polynomials) of the commuting operators $\mathbf{J}^2$ and J_Z^2. The coefficients contained in Φ and F are either deduced from *ab initio* calculations or regarded as fit parameters, which are chosen to reproduce the experimentally observed rotational levels. Note that the rigid-rotor Hamiltonian Eq. (C3) can be regarded as a special case of Eq. (C5).

The eigenvalue problem for Watson's Hamiltonian results once again in a three-term recursion relation similar to Eq. (C4). As distinct from the rigid-rotor case, its potential functions will be polynomials of K of degree higher than quadratic (Braun, 1989a). If the centrifugal effects are not too pronounced (this will be the case when J is not excessively large) the potential curves will still resemble the parabolas in Fig. 39 [cases (a), (b), and (c) correspond to the so-called reduction schemes I^r, II^r, and III^r, respectively). Accordingly the rotational spectrum will be qualitatively unchanged by the effects of nonrigidity.

Higher-order terms in K become more important in the case of quickly rotating molecules with large J. The deviation of the potential curves of Watson's tridiagonal Hamiltonian from the purely parabolic form can be a convenient way of describing the resulting complicated centrifugal distortions of the rotational spectra.

In the case of spherical-top molecules, the discrete WKB method can be used to describe the centrifugal splitting of rotational levels (Braun *et al.*, 1985). Because of this splitting the degenerate eigenvalue $AJ(J+1)$ of the Hamiltonian (C3), where $A=A_X=A_Y=A_Z$ is the molecular rotational constant, becomes a multiplet (Fox *et al.*, 1977; Harter and Patterson, 1977; Baldacchini *et al.*, 1982). The emerging spectrum has a complicated structure consisting of clusters, each containing six or eight quasidegenerate levels.

The zero-order rotational eigenfunctions are obtained by diagonalizing the effective operator of the centrifugal corrections in the basis set of generalized spherical functions. This results in a three-term recursion relation connecting C_K with K differing by ±3 or ±4, depending on the choice of quantization axis for the spherical functions.

In Sec. III.B dealing with the quadratic Zeeman splitting of atomic hydrogen in the spherical coordinates, we showed that the spectrum of a TTR relation with a step larger than 1 consists partly of quasidegenerate groups of levels. In the case of centrifugal splitting this source of degeneracy is combined with the customary double quasidegeneracy due to the symmetrical-double-well-like form of the plot of the potential functions of the corresponding TTR relation. This explains the sixfold (3×2) and the eightfold (4×2) composition of the clusters in the rotational spectra.

3. The Lipkin-Meshkov-Glick model of the transition from spherical to nonspherical nuclei

A simple model used to describe the loss of the spherical form by a nucleus when the number of valence nucleons is increased is the Lipkin-Meshkov-Glick (LMG) model (Lipkin *et al.*, 1965). It considers a system of N interacting fermions, which can occupy one of two one-particle levels separated by an energy gap ε, both of which are N times degenerate.

Let us introduce the fermion creation a_{pi}^+ and annihilation a_{pi} operators ($i=1,2$ is the number of the energy level and $p=1,2,\ldots,N$ is the number used to distinguish the degenerate states belonging to each level). The so-called quasispin operators

$$J_z=\frac{1}{2}\sum_{p=1}^{N}(a_{p2}^+a_{p2}-a_{p1}^+a_{p1})\ ,$$

$$J_+=(J_-)^+=\sum_{p=1}^{N}a_{p2}^+a_{p1}$$

obey the angular momentum commutation rules. The LMG model Hamiltonian, written in terms of the quasispin operators, is

$$H=\varepsilon J_z+\tfrac{1}{2}W(J_+J_-+J_-J_+)+\tfrac{1}{2}V(J_+^2-J_-^2)\ , \tag{C6}$$

where ε, W, and V are parameters.

The Hamiltonian (C6) commutes with the operator of the total quasispin $\mathbf{J}^2=J(J+1)$; the ground state is associated with the maximal possible $J=N/2$.

The characteristic property of the LMG model is the sharp change in the structure of its ground state and the transition energy to the first excited state when the number of fermions N exceeds a certain critical value. (It is this change that is associated with the spherical-to-nonspherical form transition in the nuclei.) Such a transformation acquired the name of "phase transition" in the ground state; see the paper of Gilmore and Feng (1978), where this phenomenon is explained in terms of the coherent-states technique.

The discrete WKB method was applied to the LMG model by Braun *et al.* (1987), making use of the fact that the eigenvalue equation for the Hamiltonian of the model is brought to a TTR relation by developing its eigenfunction in the basis set of the eigenfunctions $|JK\rangle$ of the total quasispin $\mathbf{J}^2=J(J+1)$ and its component $J_z=K$, where J is fixed. This TTR relation has the form (C4) with

$$w_K=\varepsilon K+W[J(J+1)-K^2]\ ,$$

$$p_K=\tfrac{1}{2}V[(J-K+2)(J+K-1)(J-K+1)(J+K)]^{1/2}\ .$$

The potential functions of the LMG recursion relation are presented in Fig. 40. The lower part of their plot has

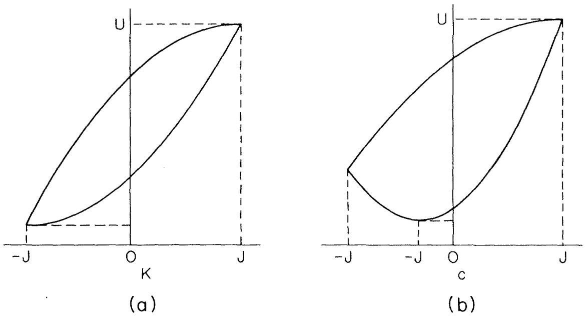

FIG. 40. Potential functions of the recursion relation associated with the Lipkin-Meshkov-Glick model. The dashed horizontal lines mark at the ordinate axis the lower and the upper bounds of the energy spectrum: (a) $J < J_{\text{crit}}$; (b) $J_{\text{crit}} < J$.

a different form depending on the relation between J and

$$J_{\text{crit}} = \frac{\varepsilon}{2(V-W)} \ . \tag{C7}$$

Assuming that $V > W$, the lowest point of the plot is either the crossing of U^+ and U^- at $K=-J$ [when $J<J_{\text{crit}}$, Fig. 40(a)] or the minimum of U^- at $K=-J_{\text{crit}}$ [when $J_{\text{crit}}<J$, Fig. 40(b)]. The ground-state wave function will correspondingly be a combination of states with the J_z value either close to $-J=-N/2$ (which means that all fermions occupy level 1) or close to $-J_{\text{crit}}$. The excitation energy equal to the classical oscillation frequency (cf. Sec. II.B) will also be different. Such a transformation of the ground-state composition, occurring when the number of fermions exceeds $2J_{\text{crit}}$, is just the "phase transition" mentioned above.

Critical effects in the case of more general quasispin Hamiltonians encountered in nuclear theory can also be dealt with by the discrete WKB method; see Braun *et al.* (1987) for a discussion and references to other works.

4. Calculation of infinite continued fractions

In a number of physical problems the result is formulated in terms of infinite continued fractions, e.g., the treatment of the Coulomb two-center problem by Komarov *et al.* (1978) and calculation of the quantum correlation functions by Lee *et al.* (1987). [General properties of the continued fractions are described in detail by Wall (1973) and Jones and Thron (1980).]

There is a close link between continued fractions and recursion relations. To show this, let us make the substitution in our standard TTR relation (2.1)

$$\mu_j = p_j C_{j-1}/C_j \ . \tag{C8}$$

The sequence μ_j obeys the recursion relation

$$\mu_j = d_j - \frac{b_{j+1}}{\mu_{j+1}} \ , \tag{C9}$$

where we denoted $d_j = E' - w_j$, $b_{j+1} = p_{j+1}^2$.

Iteration of Eq. (C9) expresses μ_j through μ_{j+2}, μ_{j+3}, etc. If this process converges, we obtain the development of μ_j into an infinite continued fraction:

$$\mu_j = d_j - \cfrac{b_{j+1}}{d_{j+1} - \cfrac{b_{j+2}}{d_{j+2} - \cdots}} \ . \tag{C10}$$

On the other hand, an infinite continued fraction of the form (C10) with arbitrary elements $d_j, d_{j+1}, \ldots$ and positive $b_{j+1}, b_{j+2}, \ldots$ can be expressed through a particular solution of a Hermitian TTR relation of the type (2.1). This means that every approximate method of solving the TTR relation provides a tool for calculation of the continued fractions.

Suppose that the elements d_j and b_j of the continued fraction are given slowly changing functions of the subscript j. Then the associated TTR relation can be investigated by the discrete WKB method. A qualitative appraisal of the properties of the sequence Eq. (C10) can be obtained using the connections with classical mechanics (Sec. II.A) and the plot of the potential functions of the related TTR relation. In particular, it is easy to show that the continued fractions with slowly changing elements converge provided the associated classical movement is finite (large j should be classically forbidden).

The WKB solutions of the TTR relation given in Sec. II.C can be used to construct closed analytical expressions for the infinite continued fractions (Braun, 1984). Denoting $D_j = d_j^2 - 4b_{j+1/2}$, we can write this expression in one of two ways:

(a) In the classically forbidden interval of j stretching to positive infinity.

$$\begin{aligned} \mu_j &= \mu_j^{(0)} + \mu_j^{(1)} + \cdots \ , \\ \mu_j^{(0)} &= (d_j + \sqrt{D_j})/2 \ , \\ \mu_j^{(1)} &= \left[2b_j \frac{\partial d_j}{\partial j} - d_j \frac{\partial b_j}{\partial j} \right] \Big/ 2D_j \ . \end{aligned} \tag{C11}$$

(b) In the classically allowed interval of j divided from positive infinity by just one turning point j_t,

$$\begin{aligned} \mu_j \approx{} & \tfrac{1}{2} d_j - \tfrac{1}{2}(-D_j)^{1/2} \tan \\ & \times \left[\int_j^{j_t} dj \arccos \frac{d_j}{2\sqrt{b_{j+1/2}}} - \frac{\pi}{4} \right] \quad (j < j_t) \ . \end{aligned} \tag{C12}$$

In both expressions it is assumed that d_j is positive for all sufficiently large j; otherwise these formulas have to be slightly modified.

As an example consider the sequence of infinite continued fractions connected with the TTR relation (2.11) for Bessel functions with $E'=0$, which corresponds to the choice $d_j = j/a$, $b_j = 1$ in Eq. (C10):

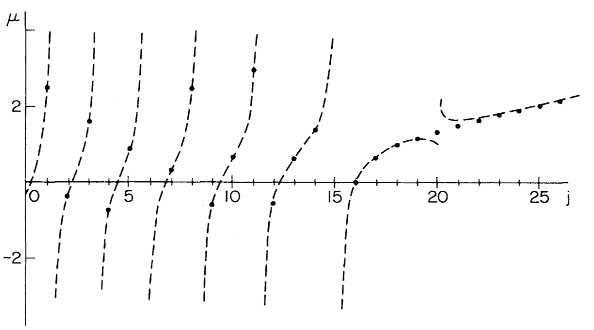

FIG. 41. The infinite continued fractions $\mu_j(a)$ [Eq. (C13)] with $a=20$ as functions of j. The circles indicate the numerical values, while the dashed lines represent the values of the WKB expressions (C11) and (C12) calculated for all (not only integer) j. Note the breakdown of the WKB approximation in the vicinity of the turning point $j_t=20$.

$$\mu_j(a)=(2j/a)-\cfrac{1}{[2(j+1)/a]-\cfrac{1}{[2(j+2)/a]-\cdots}}\ . \tag{C13}$$

The fractions (C13) converge because infinitely large positive j are classically forbidden (Sec. II). The classically allowed region is situated to the left of the turning point $j_t=a$. Figure 41 shows a plot of μ_j versus j with $a=20$, calculated both numerically and by means of the WKB formulas (C11), (C12). Note the striking difference between the behavior of μ_j as functions of j in the classically forbidden and allowed intervals. A slow monotonic change occurs to the right of the turning point and seemingly erratic jumps to the left of it.

5. The estimate of errors introduced by truncation of an infinite matrix

Numerical calculation of the eigenvalues of an infinite tridiagonal matrix entails replacing the matrix by a finite one. This amounts to truncation of the basis set used in the calculation. The eigenvalue equations for the truncated matrix are still given by a TTR relation of the type (2.1). However, instead of the boundary condition $C_j \to 0$ when $j\to\infty$, we should impose the condition $C_{j_0+1}=0$, where j_0 is the number of functions in the truncated basis set. [A similar condition, $\psi(x_0)=0$, imposed on the solution of the Schrödinger equation would mean the introduction of an infinitely high potential wall at the point x_0.]

Suppose we want to know whether a certain eigenvalue of the truncated matrix is close enough to the corresponding eigenvalue of the original infinite matrix. In the framework of the discrete WKB method the answer is obvious. The errors introduced by truncation will be small if the point j_0 of truncation lies deep enough inside the classically forbidden region (within the "classical shadow") of the recursion relation (2.1).

Drawing a plot of the potential functions of the TTR relation, we can see at once the position of the boundary of the classically forbidden region for all energies. As a result it is easy to establish a minimal size j_0 of the basis set necessary to obtain eigenvalues located in a specified energy interval with a desired accuracy.

REFERENCES

Adamov, M. N., V. K. Kagan, and T. K. Rebane, 1964, Vestnik Leningradskogo Universiteta **10**, 31.

Alhassid, Y., E. A. Hinds, and D. Meschede, 1987, Phys. Rev. Lett. **59**, 1545.

Arnold, V. I., 1974, *Mathematical Methods of Classical Mechanics* (Nauka, 1974). In Russian.

Baldacchini, G., S. Marchatti, and V. Montelatici, 1982, J. Mol. Spectrosc. **91**, 80.

Barton, G., 1987, Proc. R. Soc. London Ser. A **410**, 175.

Barton, G., 1988, Phys. Scr. **21**, 11.

Bassani, G. F., M. Inguscio, and T. W. Hänsch, 1989, Eds., *The Hydrogen Atom* (Springer, Berlin).

Baz, A. I., Ya. B. Zel'dovich, and A. M. Perelomov, 1971, *Scattering, Reactions, and Decays in Nonrelativistic Quantum Mechanics* (Nauka, Moscow). In Russian.

Belov, A. A., A. P. Kazantsev, D. V. Khveschenko, and V. L. Pokrovsky, 1985, J. Phys. B **18**, 4683.

Belov, A. A., Yu. E. Lozovik, and V. L. Pokrovsky, 1989, Zh. Eksp. Teor. Fiz. **96**, 552 [Sov. Phys.—JETP **69**, 312 (1989)].

Bender, C. W., G. S. Guralnik, and M. Silverstone, 1979, Phys. Rev. D **20**, 2583.

Beterov, I. M., and P. B. Lerner, 1989, Usp. Fiz. Nauk **159**, 665 [Sov. Phys. Usp. **32**, 1084 (1989)].

Bethe, H. A., and E. E. Salpeter, 1957, *Quantum Mechanics of One- and Two-Electron Atoms* (Springer, Berlin).

Bivona, S., W. Schweizer, P. F. O'Mahony, and K. T. Taylor, 1988, J. Phys. B **21**, L617.

Bogomolny, E. B., 1989, Zh. Eksp. Teor. Fiz. **96**, 487 [Sov. Phys. JETP **69**, 275 (1989)].

Born, M., 1960, *Mechanics of the Atom* (Ungar, New York).

Braun, P. A., 1978, Teor. Mat. Fizika **37**, 355 [Sov. Phys. Theor. Math. Phys. **37**, 1070 (1978)].

Braun, P. A., 1979, Teor. Mat. Fizika **41**, 336 [Sov. Phys. Theor. Math. Phys. **41**, 1060 (1979)].

Braun, P. A., 1981, in *Problems of the Quantum Theory of Atoms and Molecules,* edited by I. V. Abarenkov, No. 2 (Leningrad University), p. 110. In Russian.

Braun, P. A., 1983a, Zh. Eksp. Teor. Fiz. **84**, 850 [Sov. Phys. JETP **57**, 492 (1983)].

Braun, P. A., 1983b, J. Phys. B **16**, 4323.

Braun, P. A., 1984, doctoral thesis (Leningrad University).

Braun, P. A., 1985, J. Phys. B **18**, 4183.

Braun, P. A., 1986, Opt. Spectrosk. **61**, 253 [Opt. Spectrosc. (USSR) **61**, 164 (1986)].

Braun, P. A., 1989a, Opt. Spectrosk. **66**, 57 [Opt. Spectrosc. (USSR) **66**, 32 (1989)].

Braun, P. A., 1989b, Zh. Eksp. Teor. Fiz. **96**, 1650 [Sov. Phys. JETP **69**, 934 (1989)].

Braun, P. A., 1990a, Opt. Spectrosk. **69**, 252.

Braun, P. A., 1990b, Opt. Spectrosk. **69**, 1208.

Braun, P. A., 1990c, J. Phys. B **23**, 3083.

Braun, P. A., 1991a, J. Phys. B **24**, 399.

Braun, P. A., 1991b, J. Phys. B **24**, 2313.

Braun, P. A., and A. A. Kiselev, 1983, *Introduction to Theory of Molecular Spectra* (Leningrad University, Leningrad), in Russian.

Braun, P. A., and G. P. Miroshnichenko, 1980, Opt. Spectrosk. **48**, 1081.

Braun, P. A., V. N. Ostrovsky, and N. V. Prudov, 1990, Phys. Rev. A **42**, 6537.

Braun, P. A., and M. V. Senyushkin, 1991, Zh. Eksp. Teor. Fiz. **100**, 1461.

Braun, P. A., A. M. Shirokov, and Yu. F. Smirnov, 1985, Mol. Phys. **56**, 573.

Braun, P. A., A. M. Shirokov, and Yu. F. Smirnov, 1987, Izv. Akad. Nauk SSSR, Ser. Fiz. **51**, 176 [Bull. Acad. Sci. USSR, Phys. Ser. **51**, 162 (1987)].

Braun, P. A., and E. A. Solov'ev, 1984, Zh. Eksp. Teor. Fiz. **86**, 68 [Sov. Phys. JETP **59**, 38 (1984)].

Brussard, P., and J. H. Tolhoek, 1957, Physica **23**, 955.

Bruyev, A. S., 1986, Zh. Eksp. Teor. Fiz. **90**, 35 [Sov. Phys. JETP **63**, 20 (1986)].

Cacciani, P., S. Liberman, E. Luc-Koenig, J. Pinard, and C. Thomas, 1989, Phys. Rev. A **40**, 3026.

Cacciani, P., E. Luc-Koenig, J. Pinard, C. Thomas, and S. Liberman, 1986a, Phys. Rev. Lett. **56**, 1124.

Cacciani, P., E. Luc-Koenig, J. Pinard, C. Thomas, and S. Liberman, 1986b, Phys. Rev. Lett. **56**, 1467.

Cacciani, P., E. Luc-Koenig, J. Pinard, C. Thomas, and S. Liberman, 1986c, J. Phys. B **19**, L519.

Cacciani, P., E. Luc-Koenig, J. Pinard, C. Thomas, and S. Liberman, 1988a, J. Phys. B **21**, 3473.

Cacciani, P., E. Luc-Koenig, J. Pinard, C. Thomas, and S. Liberman, 1988b, J. Phys. B **21**, 3499.

Cacciani, P., E. Luc-Koenig, J. Pinard, C. Thomas, and S. Liberman, 1988c, J. Phys. B **21**, 3523.

Carruthers, P., and M. M. Nieto, 1968, Rev. Mod. Phys. **40**, 411.

Chardonnet, C., D. Delande, and J. C. Gay, 1989, Phys. Rev. A **39**, 1066.

Clark, Ch. W. 1981, Phys. Rev. A **24**, 605.

Clark, Ch. W., and K. T. Taylor, 1980, J. Phys. B **13**, L737.

Clark, Ch. W., and K. T. Taylor, 1982, J. Phys. B **15**, 1175.

Colwell, S. M., N. C. Handy, and W. H. Miller, 1978, J. Chem. Phys. **68**, 745.

Delande, D., and J. C. Gay, 1981a, Phys. Lett. A **82**, 393.

Delande, D., and J. C. Gay, 1981b, Phys. Lett. A **82**, 399.

Delande, D., and J. C. Gay, 1984, J. Phys. B **17**, L335.

Delande, D., and J. C. Gay, 1987, Phys. Rev. Lett. **59**, 1809.

Delande, D., and J. C. Gay, 1991, Phys. Rev. Lett. **66**, 3237.

Delos, J. B., and M. L. Du, 1988, IEEE J. Quantum Electron. **24**, 1445.

Delos, J. B., S. K. Knudson, and D. W. Noid, 1983a, Phys. Rev. Lett. **50**, 579.

Delos, J. B., S. K. Knudson, and D. W. Noid, 1983b, Phys. Rev. A **28**, 7.

Delos, J. B., R. L. Waterland, and M. L. Du, 1988, Phys. Rev. A **37**, 1185.

Demkov, Yu. N., B. S. Monozon, and V. N. Ostrovsky, 1969, Zh. Eksp. Teor. Fiz. **57**, 1431 [Sov. Phys. JETP **30**, 775 (1970)].

Du, M. L., and J. B. Delos, 1988, Phys. Rev. A **38**, 1896.

Edmonds, A. R., 1960, *Angular Momentum in Quantum Mechanics* (Princeton University, Princeton).

Epstein, P. S., 1926, Phys. Rev. **28**, 695.

Fabre, C., Y. Kaluzny, R. Calabrese, Liang Jun, P. Goy, and S. Haroche, 1984, J. Phys. B **17**, 3217.

Fano, U., F. Robicheaux, and A. R. P. Rau, 1988, Phys. Rev. A **37**, 3655.

Fauth, M., H. Walther, and E. Werner, 1987, Z. Phys. D **7**, 293.

Fedorov, M. V., 1977, Zh. Eksp. Teor. Fiz. **73**, 134.

Fox, K., H. W. Galbraith, B. J. Krohn, and J. D. Kouck, 1977, Phys. Rev. A **15**, 1363.

Friedrich, H., and D. Wintgen, 1989, Phys. Rep. **183**, 37.

Ganesan, K., and M. Lakshmanan, 1990, Phys. Rev. A **42**, 3940.

Gay, J. C., 1985, in *Photophysics and Photochemistry in the Vacuum Ultraviolet,* edited by S. P. McGlynn, G. L. Findley, and R. H. Huebner (Reidel, Dordrecht), p. 631.

Gay, J. C., 1986, in *Atoms in Unusual Situations,* edited by J. P. Briand (Plenum, New York), p. 107.

Gay, J. C., 1988, in *Spectrum of Atomic Hydrogen,* edited by G. W. Series (World Scientific, Singapore), p. 367.

Gay, J. C., and D. Delande, 1983, Comments At. Mol. Phys. **13**, 275.

Gay, J. C., D. Delande, and F. Biraben, 1980, J. Phys. B **13**, L729.

Gay, J. C., D. Delande, F. Biraben, and F. Penent, 1983, J. Phys. B **16**, L693.

Gay, J. C., D. Delande, and A. Bommier, 1988, in *Proceedings of 11th International Conference on Atomic Physics,* edited by C. Fabre and D. Delande (École Normale Supérieure, Paris). Book of Abstracts, VIII-51.

Gilmore, R., and D. H. Feng, 1978, Nucl. Phys. A **301**, 189.

Grozdanov, T. P., and M. J. Raković, 1988, J. Phys. B **21**, 4087.

Grozdanov, T. P., and E. A. Solov'ev, 1984, J. Phys. B **17**, 555.

Grozdanov, T. P., and H. S. Taylor, 1986, J. Phys. B **19**, 4075.

Harmin, D. A., 1984, Phys. Rev. A **30**, 2413.

Haroche, S., 1986, in *Atoms in Unusual Situations,* edited by J. P. Briand (Plenum, New York), p. 77.

Harter, W. G., and C. W. Patterson, 1977, J. Chem. Phys. **66**, 4872.

Hasegawa, H., and S. Adachi, 1988, J. Phys. Soc. Jpn. **57**, 80.

Hasegawa, H., A. Harada, and Y. Okazaki, 1984, J. Phys. A **17**, L883.

Hasegawa, H., M. Robnik, and G. Wunner, 1989, Prog. Theor. Phys. Suppl. **98**, 198.

Herrick, D., 1982, Phys. Rev. A **26**, 323.

Hinds, E. A., 1990, Adv. At. Mol. Opt. Phys. **28**, 235.

Holle, A., B. Hager, and K. H. Welge, 1985, in *Proceedings of II European Conference on Atomic and Molecular Physics,* edited by A. E. de Vries and M. J. van der Wiel (Europ. Phys. Soc., Amsterdam), Book of Abstracts, p. 6.

Holle, A., J. Main, G. Wiebusch, H. Rottke, and K. H. Welge, 1988, Phys. Rev. Lett. **61**, 161.

Jenkins, F. A., and E. Segre, 1939, Phys. Rev. **55**, 52.

Jones, W. B., and W. J. Thron, 1980, *Continued Fractions: Analytic Theory and Applications* (Addison-Wesley, Reading).

Kazantsev, A. P., and V. L. Pokrovsky, 1983a, Pis'ma Zh. Eksp. Teor. Fiz. **37**, 471.

Kazantsev, A. P., and V. L. Pokrovsky, 1983b, Zh. Eksp. Teor. Fiz. **85**, 1917.

Kazantsev, A. P., and V. L. Pokrovsky, 1983c, J. Phys. B **16**, L601.

Kazantsev, A. P., V. L. Pokrovsky, and J. Bergou, 1983, Phys. Rev. A **28**, 3659.

Komarov, I. V., T. P. Grozdanov, and R. R. Janev, 1980, J. Phys. B **13**, L573.

Komarov, I. V., L. I. Ponomarev, and S. Yu. Slavyanov, 1976, *The Spheroidal and Coulomb Spheroidal Functions* (Nauka, Moscow). In Russian.

König, A., J. Neukammer, K. Vietzke, M. Kohl, H. J. Grabka, H. Hieronymus, and H. Rinneberg, 1988, Phys. Rev. A **38**, 547.

Korevaar, E. G., and M. G. Littman, 1983, J. Phys. B **16**, L437.

Kravchenko, V. A., and A. S. Prostnev, 1973, Dok. Akad. Nauk SSSR **211**, 75.

Landau, L. D., and E. M. Lifshitz, 1989, *Quantum Mechanics: Non-Relativistic Theory* (Nauka, Moscow). In Russian.

Landau, L. D., and E. M. Lifshitz, 1988, *Mechanics* (Nauka, Moscow). In Russian.

Langer, R. E., 1937, Phys. Rev. **51**, 669.

Lee, M. H., J. Hong, and J. Florencio, Jr., 1987, Phys. Scr. **T19**, 498.

Leopold, J. G., and D. Richards, 1989, J. Phys. B **22**, 1931.

Lindgard, A., and S. E. Nielsen, 1977, At. Data Nucl. Data **19**, 533.

Lipkin, H. J., N. Meshkov, and A. J. Glick, 1965, Nucl. Phys. **62**, 188.

Lisitsa, V. S., 1987, Usp. Fiz. Nauk **153**, 379 [Sov. Phys. Usp. **30**, 927 (1987)].

Makarov, V. P., and M. V. Fedorov, 1976, Zh. Eksp. Teor. Fiz. **70**, 1185.

Maslov, V. P., 1973, *The Operator Methods* (Nauka, Moscow). In Russian.

Maslov, V. P., and M. V. Fedoryuk, 1981, *Quasiclassical Approximation for the Equations of Quantum Mechanics* (Reidel, Dordrecht).

Mur, V. D., and V. S. Popov, 1988, Zh. Eksp. Teor. Fiz. **94**, 125 [Sov. Phys.—JETP **67**, 2027 (1988)].

Nayfeh, M. H., and C. W. Clark, 1985, Eds., *Atomic Excitation and Recombination in External Fields* (Gordon and Breach, New York).

Nikitin, S. I., and V. N. Ostrovsky, 1982, J. Phys. B **15**, 1609.

O'Mahony, P. F., 1988, in *Fundamental Processes of Atomic Dynamics,* edited by J. S. Briggs, H. Kleinpoppen, and H. O. Lutz (Plenum, New York), p. 197.

O'Mahony, P. F., and K. T. Taylor, 1986a, Phys. Rev. Lett. **57**, 2931.

O'Mahony, P. F., and K. T. Taylor, 1986b, J. Phys. B **19**, L65.

Ostrovsky, V. N., and D. A. Telnov, 1987, J. Phys. B **20**, 2397.

Pauli, W., 1926, Z. Phys. **36**, 336.

Penent, F., D. Delande, F. Biraben, and J. C. Gay, 1984, Opt. Commun. **49**, 184.

Penent, F., D. Delande, and J. C. Gay, 1988, Phys. Rev. A **37**, 4707.

Ponzano, C., and T. Regge, 1968, in *Spectroscopic and Group Theoretical Methods in Physics,* edited by F. Bloch, S. G. Cohen, A. De-Shalit, S. Sambursky, and I. Talmi (Wiley, New York), p. 53.

Raithel, G., M. Fauth, and H. Walther, 1991, Phys. Rev. A **44**, 1898.

Rath, O., and D. Richards, 1988, J. Phys. B **21**, 555.

Rau, A. R. P., 1989, Phys. Rev. Lett. **63**, 244.

Rau, A. R. P., 1990, Rep. Prog. Phys. **53**, 181.

Rau, A. R. P., and Lijun Zhang, 1990, Phys. Rev. A **42**, 6342.

Rau, A. R. P., and Q. Molina, 1989, J. Phys. B **22**, 189.

Reinhardt, W. P., 1983, J. Phys. B **16**, L635.

Richards, D., 1983, J. Phys. B **16**, 749.

Richter, K., D. Wintgen, and J. S. Briggs, 1987, J. Phys. B **20**, L627.

Rinneberg, H., J. Neukammer, A. König, H. Hieronymus, M. Kohl, and G. Jönsson, 1986, in *Proceedings of Oji International Seminar on Highly Excited States of Atoms and Molecules,* edited by S. S. Kano and M. Matsuzawa (Fuji-Yoshida, Japan), p. 7.

Rinneberg, H., J. Neukammer, A. König, K. Vietzke, H. Hieronymus, M. Kohl, H. J. Grabka, and G. J. Jönsson, 1987, Hyperfine Interact. **38**, 515.

Robnik, M., 1981, J. Phys. A **14**, 3195.

Robnik, M., 1982, J. Phys. (Paris) Colloq. **43**, c2-45

Sazonov, V. N., 1978, Teor. Nat. Fizika **35**, 361 [Sov. Phys. Theor. Math. Phys. **35**, 514 (1978)].

Schiff, L. I., and H. Snyder, 1939, Phys. Rev. **55**, 59.

Schulten, K., and R. G. Gordon, 1975, J. Math. Phys. **16**, 1970.

Sokoloff, J. B., 1985, Phys. Rep. **126**, 189.

Solov'ev, E. A., 1981, Pis'ma Zh. Eksp. Teor. Fiz. **34**, 278 [JETP Lett. **34**, 265 (1981)].

Solov'ev, E. A., 1982, Zh. Eksp. Teor. Fiz. **82**, 1762 [Sov. Phys. JETP **55**, 1017 (1982)].

Solov'ev, E. A., 1983, Zh. Eksp. Teor. Fiz. **85**, 109 [Sov. Phys. JETP **58**, 63 (1983)].

Sumetsky, M. Yu., 1982, Zh. Eksp. Teor. Fiz. **83**, 1661 [Sov. Phys. JETP **56**, 959 (1983)].

Taylor, K. T., C. W. Clark, and M. H. Nayfeh, 1988, Eds., *Atomic Spectra and Collisions in External Fields* (Plenum, New York).

Uzer, T., 1990, Phys. Rev. A **42**, 5787.

van der Veldt, T., G. J. Kuik, and W. Hogervorst, 1990, in *Proceedings of 22nd European Group on Atomic Spectroscopy,* edited by K. Bethge (European Physical Society, Uppsala), Book of Abstracts, p. 529.

van der Veldt, T., W. Vassen, and W. Hogervorst, 1992, J. Phys. B **25**, 3295.

Vasil'eva, A. B., and V. F. Butuzov, 1978, *Singularly Perturbed Equations in the Critical Cases* (Moscow University, Moscow). In Russian.

Wall, H. S., 1983, *Analytic Theory of Continued Fractions* (Chelsea, New York).

Watanabe, S., 1989, Phys. Rev. A **39**, 417.

Waterland, R. L., J. B. Delos, and M. L. Du, 1987, Phys. Rev. A **35**, 5064.

Watson, J. K. G., 1967, J. Chem. Phys., **46**, 1935.

Watson, J. K. G., 1977, in *Vibrational Spectra and Structure,* edited by J. R. Durig (Elsevier, Amsterdam), Vol. 6, p. 1.

Wiebusch, G., J. Main, K. Krüger, H. Rottke, A. Holle, and K. H. Welge, 1989, Phys. Rev. Lett. **62**, 2821.

Windholz, L., 1990, Z. Phys. D **15**, 87.

Wintgen, D., and H. Friedrich, 1986a, J. Phys. B **19**, 991.

Wintgen, D., and H. Friedrich, 1986b, J. Phys. B **19**, 1261.

Wintgen, D., and H. Friedrich, 1987, Phys. Rev. A **36**, 131.

Wintgen, D., A. Holle, G. Wiebusch, J. Main, H. Friedrich, and K. H. Welge, 1986, J. Phys. B **19**, L557.

Wunner, G., 1986, J. Phys. B **19**, 1623.

Zeller, G., R. Niemeier, W. Schweizer, and G. Wunner, 1989, in *Proceedings of the III European Conference on Atomic and Molecular Physica* (Bordeaux), Book of Abstracts, p. 223.

Ziman, J. M., 1964, *Principles of the Theory of Solids* (Cambridge University, Cambridge).

Zimmerman, M. L., M. M. Kash, and D. Kleppner, 1980, Phys. Rev. Lett. **45**, 1092.

Zimmerman, M. L., M. G. Littman, M. M. Kash, and D. Kleppner, 1980, Phys. Rev. A **20**, 2251.